Mismatched Mimics: Insights and Conundrums from the Evolutionary History of Colorful Ground Beetles

by

Carlos P. Munoz Ramirez

A dissertation submitted in partial fulfillment
of the requirements for the degree of
Doctor of Philosophy
(Ecology and Evolutionary Biology)
in The University of Michigan
2017

Doctoral Committee:

Professor Lacey L. Knowles, Chair
Professor Diarmaid O'Foighil
Assistant Professor Stephen A. Smith
Assistant Professor Selena Y. Smith

Carlos P. Munoz Ramirez

carmunoz@umich.edu

ORCID iD: 0000-0003-1348-5476

© Carlos P. Munoz Ramirez 2017

DEDICATION

This dissertation is dedicated to my family—Maribel, Aleli, and Jazmin—which has been an invaluable support along these years of intense academic and human growth.

ACKNOWLEDGMENTS

I would like to thank my lab mates Rob Mazzatti, Jen-Pan Huang, Qixin He, Lucy Tran, Andrea Thomas, and Tristan McKnight, for their insightful discussions and conversations that allowed me to learn in an enjoyable and stimulating environment. I am also thankful with my advisor, Lacey Knowles, who supported me in the most difficult moments. I learnt a great deal of good science during our conversations and lab meetings.

I also want to thank Alvaro Zuñiga, Dusan Boric, Gustavo Valenzuela, Christian Muñoz, Laurent Rataj, and Dr. Viviane Jerez for donating specimens. I am especially grateful to Alvaro Zuñiga, Christian Muñoz, Alfonso Jara, Luis Correa, Jorge Avaria, Pablo Fuentes and many others for their selfless help in the field. I also thank Corporación Nacional Forestal (CONAF) for granting permits to sample within several National Parks (Authorization number: 024/2012), the Ammerman Fund from the Insect Division of Ruthven Museums for funding my fieldwork, and Becas Chile (CONICYT, Chile) (CM-R) and Fulbright scholarships for sponsorship and funding support. This research was aided with funds from Block Grants and Hinsdale-Walker scholarships from the department of Ecology and Evolutionary Biology and a National Science Foundation DDIG grant (DEB-1601260).

TABLE OF CONTENTS

LIST OF FIGURES

FIGURES CHAPTER 2:

FIGURES CHAPTER 3:

FIGURES CHAPTER 4:

LIST OF TABLES

TABLES CHAPTER 2:

TABLES CHAPTER 3:

TABLES CHAPTER 4:

ABSTRACT

A particular form of evolutionary convergence among species—known as mimicry—is a phenomenon that has stimulated great progress in the fields of ecology and evolutionary biology. In particular, the phenomenon of Müllerian mimicry (the phenotypic convergence between aposematic species driven by shared predators) has been studied for more than 100 years in butterflies from the genus *Heliconius* because the almost perfect matching of color morphs between species highlights the power of natural selection as a deterministic evolutionary force. Although many lessons have been learned from this study system, many questions still remain; for example, it is still unclear how general the principles learnt from this system are or what role it plays on generating diversity. Here, a new mimicry system—the ground beetle genus *Ceroglossus*—is uncovered and studied to test some of these important questions. First, although the evolution of color matching between some species was clearly supported by data and simulation-based analyses (Chapter 2), the most remarkable characteristic is that the strength or degree of mimicry varies across regions. This finding may provide exceptional opportunities to study aspects of mimicry that cannot be analyzed in systems where mimicry is more accurate. For example, understanding the factors causing the variation of the degree of mimicry across space might shed light on how mimicry evolves or under what scenarios mimicry can be facilitated or impeded. Second, the diversity of intraspecific forms in this system is quantified and analyzed using recently developed species delimitation methods to understand the taxonomic diversity of the *Genus* (chapter 2). The results of this chapter highlight important issues and challenges of species delimitation methods, particularly when combined with large amounts of molecular data. For example, it was found that although phenotypic diversity suggested the potential for multiple species, current delimitation

methods were not able to distinguish whether lineage diversity corresponded to population or species structure. These results are important because appropriately distinguishing taxonomic limits not only affect estimations of diversity, but also our understanding of important evolutionary processes and their role on mimicry and evolution more generally. Finally, in chapter 3, the evolutionary history of co-distributed species was studied and quantified to test coevolution, a long standing question in Müllerian mimicry research. Because Müllerian mimicry is considered a mutualistic process, it has been argued that Müllerian mimicry provides particularly good conditions for coevolution. The results showed high levels of phylogenetic congruence in agreement with the hypothesis of coevolution. However, the results also showed that the varying degrees of mimicry across regions did not affect the phylogenetic congruence, failing to support an association between mimicry and coevolution. This is the first time that the degree of mimicry is accounted for to understand these processes at a regional scale and the results suggest that the role of mimicry on speciation and diversification is complex and requires further investigation. The study of this system provides a window to deepen our understanding about the role of mimicry on generating patterns of diversity, but most importantly, its uniqueness in regards to the spatial variation in the strength of mimicry also provides a natural experiment to investigate a completely new set of questions about factors favoring or disfavoring the evolution of phenotypic convergence.

CHAPTER 1: INTRODUCTION

Among the most fundamental questions in evolutionary biology are how diversity originates, evolve and persist over time (Coyne and Orr 2004; Futuyma 2013). The study of Müllerian mimicry, the evolution of resemblance between unpalatable species, has greatly advanced our knowledge on these questions (Ruxton et al. 2004; Pfennig 2012; Merrill et al. 2015). For example, some Müllerian mimicry systems, like the genus *Heliconius*, have become classic examples of the power of natural selection to produce striking convergent phenotypic evolution (Müller 1879) and promote speciation (Jiggins et al. 2001). Unfortunately, other Müllerian systems have not been studied in the same depth, which has limited not only our understanding of the generality of the principles we have learnt from the more classic systems, but also our ability to test basic questions under different conditions (e.g. particular advantages for experimental designs) that other systems might provide, but the more classic systems might not. One of the main foci on mimicry research has been on to explain the remarkable accuracy of phenotypic matching among co-mimics (Brower 1994; Sherratt 2006). However, the study of how less accurate mimicry can evolve has attracted relatively less attention. Remarkable studies on imperfect mimicry, nevertheless, have increased our understanding on topics like cognitive predator behavior (Johnstone 2002; Pfennig and Kikuchi 2012; Smith et al. 2016), and the effects tradeoffs between gene flow and natural selections (Harper and Pfennig 2008) on the maintenance of mimetic patterns. Another aspect related with imperfect mimicry is the existence of local polymorphism in some species (e.g. one sex is mimetic, but the other is not), whose study has shed light on particularities of the genetic architecture of the mimetic traits (Mallet and Joron 1999; Stoddard 2012). In this dissertation, I uncover a remarkable new mimicry system—the ground beetle genus *Ceroglossus*—that possess several striking

characteristics that make it an excellent model system to study Müllerian mimicry (Chapter 2). It is a system of three species groups which overlap across large areas of South Chile, with high diversity of color morphs, and most remarkably, it exhibits varying degrees of mimicry across space. In other words, the degree of phenotypic matching varies geographically. Unlike other mimicry systems, the variation in the degree of mimicry in *Ceroglossus* provides an excellent opportunity to investigate what is the role of mimicry on processes like speciation and diversification. For example in Chapter 3, I conduct species delimitation analyses to study the taxonomic diversity of the genus with the aim to not only gain a better understanding on the taxonomic diversity of the genus, but also on the role of mimicry on speciation. Accurate delimitation of species in Müllerian systems is not only important to appropriately account for the diversity within the group, but also because how we delimit species might have profound consequences on our understanding of the processes generating diversity in Müllerian systems. Two main findings were that most color morphs were supported as different evolutionary units and that the degree of mimicry across species was not associated with the support for speciation. Most importantly, validation tests suggested that species delimitation analyses are highly sensitive to delimit population genetic structure, which complicate our ability to distinguish whether delimited entities represent species or populations. These results have two-fold implications. On one hand, it highlights the challenges of existing species delimitation methods, particularly when coupled with genome scale data, to delimit a process that is essentially continuous and whose limits are commonly blurred. On the other hand, they suggest that the role of Müllerian mimicry on speciation is not a generality and that additional processes (e.g. assortative mating) might be a requirement to promote speciation. Finally in Chapter 4, I investigated the role of Müllerian mimicry on the diversification of intraspecific diversity. Specifically, detailed phylogenetic analyses were used to test whether Müllerian mimicry promoted coevolution, a long standing debate in the mimicry literature. The *Ceroglossus* system offered an excellent opportunity to test this hypothesis because the variation in the degree of mimicry allowed

testing whether the degree of mimicry could predict levels of phylogenetic congruence among co-mimics. The results provided support for the hypothesis of co-divergence, although the role of mimicry could not be linked to coevolution because an association between the degree of mimicry and the degree of co-divergence was not found. This result emphasizes that co-divergence may result from mechanisms other than mimicry, and that mimicry may not be a promoter of diversity but rather a result of it, arising perhaps just by filtering of pre-existing polymorphism.

Research on mimicry has promoted the idea that mimicry can be an important driver of diversity. The results of this dissertation challenge the idea that mimicry may drive speciation and coevolution and raise the question whether mimicry evolves before—promoting diversity—or after race formation. This do not undermine the importance of mimicry on the generation of diversity, but suggest that its role might be more restricted to the formation and maintenance of the pattern of interspecific color covariation rather than the generation of polymorphism. The results of this dissertation encourage the need for more investigation in disparate taxa with different ecological and evolutionary contexts in order to gain a full understanding of the processes contributing to biodiversity.

CHAPTER 2: MIMICS HERE AND THERE, BUT NOT EVERYWHERE: MÜLLERIAN MIMICRY IN *CEROGLOSSUS* GROUND BEETLES?

2.1 ABSTRACT

The ground beetle genus *Ceroglossus* contains co-distributed species that show pronounced intraspecific diversity in the form of geographic colour morphs. While colour morphs among different species appear to match in some geographic regions, in others there is little apparent colour matching. Mimicry is a potential explanation for covariation in colour patterns, but it is not clear whether the degree of sympatric colour matching is higher than expected by chance given the obvious mismatches among morphs in some regions. Here we used reflectance spectrometry to quantify elytral colouration from the perspective of an avian predator to test whether colour similarity between species is indeed higher in sympatry. After finding no significant phylogenetic signal in the colour data, analyses showed strong statistical support for sympatric colour similarity between species despite the apparent lack of colour matching in some areas. We hypothesize Müllerian mimicry as the responsible mechanism for sympatric colour similarity in *Ceroglossus* and discuss potential explanations and future directions to elucidate why mimicry has not developed similar levels of interspecific colour resemblance across space.

2.2 INTRODUCTION

The existence of multiple geographic races is a common phenomenon in aposematic species (e.g. Brower 1994; Marek and Bond 2009; Noonan and Comeault 2009; Yeager et al. 2012) that can be

maintained by localised frequency-dependent selection. When multiple closely related or phenotypically similar aposematic species co-occur, phenotypic convergence is locally favored because species benefit from sharing the costs of teaching predators about their unpalatability. This phenomenon, known as Müllerian mimicry, is documented in several systems exhibiting geographic mosaics of mimetic forms (e.g. Brower 1994; Marek and Bond 2009; Yeager et al. 2012) and is best exemplified by Heliconius butterflies (Brower 1994) where species mimic each other across extensive geographic areas with remarkable accuracy. Although geographic variation in aposematic colouration can also occur in the absence of mimicry (Noonan and Comeault 2009), extreme variation seems to be relatively frequent in Müllerian systems(Aubier and Sherratt 2015).

In this study, we investigate whether species of ground beetles in the genus *Ceroglossus,* which are conspicuously coloured and chemically defended species endemic to the temperate forests of southern South America (Jiroux 2006), are a possible new candidate system of mimicry. The taxa are widely co-distributed and characterized by high intraspecific variation (Aubier and Sherratt 2015; figure 2.1). In addition, some striking covariation in elytral colouration has been noted among co-occurring species (Okamoto et al. 2001). For example, up to three different species with similar colouration can be collected at some localities, suggestive of colour convergence. However, such interspecific colour matching is weak or lacking at other sites (figure 2.2A) calling into question whether mimicry actually explains the pronounced phenotypic variation in *Ceroglossus*.

To examine whether mimicry plays a predominant role in the *Ceroglossus* beetles, we collected reflectance data and tested whether the degree of colour matching among coexisting species is greater than expected by chance. Failure to reject the null hypothesis would preclude the need for invoking deterministic explanations posited by mimicry. By contrast, rejecting the null hypothesis of chance would lend preliminary support for a role of mimicry.

2. 3 METHODS

We collected colour data from 195 individuals belonging to three of the most widely distributed taxa that overlap to varying degrees: *Ceroglossus chilensis* (n= 57), *C. buqueti* (n= 71), and the *C. darwini* species group (n= 67) (more sampling details can be found in Tables S1 and S2 in the electronic supplementary material). Species were identified following the diagnostic characters described by Jiroux (2006) (e.g. the number and position of antennal carinas).

Quantification of colour

Colour data was quantified with a USB4000 spectrophotometer (Ocean Optics) under a deuterium-tungsten light source (Ocean Optics) and in relation to a white reference standard (WS-1 Ocean Optics), from 300-700 nm. Data were processed with the R-package 'pavo' (Maia et al. 2013) to represent the visual system of potential predators (avian UV and VS and reptile) following Endler and Mielke (2005) and Stoddard and Prum (2008). Additional methodological details and data can be found in the electronic supplementary material.

Testing phylogenetic signal

A 680 bp-fragment of the COI gene was obtained for 42 individuals following the protocol described in (Muñoz-Ramírez 2015). Sequences were used to estimate a Bayesian phylogeny using MrBayes 3.2.6 (Ronquist and Huelsenbeck 2003). Because our colour data is multidimensional, phylogenetic signal of trait values was tested by both the Mantel test (Harmon and Glor 2010) and a multivariate implementation of Pagel's lambda test available in *Rphylopars* (Goolsby et al. 2016). See the electronic supplementary material for details about sequenced individuals and GenBank accession numbers (Table S1) and data (Table S2).

Randomization test of colour matching

Because of the lack of phylogenetic signal in colour indicated by both the Mantel test and the Pagel's lambda test (Table S3, electronic supplementary material), we tested whether colour similarity between species was higher within than between sites using randomization tests. Specifically, we calculated all pairwise interspecific colour distances—the Euclidean distance between the colour-space coordinates (e.g. Dalrymple et al. 2015) of each population's centroid—to test whether "within-site" distances were lower than "between-site" distances. Posteriorly, to test whether the mean of the within-site colour distances (n=29) was lower than expected by chance, we compared the observed mean against a random distribution generated from 1,000 mean colour values calculated by randomly picking 29 distance values (i.e. the same number of within-site distances calculated from the empirical data) from the total pool of distances without replacement.

2.4 RESULTS

Analyses using the avian UV, the avian VS, and the reptile model data produced nearly identical results. Therefore, here we only present the results for the UV model. Results for the other models can be found in the electronic supplementary material, figures S1 and S2. Spectral reflectance plots for sites containing all three species can be found in figure S3. Interspecific colour distances were lower within sites (n= 29; mean= 0.126; s.d.= 0.072) than between sites (n= 706; mean= 0.214; s.d.= 0.108) and this difference was statistically significant (one-way ANOVA, $F(2, 1078)=11.9$; $p<0.001$) (figure 2.2B). Furthermore, within-site colour distances between species were on average also lower than between-site colour distances among populations of the same species (n= 346; mean= 0.194; s.d. = 0.11). This pattern was statistically supported by the randomization test, showing that the mean colour distance within sites was much lower than random expectations (figure 2.2C).

2.5 DISCUSSION

Even though *Ceroglossus* species exhibit little evidence of colour matching in some areas (figure 2.2A), the degree of covariation of elytral colouration among species nonetheless deviates from random expectations (figure 2.2C), providing preliminary support for the potential role of mimicry in these beetles. Because all *Ceroglossus* have glands that produce noxious chemical compounds (Okamoto et al. 2001), we hypothesise that this pattern may represent a case of Müllerian mimicry. Although alternative, non-mimetic explanations for colour variation can be invoked including sexual or natural selection for certain colours in similar light environments, high colour variation across areas in close geographic proximity with similar forest (and therefore light environment) types suggests these mechanisms are unlikely to explain colour matching patterns in *Ceroglossus*. Similarly, the evolution of certain colours to match the background substrate (crypsis) seems also unlikely since many *Ceroglossus* beetles appear conspicuously coloured relative to a forest background (i.e. bright metallic red and blue) and they are very active predators in nearly constant motion (Jiroux 2006), which should make them easily visible to predators.

Although further studies are necessary to confirm mimicry, including toxicity quantification and field/lab experiments, this study represents the first step in establishing the Müllerian mimicry hypothesis as a primary determinant of colour variation across these species (figure 2.1). Below we highlight aspects of the *Ceroglossus* beetle system—in particular, and perhaps somewhat ironically, the variation in the degree of matching across geography (figure 2.2A)—that speak to its potential promise for providing insights about the evolutionary dynamics associated with mimicry.

Potential insights on mimicry from Ceroglossus beetles

Instances of imperfect mimicry may shed new light on the processes that mediate mimicry evolution (e.g. Sherratt 2002; Penney et al. 2012). Potential processes preventing mimicry might include

ecological differences across space, high levels of maladaptive gene flow, and the stability of co-distributions among taxa.

Because predators are the selective force maintaining mimicry (Mallet and Barton 1989), shifts in predator communities across regions might change the selective landscape for mimicry causing strong selection for colour convergence in some areas versus weak selection for colour convergence in others (Aubier and Sherratt 2015). Alternatively, positive frequency-dependent selection on similarly abundant aposematic morphs (Chouteau et al. 2016a), or microhabitat partitioning of mimicry patterns to exploit different predator assemblages (Elias et al. 2008) could also preclude selection for convergence. In *Ceroglossus*, differential predation pressures are possible given that the beetles are distributed across a relatively large geographic area with potentially different predator communities (Pena and Rumboll 1998). However, information on potential predators is scarce. Although mammals and reptiles may prey on beetles, birds are among the most abundant visual predators in Chilean forests, with beetles being commonly found in their diet (e.g. Correa et al. 1990; Jimenez and Jaksic 1993), suggesting they may play a dominant role in the evolution of colour patterns in *Ceroglossus*. However, without additional data, especially on the abundance of *Ceroglossus* and their predators, it remains unclear whether differences in predator communities or positive frequency-dependent selection on multiple aposematic local morphs might explain the observed variation.

Alternatively, increased connectivity between populations might counteract the evolution of mimicry if gene flow introduces colour genes that do not match local phenotypes (Harper and Pfennig 2008). In *Ceroglossus*, this possibility seems unlikely due to the flightlessness of the beetles. In addition, the geographic proximity of some different colour morphs suggests selection is strong enough to override the effect of gene flow (figure 2.2A). Nevertheless, this possibility could be investigated in the future with detailed genetic analyses in areas with different degrees of mimicry.

Lastly, Pleistocene glaciations may have also played a role in preventing the evolution of mimicry. Postglacial expansions may have resulted in mismatching of phenotypes, with “incomplete” mimicry possibly reflecting recent co-occurrence, or reduced rates of evolution resulting from limited standing genetic variation due to bottlenecks (i.e., a possible example of genetic constraint; Pfennig and Kikuchi (2012)). The distribution of *Ceroglossus* species encompasses regions known to have been impacted by glaciations (Sérsic et al. 2011; Muñoz-Ramírez et al. 2014), suggesting investigations into the role of stability should be considered in future studies.

A potential new mimicry complex among Ceroglossus ground beetles would complement well-studied systems like Heliconius. In particular, the variation in degree of phenotypic matching among the species provides a potential window into the mechanisms that drive, or conversely impede, the evolution of mimicry, in contrast with taxa that show uniform patterns of morphological variation clearly consistent with mimicry predictions.

2.6 FIGURES

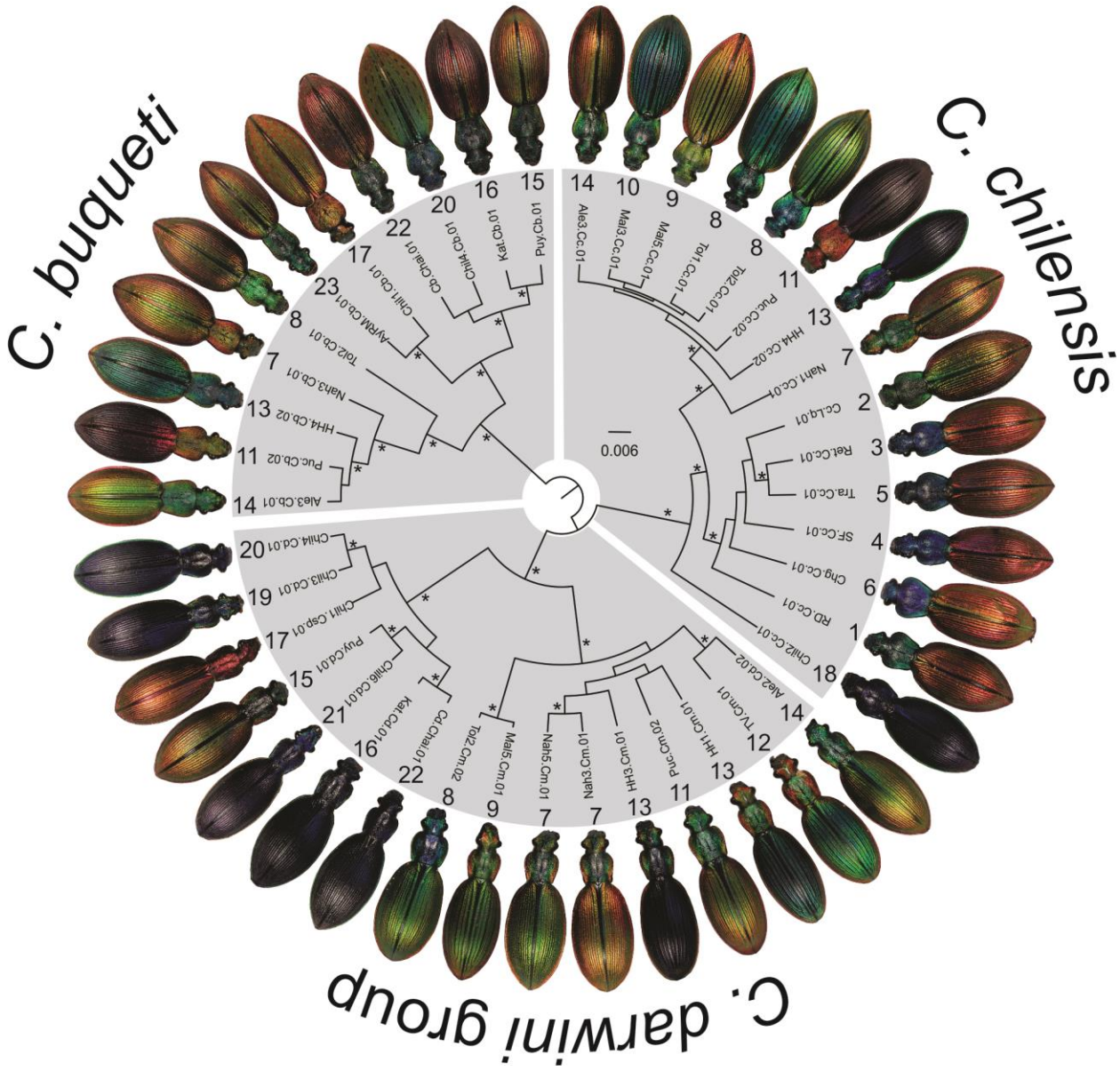

Figure 2.1: Colour diversity across the three Ceroglossus taxa analysed in this study. Relationships based on a Bayesian tree for COI recovered each of the three taxa as monophyletic (highlighted in grey). The * symbol indicates Bayesian posterior probabilities above 0.9.

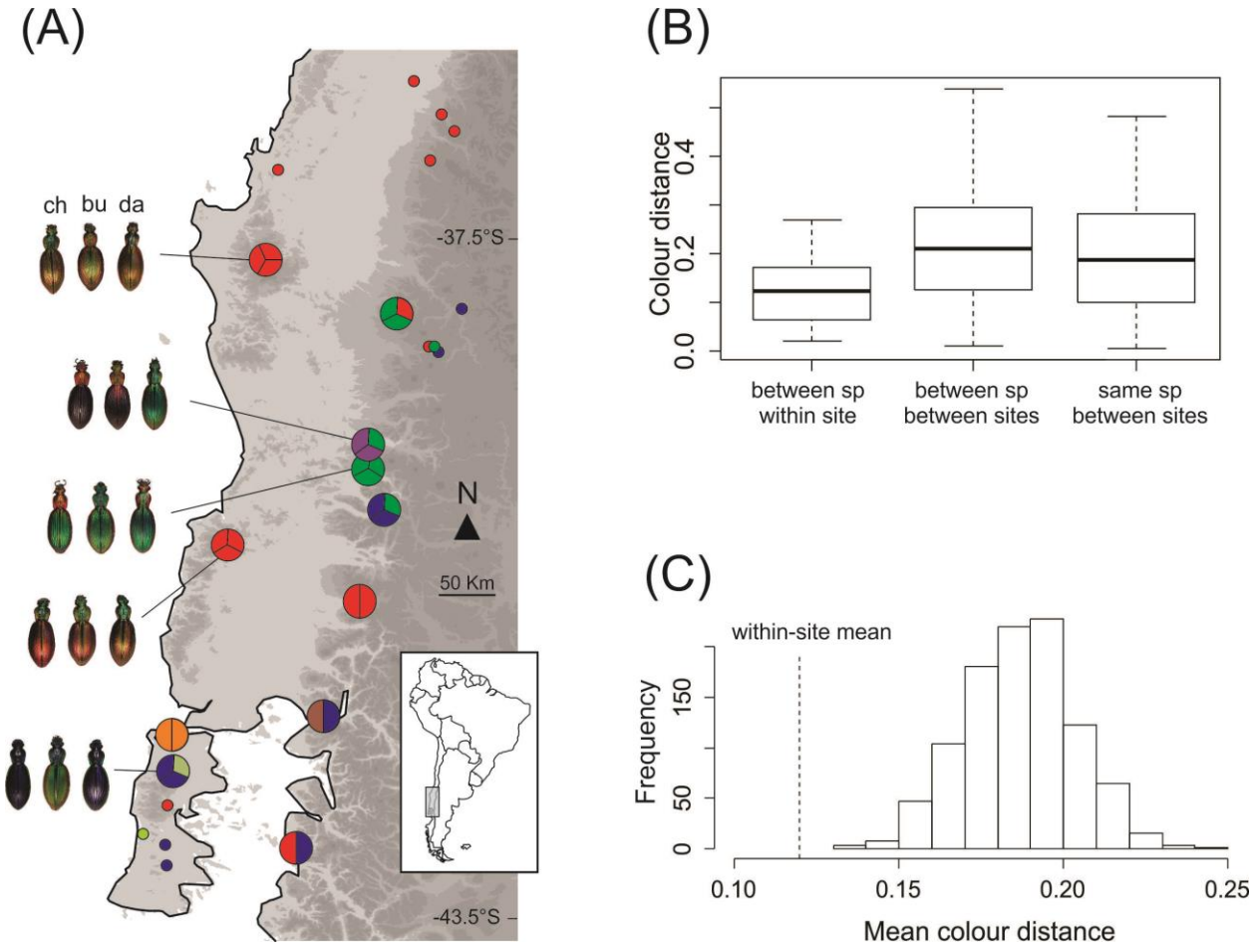

Figure 2.2: (A) Distribution map of *Ceroglossus* beetles highlighting by reference to sampled localities for three species (ch= *Ceroglossus chilensis*, dar= *Ceroglossus darwini* group, and buq= *Ceroglossus buqueti*) geographic areas where the taxa co-occur (shown by pie diagrams). Colour in the pie diagrams represents approximate species colouration in that area. The small coloured dots refer to localities where only a single species was collected. (B) Boxplots showing how within-site colour distances compare to between-site distances. (C) Randomization test showing the distribution of random colour-distance means versus the empirical within-site distance mean (dashed line).

2.7 APPENDIX

Additional details on phylogenetic estimation and phylogenetic signal test

The Bayesian phylogeny was estimated with MrBayes 3.2.6 (Ronquist and Huelsenbeck 2003) under a model of molecular evolution identified with JModeltest [7] based on Bayesian information criterion (BIC)—specifically, a HKY+I+G—and under a relaxed clock model to produce an ultrametric tree. The relaxed clock model is set in two steps. First, we set an underlying strict clock model using a coalescent model. Then, we select the independent gamma rates model (IGR), which is a continuous uncorrelated model of rate variation across lineages. Two independent analyses were run for 5,000,000 generations sampling every 1000 generations. After convergence between the two runs was confirmed, sampled trees were combined and the maximum clade credibility tree was obtained with the software TreeAnnotator v2.3.0 (distributed as part of the BEAST2 package (Bouckaert et al. 2014)) discarding 20% of the trees as burnin. Because our data can only be properly represented as multidimensional (not as a single trait), phylogenetic signal was tested via both the Mantel test, which assesses the correlation between phylogenetic distance and trait distance, and the Pagel's lambda test for multivariate traits implemented in the R-package Rphylopars (Goolsby et al. 2016). Data associated to the tree can be found in Table S2. For tips representing localities with multiple individuals quantified for colour, we used the mean trait value to represent the trait for that tip. For the Mantel test, we calculated phylogenetic distances with the "phytools" R-package (function fastDist), while colour distances were calculated as Euclidean distances for all pairwise combinations of taxa in the tree. For the Pagel's lambda test, we compared the likelihood of the empirical lambda (i.e. the tree transformation parameter that maximizes de likelihood of the Brownian motion model) against the likelihood of a star phylogeny (lambda=0) using the likelihood ratio test. Then we conducted the Mantel test with 1000 permutations using

the R-package "vegan" [10]. Because both approaches indicated a lack of phylogenetic signal (see Table S3), we tested the hypothesis of colour matching by randomization [11].

Table S1. Information for the 42 sequenced individuals used for the phylogenetic analysis representing the three species analyzed in this study, *Ceroglossus chilensis* (ch), *C. buqueti* (bu), and the *C. darwini* group (dar).

Site No	Site name	Latitude	Longitude	Voucher	GenBank code	ch	bu	dar
1	PN Radal-Siete Tazas	-35.4756	-70.9938	RD.Cc.01	KT997735	x		
2	Los Queules	-35.9900	-72.7003	Cc.Lq.01	KT997731	x		
3	Retiro	-36.0908	-71.7834	Ret.Cc.01	KT997732	x		
4	San Fabian	-36.5500	-71.4310	SF.Cc.01	KT997734	x		
5	Las Trancas	-36.8040	-71.6456	Tra.Cc.01	KT997733	x		
6	Chiguayante	-36.9355	-73.0011	Chg.Cc.01	KT997736	x		
7	PN Nahuelbuta	-37.8163	-73.0094	Nah3.Cm.01	KT997750			x
7		-37.8163	-73.0094	Nah3.Cb.01	KT997765		x	
7		-37.8193	-73.0283	Nah1.Cc.01	KT997737	x		
7		-37.8261	-72.9863	Nah5.Cm.01	KT997749			x
8	PN Tolhuaca	-38.2101	-71.8053	Tol1.Cc.01	KT997742	x		
8		-38.2220	-71.7504	Tol2.Cc.01	KT997743	x		
8		-38.2220	-71.7504	Tol2.Cm.02	KT997751			x
8		-38.2220	-71.7504	Tol2.Cb.01	KT997770		x	
9	Malalcahuello, Area1	-38.4710	-71.5760	Mal5.Cm.01	KT997753			x
9		-38.4710	-71.5760	Mal5.Cc.01	KU978918	x		
10	Malalcahuello, Area 2	-38.5138	-71.5137	Mal3.Cc.01	KU978917	x		
11	PN Villarrica, Pucon	-39.3508	-71.9680	Puc.Cc.02	KT997740	x		
11		-39.3508	-71.9680	Puc.Cm.02	KT997752			x
11		-39.3508	-71.9680	Puc.Cb.02	KT997768		x	
12	Termas Vergara	-39.5098	-71.8928	TV.Cm.01	KT997755			x
13	Neltume	-39.8538	-71.9517	HH1.Cm.01	KT997747			x
13		-39.8903	-71.9568	HH4.Cc.02	KT997741	x		
13		-39.8903	-71.9568	HH4.Cb.02	KT997766		x	
13		-39.9106	-71.9540	HH3.Cm.01	KT997748			x

14	PN Alerce Costero	-40.1825	-73.4386	Ale2.Cd.02	KT997758				x
14		-40.1967	-73.4321	Ale3.Cc.01	KT997745	x			
14		-40.1967	-73.4321	Ale3.Cb.01	KT997767			x	
15	PN Puyehue	-40.6641	-72.1720	Puy.Cd.01	KT997754				x
15		-40.6641	-72.1720	Puy.Cb.01	KT997764			x	
16	Puerto Montt	-41.5142	-72.7554	Kat.Cd.01	KT997746				x
16		-41.5142	-72.7554	Kat.Cb.01	KT997763			x	
17	Ancud, Chiloe	-41.8820	-73.8799	Chil1.Csp.01	KT997761				x
17		-41.8820	-73.8799	Chil1.Cb.01	KT997769			x	
18	Puntra, Chiloe	-42.1195	-73.8066	Chil2.Cc.01	KT997744	x			
19	Abtao, Chiloe	-42.3996	-73.8507	Chil3.Cd.01	KT997756				x
20	Cucao, Chiloe	-42.6481	-74.0653	Chil4.Cd.01	KT997757				x
20		-42.6481	-74.0653	Chil4.Cb.01	KT997762			x	
21	Las Margaritas, Chiloe	-42.7792	-73.7958	Chil6.Cd.01	KT997759				x
22	Chaiten	-42.9097	-72.7074	Cd.Chai.01	KT997760				x
22		-42.9097	-72.7074	Cb.Chai.01	KT997771			x	
23	Aysen	-45.1327	-73.0154	AyRM.Cb.01	KT997772			x	

Table S2. Colour data associated to the phylogenetic tree (tip data) used for testing phylogenetic signal. Column names with the prefix uv correspond to data for the UV avian visual system, while the prefix vs represents columns with the avian VS model data. The prefix rep identifies the data projected to model the reptile visual system

tip name	uv.x	uv.y	uv.z	vis.x	vis.y	vis.z	rep.x	rep.y
Ceroglossus chilensis HH4.Cc.02	-0.0257	-0.0178	0.0038	-0.0019	-0.0040	0.0483	-0.0159	0.0583
Ceroglossus chilensis Ale3.Cc.01	0.2460	-0.0326	-0.1532	0.2378	-0.0348	-0.1509	0.2233	-0.1712
Ceroglossus chilensis Tol1.Cc.01	-0.0129	0.0567	-0.0514	-0.1177	0.0439	-0.0884	0.0081	-0.1250
Ceroglossus chilensis Tol2.Cc.01	0.0269	0.2288	-0.1185	-0.0065	0.1925	-0.1323	0.0081	-0.1250
Ceroglossus chilensis Mal5.Cc.01	0.1520	-0.0077	-0.1010	0.1473	-0.0095	-0.0970	0.1310	-0.1026
Ceroglossus chilensis Mal3.Cc.01	-0.0997	-0.0284	-0.0638	-0.1198	-0.0425	-0.0393	-0.0722	-0.0062
Ceroglossus chilensis Puc.Cc.02	0.0409	-0.0221	-0.0214	0.0434	-0.0193	-0.0120	0.0212	-0.0062
Ceroglossus chilensis Nah1.Cc.01	0.2374	-0.0069	-0.1448	0.2327	-0.0099	-0.1468	0.2376	-0.1796
Ceroglossus chilensis Chg.Cc.01	0.2343	0.0317	-0.1468	0.2292	0.0243	-0.1550	0.2516	-0.2008

Ceroglossus chilensis RD.Cc.01	0.3596	-0.1421	-0.1582	0.3664	-0.1373	-0.1622	0.3380	-0.1930
Ceroglossus chilensis SF.Cc.01	0.2835	-0.1502	-0.1123	0.2860	-0.1437	-0.1089	0.3380	-0.1930
Ceroglossus chilensis Ret.Cc.01	0.2973	-0.1266	-0.1282	0.2948	-0.1228	-0.1311	0.2213	-0.1359
Ceroglossus chilensis Tra.Cc.01	0.3028	-0.1443	-0.1305	0.3020	-0.1383	-0.1260	0.2164	-0.1212
Ceroglossus chilensis Cc.Lq.01	0.2226	0.0201	-0.1517	0.2166	0.0165	-0.1483	0.2233	-0.1795
Ceroglossus chilensis Chil2.Cc.01	-0.0550	-0.0355	-0.0009	-0.0373	-0.0251	0.0340	-0.0317	0.0483
Ceroglossus darwini Cd.Chai.01	-0.0115	-0.0060	0.0203	-0.0070	-0.0034	0.0225	-0.0081	0.0180
Ceroglossus darwini Kat.Cd.01	-0.0867	-0.0599	0.0454	-0.0390	-0.0320	0.1247	-0.0462	0.1152
Ceroglossus darwini Chil6.Cd.01	-0.0597	-0.0437	0.0096	-0.0362	-0.0297	0.0564	-0.0358	0.0656
Ceroglossus darwini Puy.Cd.01	0.1829	0.0327	-0.1259	0.1772	0.0273	-0.1310	0.1883	-0.1577
Ceroglossus darwini Chil4.Cd.01	-0.0169	-0.0078	0.0178	-0.0140	-0.0061	0.0184	-0.0118	0.0172
Ceroglossus darwini Chil3.Cd.01	-0.0534	-0.0379	0.0530	-0.0275	-0.0229	0.0868	-0.0319	0.0768
Ceroglossus speciosus Chil1.Csp.01	0.2374	-0.0728	-0.1264	0.2284	-0.0722	-0.1268	0.1805	-0.1317
Ceroglossus magellanicus Tol2.Cm.02	0.1858	0.0355	-0.1246	0.1852	0.0252	-0.1314	0.2028	-0.1577
Ceroglossus magellanicus Mal5.Cm.01	0.0812	0.1171	-0.0959	0.0775	0.1066	-0.0979	0.1227	-0.1240
Ceroglossus magellanicus HH3.Cm.01	-0.0723	-0.0416	0.0412	-0.0421	-0.0241	0.0892	-0.0512	0.0397
Ceroglossus magellanicus Nah5.Cm.01	0.2162	-0.0058	-0.1253	0.2628	-0.0214	-0.1511	0.2254	-0.1575
Ceroglossus magellanicus Nah3.Cm.01	0.2162	-0.0058	-0.1253	0.1673	-0.0077	-0.0998	0.2254	-0.1575
Ceroglossus magellanicus Puc.Cm.02	0.1136	0.0988	-0.1200	0.1058	0.0868	-0.1209	0.1456	-0.1470
Ceroglossus magellanicus TV.Cm.01	-0.0653	0.1795	-0.0784	-0.0888	0.1484	-0.0693	-0.0247	-0.0892
Ceroglossus magellanicus Ale2.Cd.02	0.1810	0.0542	-0.1350	0.1744	0.0461	-0.1383	0.1984	-0.1705
Ceroglossus magellanicus HH1.Cm.01	-0.0667	-0.0073	-0.0050	-0.0899	-0.0223	-0.0097	-0.0512	0.0397
Ceroglossus buqueti AyRM.Cb.01	0.1356	-0.0036	-0.0865	0.1322	-0.0051	-0.0856	0.1177	-0.0953
Ceroglossus buqueti Chil1.Cb.01	0.2534	-0.0561	-0.1426	0.2439	-0.0579	-0.1469	0.2186	-0.1652
Ceroglossus buqueti Cb.Chai.01	0.0964	-0.0284	-0.0481	0.0941	-0.0284	-0.0511	0.0625	-0.0448
Ceroglossus buqueti Chil4.Cb.01	0.0609	0.1093	-0.0653	0.0439	0.0936	-0.0885	0.0773	-0.1159
Ceroglossus buqueti Kat.Cb.01	0.0628	-0.0259	-0.0204	0.0600	-0.0262	-0.0297	0.0333	-0.0233
Ceroglossus buqueti Puy.Cb.01	0.2407	-0.0396	-0.1362	0.2400	-0.0391	-0.1366	0.2234	-0.1548
Ceroglossus buqueti Tol2.Cb.01	0.1563	0.0124	-0.0905	0.1538	0.0087	-0.0955	0.1374	-0.1062
Ceroglossus buqueti Nah3.Cb.01	0.1135	0.1746	-0.1349	0.1071	0.1594	-0.1378	0.1738	-0.1853
Ceroglossus buqueti HH4.Cb.02	-0.0612	-0.0043	-0.0495	-0.0827	-0.0190	-0.0369	-0.0470	-0.0174
Ceroglossus buqueti Puc.Cb.02	0.0432	0.0495	-0.0533	0.0428	0.0465	-0.0375	0.0563	-0.0584

Ceroglossus buqueti Ale3.Cb.01	0.1879	0.0350	-0.1342	0.1836	0.0298	-0.1333	0.1961	-0.1587

Table S3. Results from the Mantel and Pagel's lambda tests of phylogenetic signal. Both tests were applied to all three color data projections: avian UV, avian VS, and reptile. All results were non-significant, indicating a lack of phylogenetic signal.

	Mantel test		Pagel's lambda test	
Trait based on:	Mantel statistic r	p-value	Pagel's lambda	p-value
Avian UV model	0.022	0.241	0.216	0.057
Avian VS model	0.01	0.319	0.19	0.075
Reptile model	0.009	0.334	0.328	0.082

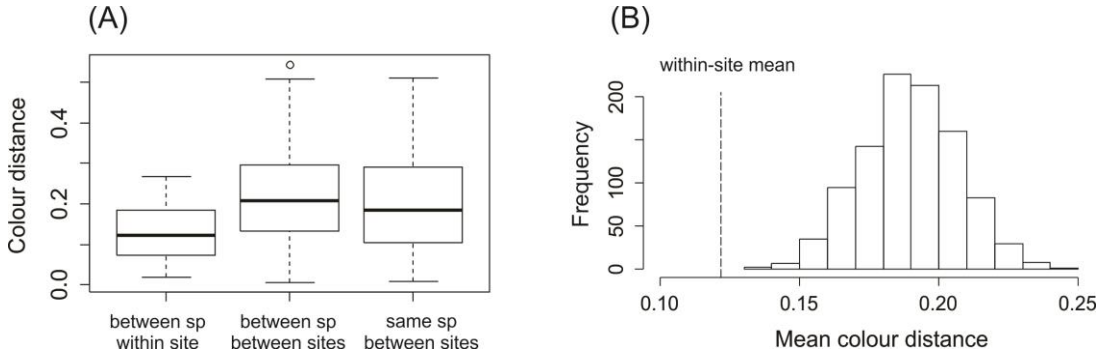

Figure S1: Analysis of the data using an avian VS visual model. (A) Comparison between different sets of distances and (B) the randomization test showing the distribution of random colour-distance means versus the empirical within-site mean (dashed line). Note that the empirical within-site mean distance between species is smaller than expected by a random distribution.

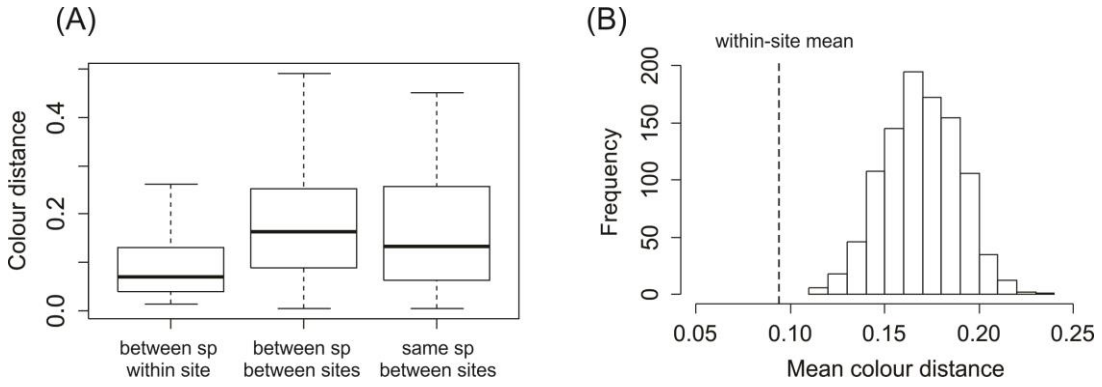

Figure S2: Analysis of the data using a reptilian visual model. (A) Comparison between different sets of distances and (B) the randomization test showing the distribution of random colour-distance means versus the empirical within-site mean (dashed line). Note that the empirical within-site mean distance between species is smaller than expected by a random distribution.

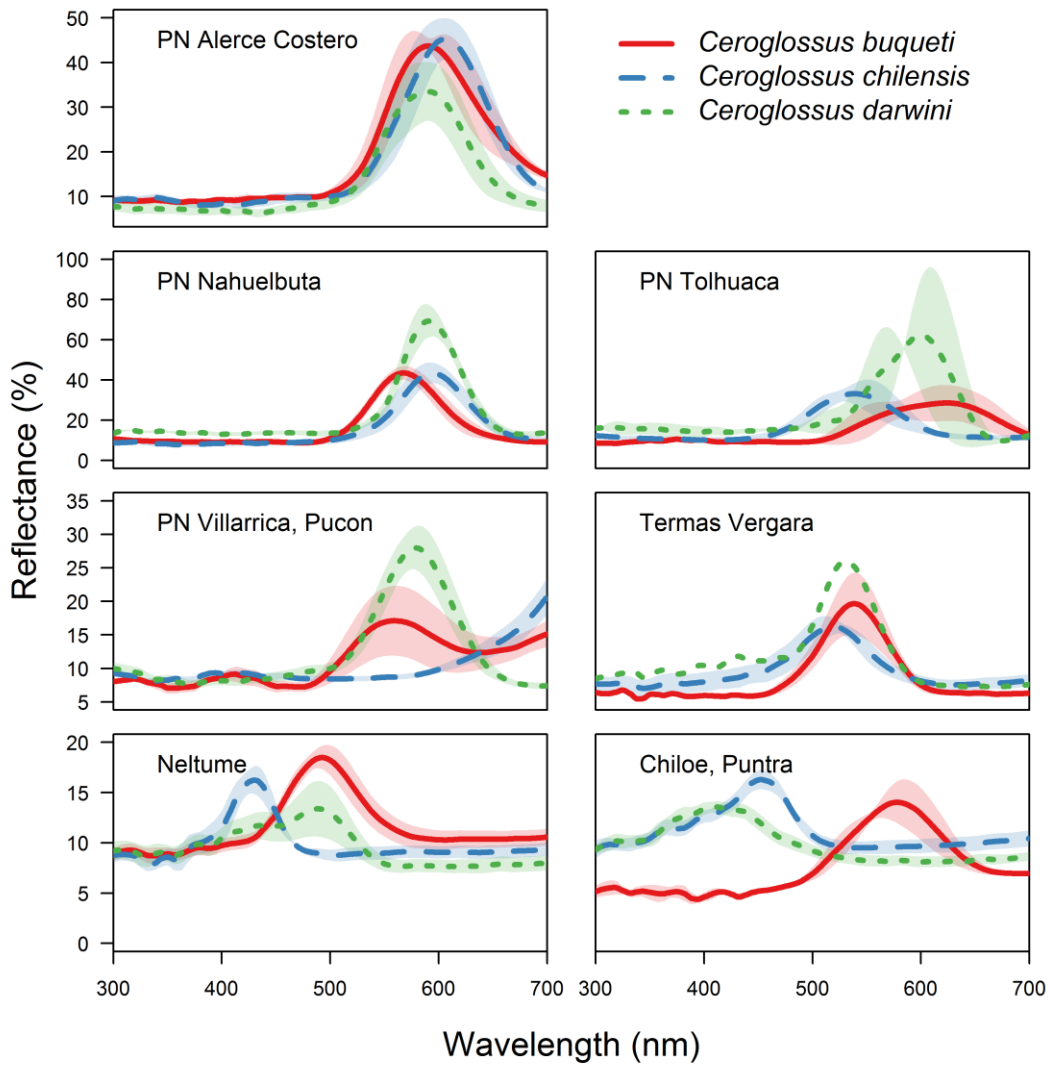

Figure S3: Average spectral curve ± SE (calculated at each wavelength) of *Ceroglossus chilensis*, *C. buqueti*, and *C. darwini*, for seven Chilean localities where all three species are sympatric.

CHAPTER 3: COALESCENT SPECIES DELIMITATION IN MIMETIC BEETLES: ARE COLOR MORPHS DIFFERENT SPECIES? DOES IT MATTER FOR UNDERSTANDING THE EVOLUTION OF MIMICRY?

"*With great power comes great responsibility*" (Benjamin Parker, from: Spiderman, Marvel comics).

3.1 ABSTRACT

Current species delimitation methods provide great power to quantify species diversity. However, some challenges may arise due to the inability of these methods to distinguish population structure from species structure, particularly when combined with the power of large amounts of molecular data. Here we applied a coalescent species delimitation method to a mimetic radiation of ground beetles to i) characterize the diversity within the group, ii) investigate the role of mimicry in the probability of species formation (i.e., do supported lineages correspond to distinct color morphs), and iii) investigate empirically whether the delimited lineages under the multispecies coalescent may be detecting population structure as opposed to species structure. The results showed that species delimitation analyzes supported most color morphs as species. However, the multispecies coalescent also identified several distinct lineages within a single color morph, suggesting that genetic structure, not species structure was detected. Moreover, the degree of mimicry did not predict the probability of

support for delimited lineages, suggesting that mimicry itself might be unrelated with lineage divergence as measured by genetic structure.

3.2 INTRODUCTION

Species delimitation methods using molecular data are growing in application and prominence and have been the focus of considerable research in recent times (Fujita et al. 2012; Camargo and Sites 2013). Among the reasons for the increased interest in using these methods are their objectivity, the increased availability of molecular data, and their ability to delimit species in the presence of incomplete lineage sorting (Fujita et al. 2012). For instance, methods based on the multispecies coalescent model, like the popular BPP (Yang and Rannala 2010), can delimit species that have extremely low divergence times (Zhang et al. 2011). Despite the obvious progress gained with methods that take full advantage of molecular data, they are however, not free of challenges. Paradoxically, the advent of new sequencing technologies that have lower the cost and increased the availability of large datasets may have also opened a new challenge—the increase in statistical power that could detect even the slightest genetic structure raises the question whether we are delimiting species or intraspecific genetic structure (Sukumaran and Knowles 2017). Whether genetic structure is caused by reproductive isolation or intraspecific processes is, therefore, an emerging question (e.g. Hedin et al., 2015) that has passed relatively overlooked.

Blurred boundaries between intraspecific genetic structure versus species have important implications not only for biodiversity assessments, but also for understanding ecological and evolutionary processes that generates biodiversity (Agapow et al. 2004; De Queiroz 2005), with ramifications across multiple fields including macroecology, biogeography, and conservation biology. However, for systems where understanding the evolution of extraordinary levels of polymorphism is the primary aim—as with mimetic systems— accurate delimitation is not only specifically challenging, but

errors with such inferences has a direct impact on interpreting the processes underlying the variation that we seek to understand (Twomey et al. 2014; Merrill et al. 2015; Rabosky et al. 2016).

Mimetic systems are comprised by groups of species that converge phenotypically in response to interactions with shared predators. It is widely recognized that mimetic systems are highly diverse, with species harboring elevated polymorphism and forming geographic mosaics of phenotypic matching (e.g. Joron and Mallet, 1998; Mallet and Joron, 1999; Twomey et al., 2014). Müllerian mimicry in *Heliconius* butterflies have been recently linked with ecological speciation (Jiggins 2008). Here, divergence in color patterns between races, which may result from adapting to different co-mimics or co-mimic's races, has the potential to reduce gene flow due to strong localized frequency-dependent selection (Chouteau et al. 2016a). Gene flow is predicted to be reduced between different color races because migrants and hybrids between races have lower fitness and suffer stronger predation rates; their phenotypes are not recognized as aposematic locally. This form of isolation by adaptation (Nosil and Crespi 2004) could theoretically maintain some degree of population structure (as in a metapopulation), or lead eventually to speciation (Jiggins et al. 2001, 2004; Twomey et al. 2014). Identifying these units as species or populations, however, may have profound impacts on the process that we infer as relevant in the evolution of biodiversity. For example, if species are represented by all geographically localized and phenotypically differentiated groups of individuals, then the proximate mechanism driving the divergence in phenotype across space (e.g., predation pressures), becomes synonymous with drivers of speciation and diversification. That is, any other differences that accumulate are a consequence and not a cause of speciation (Coyne and Orr 2004). On the other hand, if all phenotypically differentiated races are recognized as populations of a single species, understanding the processes underlying the phenotypic matching becomes a study of just one phenomena in a protracted speciation process (Etienne and Rosindell 2012; Dynesius and Jansson 2013; Sukumaran and Knowles 2017). As such, speciation would be less clear and conditional maybe to the presence or absence of

other drivers like assortative mating or geographic isolation. Similarly, mimicry has been considered as an important example of coevolution in which the diversification of one species may drive the simultaneous diversification of co-mimics (see Chapter 4).

Ceroglossus system

The ground beetle genus *Ceroglossus* (Coleoptera: Carabidae) encompasses several conspicuously colored species endemic to the temperate forest of Southern South America that have been recently associated with Müllerian Mimicry (Jiroux 2006; Muñoz-Ramírez and Knowles 2016). Like several other Müllerian mimicry systems (e.g. Chouteau and Angers, 2011; Marek and Bond, 2009; Merrill et al., 2015), *Ceroglossus* species exhibit extensively overlapping distributions and multiple geographic color morphs that tend to match their generic counterparts in several areas across their range (Okamoto et al., 2001; Muñoz-Ramírez & Knowles in prep.). Despite their high phenotypic diversity, only eight species are recognized in recent revisions of the genus (Jiroux 1996, 2006) based on morphological characters (e.g. male genitalia and male antennae). Nonetheless, multiple color morphs have been designated as subspecies (i.e. using mainly color differences as diagnostic character), although neither geographic nor climatic barriers are evident between these aposematic morphs. Mitochondrial DNA has showed support for the morphology-based subdivision of the genus into 4 major groups (Okamoto et al. 2001) and for at least seven out of the eight species currently recognized (Muñoz-Ramírez 2015). However, no further genetic structure within species seems to be associated with differences in color morphs (Okamoto et al. 2001).

Because of this geographically structured, yet lack of consistent phenotypic matching, the genus *Ceroglossus* provides an intriguing system to study species delimitation. The species have been well studied taxonomically, and recent reviews (Jiroux 1996, 2006) have provided detailed information regarding diagnostic characteristics and geographic distribution for most species and color morphs.

There is high intraspecific phenotypic diversity, with each species having a number of color morphs with well-defined distribution ranges—this aspect is particularly convenient because it provides clearly defined units (i.e. taxonomic hypotheses) for testing in species delimitation analyses. Moreover, most color morphs are distributed across relatively homogeneous landscapes, with no obvious geographic barriers separating them (except for a few morphs that are present in islands), minimizing the chance of geographic barriers as a potential mechanism causing abrupt genetic structure between morphs.

Here, we conduct delimitation analyses for three species complex of *Ceroglossus* ground beetles, using hundreds of loci obtained from NGS technologies. However, we also consider how genetic divergence is associated with phenotypic divergence given that difference in colour have been suggested as a potential driver of speciation (Jiggins et al. 2004; Jiggins 2008). Specifically, we investigated whether the color distance among lineages is correlated with the posterior probability of a split between the lineages (i.e., hereafter referred to as the BPP score, which refers to the statistical package BPP used in the delimitation analyses). We also test whether supported species were more often associated to areas with higher degrees of mimicry. A positive correlation for these tests would suggest a possible link between genetic divergence and phenotypic differentiation of color morphs (i.e., a direct role of mimicry in speciation). However, because other factors might also contribute to the formation of genetic distinctiveness – namely, geographic isolation given the regional localization of color morphs, we also conduct two additional tests. To rule out the possibility that undetected isolating barriers could be causing both color and genetic differentiation (i.e. color and genetics may co-vary as a result of drift due to isolation by geographic barriers or habitat fragmentation), we also collected morphological data unrelated to color to test whether morphology also correlated with speciation probability. If drift (not mimicry) were the main cause of genetic differentiation between color morphs, differences in traits other than color can also be expected (e.g. Runemark et al., 2010; Solis-Lemus et al., 2014). In this case, a positive correlation between morphology differentiation and BPP scores would

suggest that color morphs and genetic differences might have evolved as a result of isolation (i.e. otherwise gene flow would have homogenized any differentiation), while a lack of correlation would support isolation by adaptation. Second, as a means for empirically validate that the delimited units correspond to species (as opposed to populations; see Sukumaran and Knowles 2017), we conducted species delimitation analyses within a single color morph (using sampling localities as putative species). With this test, if lineages are delimited, despite similar color across geography, it suggests that other lineages may simply represent population genetic structure and not genetic divergence associated with species boundaries.

3.3 MATERIAL AND METHODS

Specimen and genomic data collection

We collected individuals from 29 subspecies/color morphs belonging to *C. chilensis*, *C. buqueti* and the *C. darwini* species groups (Jiroux 2006), which are co-distributed in southern Chile (see Table 3.1). Specimens were preserved in ethanol and all material deposited in the Museum of Zoology, University of Michigan (UMMZ).

DNA was extracted from legs (usually one leg per individual) using the DNeasy Blood & Tissue Kit (Cat. No. 69581; Qiagen Inc) following the manufacturer's protocol.

A total of 96 *Ceroglossus* individuals were selected to collect RADseq data from localities that would maximize the geographical range and color morph diversity in each species group. For each location, two individuals of each species group were sequenced, with the exception of a couple locations in which we only had a single representative of a species group (Table 3.1). Specifically, 38 individuals from *C. chilensis*, 30 from *C. buqueti*, and 28 from the *C. darwini* species group were sequenced in two genomic library preparations (for details, see Peterson et al. 2012). Briefly, DNA was double-digested

with EcoRI and MseI restriction enzymes, followed by the ligation of Illumina adaptor sequences and unique 10-base-pair barcodes. Ligation products were pooled among samples and size-selected using a Pippin Prep (Sage Science) machine, amplified by iProofTM High-Fidelity DNA Polymerase (BIO-RAD) with 12 cycles. The libraries were sequenced at The Centre for Applied Genomics (Hospital for Sick Children, Toronto, Canada) on the Illumina HiSeq2500 platform to generate 100-bp, single-end reads. Note that to correct for low coverage for one of the species groups (*C. buqueti*) in a first library, which may have occurred due to a small fragment-size selection (i.e., fragments of 180-280 bp), a second library was sequenced with fragments of 350-450 bp. This improved the coverage and number of homologous loci; however, because of problems with the first library or the small genome size of carabids (Sota et al. 2013), the total number of loci was lower than typically expected (e.g., compare with Massatti and Knowles 2014; Prado et al. 2017).

More than 241 million reads were produced from the two lanes of Illumina sequencing (124 and 116 million reads for the first and second libraries, respectively; for details see Table S1 in Appendix). Approximately, 26,250 loci per sample were recovered after bioinformatics processing with an estimated sequencing error rate of $E = 9.7 \times 10^{-4}$. However, because the number of loci shared among individuals was relatively low, we targeted analyses that were not sensitive to missing data. Specifically, we focus on pair-wise population analyses to maximize the number of loci informing each inference. Given that the number of loci varied among analyses, we provide details on the number of loci analyzed below in the context of each of the analyses.

Bioinformatic processing

Sequences were demultiplexed using *process_radtags.pl*, which is distributed as part of the Stacks pipeline (Catchen et al. 2013). Only reads with Phred scores ≥ 32, no adaptor contamination, and unambiguous barcode and restriction cut sites were retained. Demultiplexed reads were processed

using PyRAD v.3.0.5 (Eaton 2014); parameter used in our analyses can be seen in the 'params.txt' files deposited in Dryad (or available upon request). We used a clustering similarity threshold of 0.9 and a minimum cluster depth of 5, excluding clusters with lower coverage. Reads with more than 4 sites with a Phred quality score lower than 20 were also excluded, as were sites at the terminal portion of reads because of an increased frequency in the number of segregating sites that might reflect assembly errors; Fig. S1 in Appendix); the program Fastqc v.0.11.3 (available at <https://github.com/lh3/seqtk>) was used to trim loci, which were then reprocessed (i.e., steps 3 to 7 in pyRAD's protocol), producing loci with a minimum length of 78 bp.

Species delimitation analyses

We conducted Bayesian species delimitation analyses as implemented in BPP (Yang and Rannala 2010), using the color morph (i.e., subspecies designations from Jiroux, 2006) as hypotheses about species boundaries. Although current implementations of the program BPP allows for the joint estimation of the species tree and delimited species, we chose to estimate the species tree that is used as the guide tree in BPP separately (see Yang and Rannala, 2010; Zhang et al., 2014). This strategy may be preferred because of computational demands (e.g. Huang and Knowles 2015; Hotaling et al., 2016), but in this study in particular, it also allows us to reconstruct the guide tree (i.e., the species/population tree; Knowles and Carstens, 2007) with a larger data set than the number of loci used to delimit species because of different constraints on missing data associated with the separate analyses. Specifically, 7889 to 20842 loci across the 29 different color morphs of *C. chilensis*, *C. buqueti*, and *C. darwini* species groups (see Table 3.2) were used to estimate the guide tree for each species group. These analyses were conducted for each species group separately because (i) the focus of the study is on species delimitation and analyzing smaller numbers of putative taxa improves the computational tractability of the BPP analyses and (ii) this also increases the number of loci shared among individuals because of allele drop-

out that occurs with increasing evolutionary distance among individuals in RADseq data due to mutations in the enzyme restriction sites (DaCosta and Sorenson 2016; Eaton et al. 2016; Huang and Lacey Knowles 2016). Datasets used for species tree analyses were generated by including only loci observed in a minimum number of 8 individuals (i.e., at least 4 color morphs were represented at each locus), and included 2 individuals from one of the other species groups as an outgroup, which was selected based on the individuals with the highest number of loci to maximize the likelihood of shared loci with the ingroup.

The population trees used as guide trees in BPP analyses were estimated with SVDQuartets (Chifman and Kubatko 2014), which is available as part of the software PAUP version 4.0 (Swofford 2002). This is a fast species tree method that accounts for both mutational and coalescent stochasticity, scales well with genomic datasets, and allows for missing data (Chifman and Kubatko 2014). In addition to its better performance over concatenated datasets (Chou et al. 2015), for shallow levels of divergence with high levels of incomplete lineage sorting only a species tree analyses provides the appropriate framework for species delimitation because species/populations, not individuals, are the unit of study. SVDQuartets was run using the exhaustive option (it finds all possible quartets) and using the taxon partition option with color morphs as the partitions. Tree inference was conducted with the QFM quartet assembly under the multispecies coalescent model (Chifman and Kubatko 2014), and branch support was assessed by running 200 bootstrap replicates.

Using the guide trees estimated in SVDQuartets (Chifman and Kubatko 2014), BPP analyses were run using a dataset with no missing data (i.e., a subset of the loci used in the SVDQuartets analysis). Specifically, BBP analyses were conducted using 398, 617, and 935 loci in *C. chilensis*, *C. buqueti*, and *C. darwini* species groups, respectively. Analyses were conducted with conservative priors to avoid oversplitting (e.g. Leache and Fujita 2010; Yang and Rannala 2010); specifically, gamma distributed

priors of G(1, 10) and G(2, 2000) were used for estimating the ancestral population size (ϑ) and root age (τ_0) parameters, respectively. Locus-specific rates of evolution were estimated and default settings for parameter tuning and scaling were used in the analyses. The MCMC chains for each analysis were run for 5 x 10^5 generations with parameters sampled every five generations, and a burnin period of 5 x 10^4 generations, using the algorithm option 1 (tuning parameter of 1 and 5) for the reversible-jump MCMC searches (rjMCMC). Five independent runs were run for each delimitation analysis to check for convergence.

To address whether the structure detected from the species delimitation analyses may represent intraspecific genetic structure rather than species divergences (see Sukumaran and Knowles 2017), we conducted a "validation" test in which we conducted a species delimitation analysis on a single, geographically widespread color morph (i.e., subspecies *C. darwini darwini*; Jiroux, 2006), for which samples were available for several sites (Fig. S3). The rationale for this test was that if multiple lineages within a single color morph were identified as putative species (i.e., high posterior probabilities scores), then putative species boundaries inferred between color morphs could likewise be attributable to genetic structure that accumulates among isolated populations (Hey and Pinho 2012). In addition, the robustness of inferred species boundaries to the inclusion of a more distantly related, and recognized species, was explored with a series of BPP analyses including and excluding individuals from the distinct species (two *C. magellanicus boeufi* individuals from locality 11; figure 3.1-C).

Correspondence between genomic structure and color, geographic, and morphological distances

We evaluated the degree to which genetic structure (specifically, the posterior probability of putative species) correlates with color, geographic, and morphological distances. Specifically, separate correlation analyses were conducted for each corresponding variable (i.e., color, geographic, and morphological distances) for data from 9 nodes combined across BPP analyses of species (i.e., combined

data across BPP analyses of *C. chilensis*, *C. buqueti*, and *C. darwini*) using R (R Development Core Team 2013). No color data was available for the color morph in *C. chilensis* corresponding to node 6 (see Fig. 3.2) subspecies *C. chilensis latemarginatus*, and consequently, it was not included in correlations tests of genomic and color distance. Spectral data was collected from beetle's elytra and measured from the same angle (specular near-normal incidence 85°; for details see Muñoz-Ramírez et al. 2015). Posteriorly, the spectral data was projected in a tetrahedral color space (Supplementary figure S1) to represent color differences as they are perceived by a potential avian predator (Andersson and Praguer 2006, Montgomerie 2006). We used the Euclidean distance between the centroid of each color morph in a tridimensional color space coordinates as a measure of color distance between color morphs. A morphological distance between color morphs was calculated using geometric morphometric data collected for the same specimens that color spectral data were collected (Table S1). Using digital images of the ventral side of specimens, 17 landmarks (fig. S2-A) were digitalized using the program TpsDig2 version 2.22 (Rohlf 2013). The raw coordinate data were superimposed (i.e. made invariant to scaling, translation, and rotation) by performing a generalized Procrustes analysis (Rohlf and Slice 1990) taking into account bilateral symmetry. The first two principal components from a principal component analysis (PCA; Supplementary figure S2-B) were retained to calculate a shape distance based on the Euclidean distance between the centroid of color morphs. All geometric morphometric analyses were conducted with the R-package Geomorph (Adams and Otárola-Castillo 2013).

Finally, to evaluate whether color morphs supported as species were more prevalent at sites with the degree of mimicry, we counted how many supported species were found at sites with highest versus lowest degree of mimicry. Specifically, of the 12 sites that contained 2 or 3 co-occurring species, we divided the dataset by the second quartile of the average color distance between co-mimics (i.e., divided the data into one group with higher than the median average color distance between co-mimics, and another group with lower than the median values.(see supplementary figure S4). Color was

measured .. BRIEFLY DESCRIBE …..rather than just saying this: assuming avian visual models (see Muñoz-Ramírez et al. 2016 for more details)

3.4 RESULTS

Guide trees

The population trees estimated for each species were fairly well resolved with many nodes supported by bootstrap values greater than 90 (fig. 3.2), which is strong support given levels of incomplete lineage sorting (Chifman and Kubatko 2014). The only surprising difference with traditional taxonomy occurred within the *C. darwini* species group, where color morph dar5 (subspecies *C. darwini ugartei* in Jiroux 2006) clustered within the clade that forms *C. magellanicus* instead of within *C. darwini* as had been suggested based on genitalia.

The phylogenetic relationships estimated among color morphs show some concordance with geography, with northern and southern populations forming reciprocally monophyletic clades in each species groups (fig. 3.2). However, the geographic extent of the clades was not concordant across species.

Species delimitation among color morphs

For two species, *C. chilensis* and *C. buqueti*, the analyses greatly increased the number of species, as traditional taxonomy had only recognized one species within each of these groups. Within each species group, several, but not all, color morphs were delimited as species. These results were also robust to inclusions to a divergent species (e.g., outgroup), except for *C. darwini* (Fig. 3.3). Assuming the most conservative approach, which involved the inclusion of a more divergent species (i.e. the "outgroup-included" treatment), and considering a BPP score of at least 0.95 as strong support for a lineage split, *C. chilensis* would have at least 9 independent lineages, *C. buqueti* would have 5 independent lineages, and

C. darwini would have 3 independent lineages. Interestingly, the analysis supported for *C. darwini* the same number of independent lineages that are already recognized within this species group based on morphology, although the assignments were different. The main difference is that species *C. darwini* (*sensu stricto*) is merged with *C. speciosus* (node 6, fig. 3.3F; fig. 3.1C), whereas the subspecies *C. darwini ugartei* (dar5 in fig. 3.3F; see also locality 18 in fig. 3.1C) appears supported as a species that splits from *C. magellanicus*. For the other two species group, *C. chilensis* and *C. magellanicus*, the analyses greatly increased the number of species, as traditional taxonomy only recognizes one species in each group.

The comparison between BPP analyses with and without outgroup revealed that the analysis was robust to the inclusion of divergent species, especially at deeper nodes, and suggested several putative species in each group (see Fig. 3.3). For *C. chilensis* (fig. 3.3A), 8 out of 11 nodes showed high support for a speciation event (BPP score > 0.98) despite the inclusion of a divergent species (outgroup), and suggested the existence of 9 putative species (ch1ch2ch4; ch3; ch9; ch5; ch6; ch7ch8; ch10; ch11; ch12; figure 3.3, A and D). The same pattern was observed within the *C. buqueti* group (fig. 3.3B), with 5 out of 7 nodes (nodes 1 to 5) showing high BPP regardless the inclusion or exclusion of an outgroup (BPP> 90). Only 2 nodes (nodes 6 and 7) showed a clear decrease in BPP scores for the treatment including outgroup. Based on these results, the *C. buqueti* group would contain at least 5 species (bu1; bu2; bu3; bu4bu5; bu6bu7bu8; figure 3.3, B and E). In the *C. darwini* species group, nodes 1 and 2 showed high BPP scores regardless the treatment with discrepancies only present at shallower nodes (fig. 3.3C). These results suggest 3 species within the *C. darwini* group (dar1dar2dar3dar4; dar5; dar6dar7dar8; figure 3.3, C and F).

Correlation analyses aimed to test potential explanations for variation in BPP scores showed a lack of significant correlation for most predictor variables, except geographic distance (figure 3.4). Because BPP scores obtained from the outgroup-excluded treatment were generally high and showed

low variability, here we focus on BPP scores obtained from the more conservative approach, the outgroup-included treatment, which showed higher variation across tree nodes. Correlation analyses testing whether geographic distance between populations contributes to increasing BPP scores (as expected if genetic differences between morphs represent intraspecific processes) showed that speciation probabilities were positively and significantly correlated with geographic distance (R^2= 0.73; p= 0.024; figure 3.4A). In contrast, BPP scores were not correlated with either differences in color (R^2= 0. 046; p= 0.91) or differences in body shape (R^2= -0.31; p= 0.41) between morphs.

We also looked at whether support for a speciation event was more or less prevalent for morphs that were associated with areas with a higher degree of mimicry (see supplementary figure S4). We found that within the *C. chilensis* species group, three supported species were found at sites with high degree of mimicry, while three other supported species where found at sites with lower degree of mimicry. Within the *C. buqueti* species group, three supported species were associated with sites with high degree of mimicry, while two other supported species were associated with areas of low degree of mimicry. Finally, within *C. darwini* species group the only color morph supported as a species was associated to a site with high degree of mimicry. These results indicate no evidence for an association between the degree of mimicry and the probability of speciation.

Species delimitation within a single color morph

Species delimitation focusing on a subclade of the *C. darwini* group revealed that BPP was able to split lineages even within a single color morph (i.e. different localities of *C. darwini* ssp. *Darwini*; see figure S5). Within *C. darwini darwini* (a blue color morph represented by 5 site localities in our analysis), we found support for 4 species, with 3 out of 5 localities (sites 25, 28, and 29) highly supported as independent lineages (BPP scores of 1), while the other two populations (sites 19 and 23) were merged as one supported species (BPP score of ~0.71).

3.5 DISCUSSION

For mimetic taxa, given that phenotypic divergence is expected to be structured geographically, and is hypothesized to drive diversification, it may seem that a question like what are species should be relatively clear. However, the complications of mimicry systems make it anything but straightforward. For example, there are systems in which the entire genome except for the loci determining color variants move between putative species boundaries. Or in the beetles studied here, there are conspicuous mismatches in phenotypes among some lineages, that raises the question of how and whether mimicry is actually a cause of lineage divergence. Below we discuss the insights and quandaries mimicry systems raise that are critical to interpreting the role of mimicry is speciation, but also more generally, the application of genetic-based delimitation approaches for inferences about species boundaries.

Do mimics correspond to species boundaries?

Here we studied a group of mimetic species of ground beetles that shows high phenotypic diversity that is geographical structured. This aspect is relevant because by being geographically structured, these phenotypic differences will likely co-vary with genetic differences associated with geographic distance (e.g. IBD). In addition, these beetles are involved in Müllerian mimicry, which assumes that phenotypic differences are likely explained by strong local selection for a given aposematic phenotype (i.e. positive frequency-dependent selection) rather than by a lack of gene flow due to reproductive isolation. All these factors make the question about species limits very challenging and with the increased power genomic data provides to detect genetic patterns, knowing whether we are delimiting species structure or population structure becomes central (Sukumaran & Knowles 2016). This is why it is so important to understand the biological particularities of the system being investigated so results from species delimitation analyses can be properly interpreted.

Our analyses show support for a number of delimited lineages within each taxa that may or may not represent true species because BPP analyses coupled with genomic data has the power to detect genetic differentiation that do not necessarily correspond to species differences, but to population differences (Sukumaran and Knowles 2017). It is worth noting that these results were obtained with a few hundred loci and only two individuals per putative species. Although some of these lineages in *Ceroglossus* may actually correspond to incipient species, it is highly likely that most of the phenotypic variation within taxa represent population structure. First, mimetic radiations are known for harboring high intraspecific phenotypic diversity that is maintained by strong positive frequency-dependent selection (e.g. Mallet and Joron, 1999; Mallet, 2010; Wang and Shaffer, 2008). Although non-significant, our data shows a tendency for BPP scores to correlate with color differences suggesting color may be slowing down gene flow. Unfortunately, the power to test this prediction is low from our data, which would require more populations and individuals from different color morphs. A more detailed analysis using landscape genetic tools should be more appropriate to test this prediction. Second, our data shows a positive correlation between BPP scores and geographic distance, indicating that geographic distance is playing a role on genetic differentiation. This type of genetic pattern is typical of population-level processes—such as isolation by distance produced by dispersal limitation (Wright 1943; Orsini et al. 2013)—and therefore, expected between populations with limited dispersal capabilities such as the flightless beetles *Ceroglossus*. Third, BPP analyses also supported multiple populations within a single color morph—*C. darwini darwini* (dar7)—as independent lineages, even though these populations clearly belong to the same subspecies. These genetic differences are most likely the result of a combination of intraspecific processes like limited dispersal and genetic drift.

This empirical work shows that species delimitation analyses can be sensitive to population structure and agrees with simulations (Sukumaran and Knowles 2017) in that analysis like BPP might over split alpha diversity if not used with caution because it can detect population structure rather than

species structure. *Ceroglossus* beetles have been well studied in regards of their morphology and this has led to a relatively well understood taxonomy based on morphological characters (Jiroux 1996; 2006). Although there is an extraordinary phenotypic diversity within *Ceroglossus* species that has confused early taxonomists (e.g. Germain, 1895; Ruíz, 1931), well-known intraspecific processes can explain these external phenotypic differences. High intraspecific diversity is known to occur in several systems involved in mimicry including butterflies (Merrill et al. 2015), millipedes (Marek and Bond 2009), amphibians (Wang and Shaffer 2008), and birds (Dumbacher and Fleischer 2001), which can be maintained by processes like positive frequency-dependent selection (Mallet and Joron 1999; Chouteau et al. 2016b). As this phenotypic diversity is geographically structured—often occurring in parapatry or allopatry—genetic differences between color morphs can develop through isolation by distance and isolation by adaptation (Orsini et al. 2013). However, the extent to which genetic differences between color morphs can be driven by adaptive divergence remains unknown for *Ceroglossus* as our results only supported the role of geography. This does not necessarily rule out a role of color divergence in driving genetic differences, but it may suggest that at the geographic scale examined in this study, geographic distance plays a dominant role.

Differences when including or excluding a more distant relative

Another aspect of the species delimitation analysis with BPP is that it seems to be sensitive to the addition of more divergent species. Our results showed that at some nodes, particularly at the tips, BPP scores were lower when a subspecies from another species was included in the analysis (the "outgroup-included treatment") relative to the same analysis excluding that species. This suggests that there might be an effect of including more diverged species on how the analysis performs on more recently diverged lineages. A potential explanation for this difference could be related with the change in the proportional time depth of the "ingroup". With a constant value for the root age parameter (θ),

the longer branch length to the root caused by the inclusion of another species makes the relative time depth assigned to the ingroup smaller. Therefore, a shallower divergence between the lineages in the ingroup can increase the uncertainty of estimations and impact on posterior probabilities of the estimates. Although this seems reasonable given that all species showed a lower number of supported lineages when including a color morph from another species (outgroup-included treatment), the fact that the most affected species (*C. darwini*) was the one with smaller increase in total time depth (and consequently proportionally longer branches separating "intraspecific" color morphs) suggest that this explanation might not account for the difference in species support. The sensitivity of the analysis to the addition of another species suggests that this could be an important issue that can affect subsequent inferences that rely on accurate species delimitations. Given the known issue of species over-splitting (Sukumaran & Knowles 2017 and this chapter), the use of the "more conservative" results from the "outgroup-included treatment" seems a reasonable approach to analyze our data; they also provided a wider range of BPP scores for analyses (the results from the outgroup-excluded treatment were all very high and thus low variable). However, the use of the results from the "outgroup-excluded treatment", although more difficult to analyze, would have not affected our general results and conclusions as they would have just prove the point that the analysis provided high support for the slightest genetic structure regardless of its main cause (population or species level processes).

Simulation studies comparing the effect of including species with different divergence times (branch lengths) and, for example, varying the ratio between tip branches length and the total tree depth should increase our understanding of this potential issue. Because our results suggest that BPP detects population structure rather than species structure, it could be advisable to include more divergent species in the analyses if the intention is to take a more conservative approach and avoid over-splitting until new methods accounting for the continuum nature of the speciation process are developed.

Taxonomic implications within Ceroglossus

The high variability of most morphological traits, which has been recognized by early researchers as a problem for their taxonomic study (Germain 1895; Ruíz 1931; Jiroux 2006), makes species delimitation within the genus *Ceroglossus* particularly challenging. This is why additional evidence, such as molecular data, seems essential to aid solving this problem. However, our delimitation analyses (fig s3), including the validation tests, suggest that most of these entities could correspond to intraspecific-level genetic structure, which make decisions about species limits extremely difficult, particularly at very small scale (recently evolved and geographically adjacent tips). Sufficient molecular divergence exists between some areas that may suggest species level differences. Specifically, two major clades within *C. chilensis* (fig. 3.2) are deeply differentiated; a north clade consisting of morphs ch1, ch2, ch3, and ch4 and a south clade consisting of morphs ch6, ch7, ch8, ch10, ch11, and ch12. A third clade consisting of morphs ch5 and ch9 was also differentiated, but the position of this clade was not consistently related to any of the north and south clades as shown by low bootstrap support. These major subclades (north and south) are consistent with mtDNA data published in Okamoto et al. (2001), Muñoz-Ramirez (2015), and Muñoz-Ramirez et al. (2016) and the age for the divergence between these clades was 2.1 Mya based on the molecular rate for the COI gene (see Chapter 4, fig. 3.2 of this dissertation). However, the genitalia do not seem to support a split within this species complex (Jiroux 1996; 2006). A similar situation exists within the *C. darwini* species complex, but here, the two main clades are already recognized as species (*C. magellanicus* and *C. darwini*) based on slight morphological differences in the genitalia and body size (Jiroux 2006). Another species that is also recognized as valid species within the *C. darwini* complex is *C. speciosus*. However, this species was not supported by our species delimitation analysis (figure 3.2C).

Although the coalescent delimitation analyses offer support for several entities within each taxa, our knowledge of the processes underlying their phenotypic diversity and the results of our complementary analyses (fig s3) suggest most of these entities likely correspond to intraspecific-level genetic structure. Therefore, we do not recommend changing the current taxonomic view until more evidence is gathered. We cannot rule out the existence of at least some lineages that may have completed the speciation process and deserve the status of species. However, Additional evidence from ecological, chemical, behavioral data as well as detailed analyses of the genitalia could potentially help disentangling this taxonomic problem.

3.6 CONCLUSION

Understanding the processes underlying important phenomena such as mimicry requires an accurate understanding of species limits. This study demonstrates that coalescent species delimitation analyses have the power to detect fine scale genetic structure. This support for the slightest genetic structure, however, do not distinguish population from species structure as shown by the high support for splits clearly corresponding to population structure within a single color morph in *C. darwini* (figure 3.2). The inability of distinguishing between population and species structure makes species delimitation extremely challenging and misinterpretation of species limits may impact inferences about processes in mimicry. For instance, misidentifying color morphs as species may suggest a role of mimicry and color divergence in speciation, whereas assuming color differences as population-level differences may emphasize the role of processes other than mimicry and color divergence (e.g. geographic barriers) in the process of species formation. Our results also failed to support a role of mimicry in the probability of species formation suggesting that perhaps mimicry do not represent a driver of speciation. We call for careful interpretations of results from species delimitation analyses and suggest that a good

understanding of the potential process driving speciation may not only help interpreting species boundaries, but also a deeper understanding of the processes involved in species formation.

3.6 TABLES

Table 3.1: Sampling of individuals across species for molecular data collection with information about subspecies designations, coordinates, and color-morph coding used in delimitation analyses.

specimen	species	subspecies	ssp code	latitude	longitude
ST_Cc_01	C. chilensis	colchaguensis	ch1	-35.4459	-71.0411
RD_Cc_01	C. chilensis	colchaguensis	ch1	-35.4459	-71.0411
Cc_LQ_01	C. chilensis	fallaciosus	ch3	-35.99	-72.7003
Cc_LQ_02	C. chilensis	fallaciosus	ch3	-35.99	-72.7003
Ret_Cc_02	C. chilensis	cyanicollis	ch2	-36.0908	-71.7834
VB_Cc_01	C. chilensis	cyanicollis	ch2	-36.3922	-71.5429
VB_Cc_02	C. chilensis	cyanicollis	ch2	-36.3922	-71.5429
SF_Cc_01	C. chilensis	cyanicollis	ch2	-36.55	-71.431
Tra_Cc_01	C. chilensis	cyanicollis	ch2	-36.804	-71.6456
Tra_Cc_02	C. chilensis	cyanicollis	ch2	-36.804	-71.6456
Chg_Cc_01	C. chilensis	chilensis	ch4	-36.9355	-73.0011
Chg_Cc_02	C. chilensis	chilensis	ch4	-36.9355	-73.0011
Nah1_Cc_02	C. chilensis	ficheti	ch9	-37.8193	-73.0283
Nah1_Cc_03	C. chilensis	ficheti	ch9	-37.8193	-73.0283
Cc_Ct_01	C. chilensis	latemarginatus	ch5	-38.0128	-73.1874
Cc_Ll_01	C. chilensis	evenoui	ch6	-38.15	-71.2997
Tol1_Cc_01	C. chilensis	gloriosus	ch8	-38.222	-71.7504
Tol1_Cc_03	C. chilensis	gloriosus	ch8	-38.222	-71.7504
Tol2_Cc_01	C. chilensis	gloriosus	ch8	-38.222	-71.7504
Mal3_Cc_01	C. chilensis	seladonicus	ch7	-38.4361	-71.5258
Mal4_Cc_02	C. chilensis	seladonicus	ch7	-38.4658	-71.5193
Cur_Nn_04	C. chilensis	gloriosus	ch8	-38.4682	-71.7164
Mal5_Cc_01	C. chilensis	gloriosus	ch8	-38.471	-71.576
Mal5_Cc_02	C. chilensis	gloriosus	ch8	-38.471	-71.576
Cur_Cc_01	C. chilensis	gloriosus	ch8	-38.5138	-71.5137
Cur_Cc_03	C. chilensis	gloriosus	ch8	-38.5138	-71.5137
Cur_Cc_02	C. chilensis	seladonicus	ch7	-38.5575	-71.4971
Nel_Cc_02	C. chilensis	resplendens	ch10	-39.8511	-71.9256
Nel_Cc_03	C. chilensis	resplendens	ch10	-39.8511	-71.9256
Ale3_Cc_02	C. chilensis	kraatzianus	ch11	-40.1967	-73.4321
Ale4_Cc_08	C. chilensis	kraatzianus	ch11	-40.1967	-73.4321
Cc_Chil2_07	C. chilensis	solieri	ch12	-42.1195	-73.8066
Chil2_Cc_06	C. chilensis	solieri	ch12	-42.1195	-73.8066
Nah3_Cb_01	C. buqueti	deuvei	bu1	-37.8163	-73.0094
Nah3_Cb_03	C. buqueti	deuvei	bu1	-37.8163	-73.0094
Tol2_Cb_01	C. buqueti	cherquencoensis	bu2	-38.222	-71.7504
Tol2_Cb_02	C. buqueti	cherquencoensis	bu2	-38.222	-71.7504

Puc_Cb_01	C. buqueti	subnitens	bu3	-39.3508	-71.968
Puc_Cb_02	C. buqueti	subnitens	bu3	-39.3508	-71.968
Puc_Cb_10	C. buqueti	subnitens	bu3	-39.3508	-71.968
Cb_Nel_04	C. buqueti	andestus	bu4	-39.8511	-71.9256
Cb_Nel_05	C. buqueti	andestus	bu4	-39.8511	-71.9256
Ale3_Cb_01	C. buqueti	buqueti	bu5	-40.1967	-73.4321
Ale3_Cb_02	C. buqueti	buqueti	bu5	-40.1967	-73.4321
Puy_Cb_01	C. buqueti	chiloensis	bu6	-40.6641	-72.172
Puy_Cb_02	C. buqueti	chiloensis	bu6	-40.6641	-72.172
Kat_Cb_04	C. buqueti	chiloensis	bu6	-41.5142	-72.7554
Chil1_Cb_06	C. buqueti	calvus	bu7	-41.882	-73.8799
Chil1_Cb_07	C. buqueti	calvus	bu7	-41.882	-73.8799
Chil2_Cb_01	C. buqueti	sybarita	bu8	-42.1195	-73.8066
Chil2_Cb_02	C. buqueti	sybarita	bu8	-42.1195	-73.8066
Chil3_Cb_04	C. buqueti	chiloensis	bu6	-42.3996	-73.8507
Chil3_Cb_05	C. buqueti	chiloensis	bu6	-42.3996	-73.8507
Chil3_Cb_12	C. buqueti	chiloensis	bu6	-42.3996	-73.8507
Chil4_Cb_01	C. buqueti	sybarita	bu8	-42.6481	-74.0653
Chil4_Cb_05	C. buqueti	sybarita	bu8	-42.6481	-74.0653
Cb_Chai_03	C. buqueti	chiloensis	bu6	-42.9097	-72.7074
Cb_Chai_04	C. buqueti	chiloensis	bu6	-42.9097	-72.7074
Cb_Ay_01	C. buqueti	chiloensis	bu6	-45.6335	-72.9895
Cb_Ay_02	C. buqueti	chiloensis	bu6	-45.6335	-72.9895
Nah3_Cm_04	C. magellanicus	dolhemi	dar1	-37.8163	-73.0094
Nah5_Cm_03	C. magellanicus	dolhemi	dar1	-37.8261	-72.9863
Tol2_Cm_02	C. magellanicus	boeufi	dar2	-38.222	-71.7504
Tol2_Cm_03	C. magellanicus	boeufi	dar2	-38.222	-71.7504
Mal5_Cm_01	C. magellanicus	similis	dar3	-38.471	-71.576
Mal3_Cc_02	C. magellanicus	similis	dar3	-38.4361	-71.5258
Mal4_Cc_03	C. magellanicus	similis	dar3	-38.4658	-71.5193
Puc_Cm_03	C. magellanicus	similis	dar3	-39.3508	-71.968
Puc_Cm_04	C. magellanicus	similis	dar3	-40.6641	-72.172
Tv_Cm_01	C. magellanicus	similis	dar3	-39.5098	-71.8928
Nel_Cm_01	C. magellanicus	caburgansis	dar4	-39.8511	-71.9256
Nel_Cm_02	C. magellanicus	caburgansis	dar4	-39.8511	-71.9256
Ale2_Cd_01	C. magellanicus	ugartei	dar5	-40.1967	-73.4321
Ale4_Cd_07	C. magellanicus	ugartei	dar5	-40.1967	-73.4321
Puy_Cd_05	C. darwini	reedi	dar6	-40.6641	-72.172
Puy_Cd_06	C. darwini	reedi	dar6	-40.6641	-72.172
Kat_Cd_05	C. darwini	darwini	dar7	-41.5142	-72.7554
Kat_Cd_06	C. darwini	darwini	dar7	-41.5142	-72.7554
Chil2_Cd_06	C. darwini	darwini	dar7	-42.1195	-73.8066

Chil2_Cd_07	C. darwini	darwini	dar7	-42.1195	-73.8066
Chil3_Cd_01	C. darwini	darwini	dar7	-42.3996	-73.8507
Chil3_Cd_02	C. darwini	darwini	dar7	-42.3996	-73.8507
Chil6_Cd_01	C. darwini	darwini	dar7	-42.7792	-73.7958
Chil6_Cd_02	C. darwini	darwini	dar7	-42.7792	-73.7958
Cd_Chai_02	C. darwini	darwini	dar7	-42.9097	-72.7074
Cd_Chai_03	C. darwini	darwini	dar7	-42.9097	-72.7074
Chil1_Csp_08	C. speciosus	-	dar8	-41.882	-73.8799
Chil1_Csp_09	C. speciosus	-	dar8	-41.882	-73.8799
Puc_Cc_01	C. chilensis	villarricensis	ch13	-39.3508	-71.968
Puc_Cc_04	C. chilensis	villarricensis	ch13	-39.3508	-71.968
Ret_Cc_05	C. chilensis	cyanicollis	ch2	-36.0908	-71.7834
TV_Cb_02	C. buqueti	andestus	bu4	-39.5098	-71.8928
TV_Cb_03	C. buqueti	andestus	bu4	-39.5098	-71.8928
TV_Cc_01	C. chilensis	resplendens	ch10	-39.5098	-71.8928
TV_Cc_03	C. chilensis	resplendens	ch10	-39.5098	-71.8928
Kat_Cb_05	C. buqueti	chiloensis	bu6	-41.5142	-72.7554

Table 3.2: Data on the degree of mimicry based on color distance between co-mimics and the support for speciation of color morphs at those sites (1= positive support; 0= no support). Sites were ranked from high to low degree of mimicry (i.e. low to high mean color distance) based on the UV visual system. The VS avian system produced a nearly identical rank, except for a few sites and did not impact the counting of supported speciation events at each category of mimicry.

	Mean color distance		Support for speciation			
locality	UV	VS	ch	bu	dar	morphs
Chil1	0.029	0.028	1	0	0	ch12, bu8, dar7
Ale	0.070	0.074	1	1	1	ch11, bu5, dar5
Puy	0.091	0.093	NA	NA	0	dar6
Nel	0.092	0.059	1	1	0	ch10, bu4, dar4
Puc	0.116	0.120	NA	1	NA	bu3
Mal3	0.123	0.135	0	NA	NA	ch7, dar3
Chai	0.127	0.130	NA	0	0	bu6, dar7
Mal5	0.135	0.144	0	NA	0	ch8, dar3
Nah	0.144	0.152	1	1	0	ch9, bu1, dar1
Chil2	0.161	0.164	1	0	0	ch12, bu8, dar7
Tol	0.182	0.169	1	1	0	ch6, bu2, dar2
Kat	0.184	0.167	NA	NA	0	dar7

Table 3.3: Summary on the number of loci per species group used for the species tree analyses and species delimitation analyses.

Taxon	total	polymorphic
BPP analyses		
C. chilensis	412	**398**
C. buqueti	644	617
C. darwini group	974	935
Species tree analyses		
C. chilensis	21782	20842
C. buqueti	8403	7889
C. darwini group	19157	18104

3.7 FIGURES

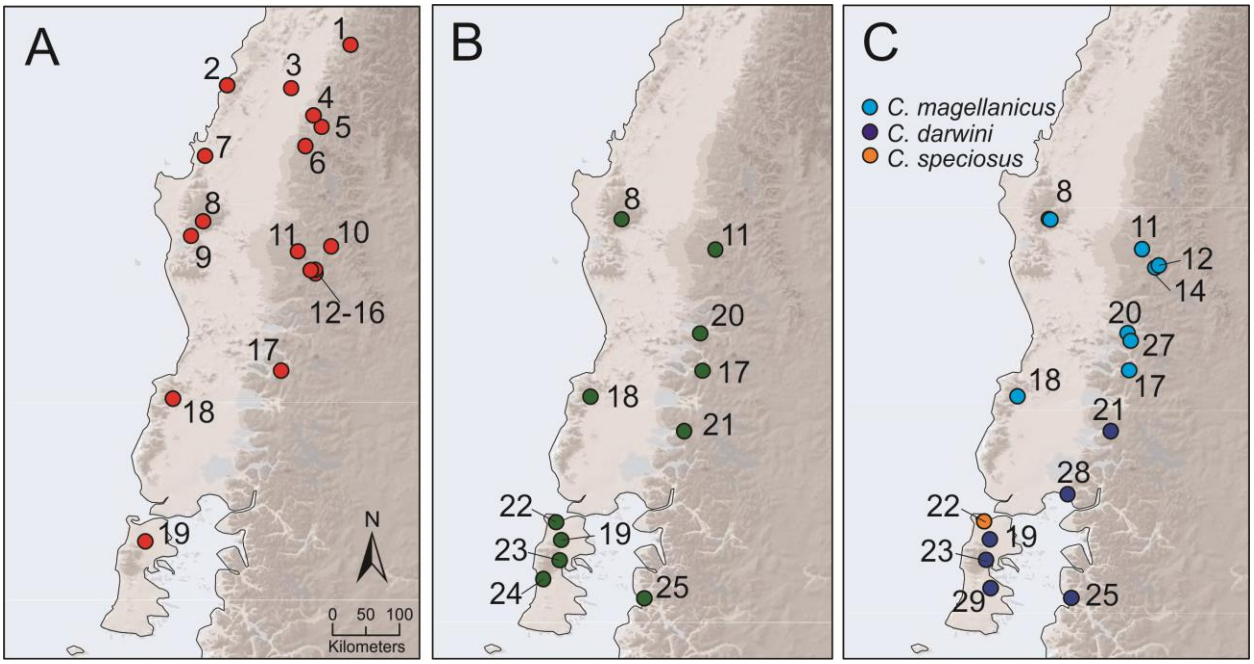

Figure 3.1: Sample sites for three taxa of *Ceroglossus* ground beetles. (A), *C. chilensis*; (B), *C. buqueti*; and (C), the *C. darwini* species group that includes the species *C. magellanicus*, *C. darwini* and *C. speciosus*.

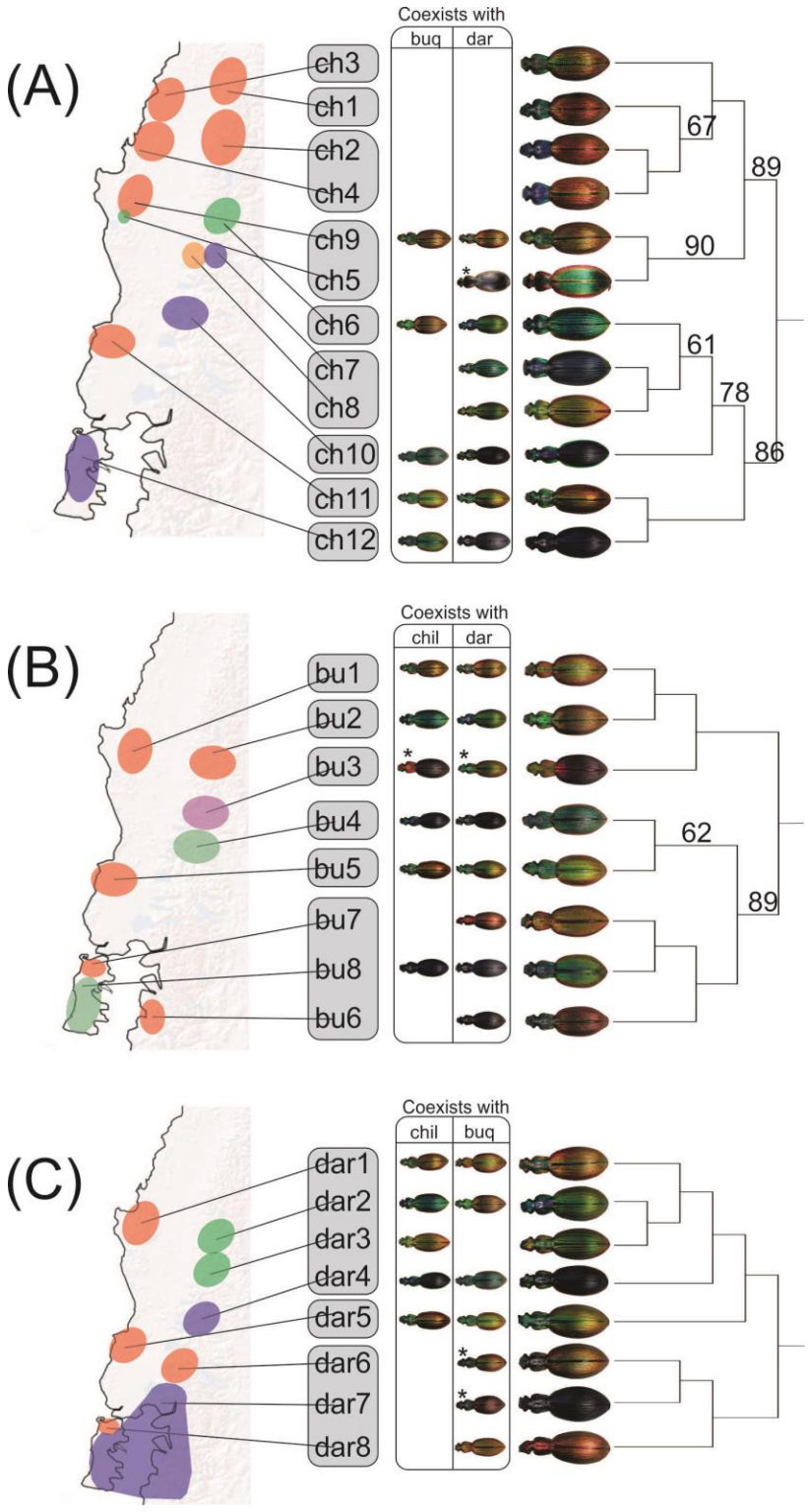

Figure 3.2: Population trees for the three major species groups of *Ceroglossus* analyzed in this study inferred with SVDQuartets (Chifman and Kubatko 2014). (A), *Ceroglossus chilensis*, (B) *Ceroglossus buqueti*, and (C) *Ceroglossus darwini* species group. Bootstrap support below 90 is shown above branches. Bootstrap support above 90 not shown.

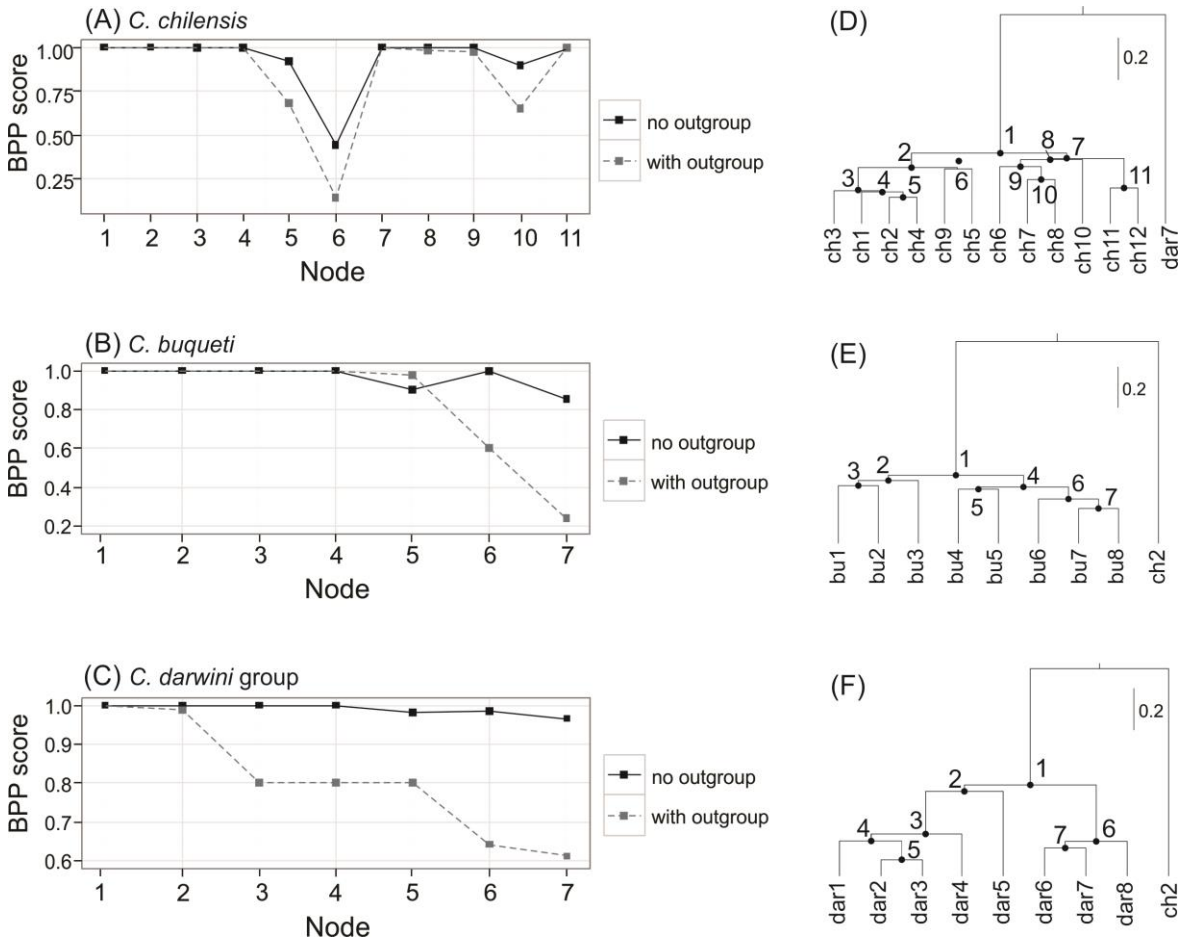

Figure 3.3: BPP scores, with and without outgroup, for all three *Ceroglossus* species groups detailed by node. (A), *Ceroglossus chilensis*. (B), *Ceroglossus buqueti*. (C), *Ceroglossus darwini* species group. (D-F), Species trees showing the position of nodes referenced in A-C for *C. chilensis* (D), *C. buqueti* (E), and *C. darwini* (F), respectively.

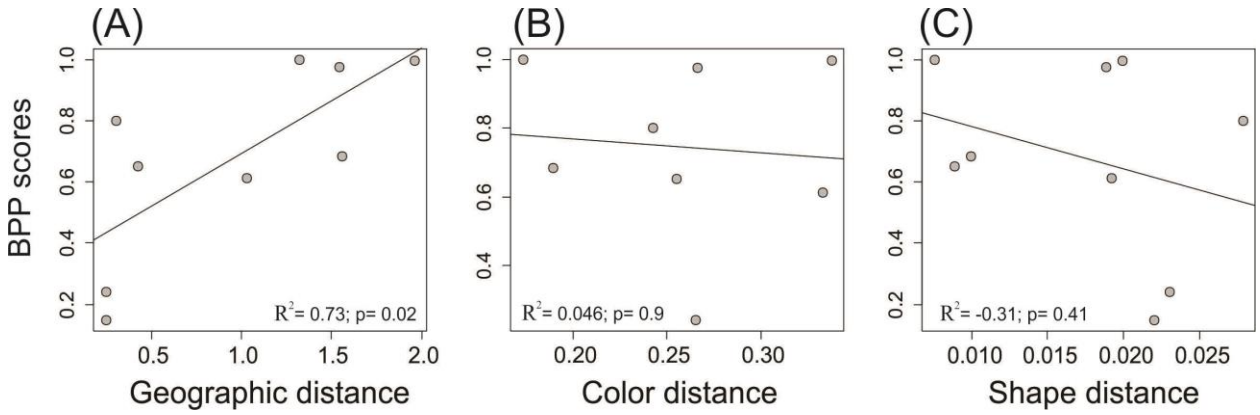

Figure 3.4: Correlation between geographic (A), color (B), and morphology (C) distance versus BPP scores.

3.8 APPENDIX

Table S1: Summary statistics of the data processed in pyRAD. Rows shaded in grey are samples with low number of loci that were discarded for downstream analyses.

species	sample	reads_raw	Nloci	avg_depth_stat	nsites	nhetero	heterozygosity
buq	TV_Cb_03	71363	142	63.098765	12732	181	0.014216
buq	TV_Cb_02	577680	326	129.764069	29284	732	0.024997
buq	Kat_Cb_05	278165	357	32.423154	32040	650	0.020287
buq	Kat_Cb_04	567099	783	40.966738	70246	999	0.014221
buq	Tol2_Cb_02	2854346	23006	28.675301	2068263	10602	0.005126
buq	Nah3_Cb_03	2542010	18743	25.460221	1684195	8810	0.005231
buq	Cb_Ay_02	1580721	9962	18.829544	895026	5003	0.00559
buq	Nah3_Cb_01	699109	4984	19.459598	447677	2601	0.00581
buq	Puy_Cb_01	5194428	26536	33.039832	2385884	15187	0.006365
buq	Puy_Cb_02	9265081	36878	43.416671	3316821	21954	0.006619
buq	Chil4_Cb_05	5355180	34324	63.981347	3087604	21697	0.007027
buq	Cb_Ay_01	1177698	4213	18.525056	378213	2756	0.007287
buq	Chil3_Cb_05	1298484	6779	25.624561	609175	4582	0.007522
buq	Puc_Cb_02	638667	5012	19.24631	450409	3399	0.007546
buq	Chil1_Cb_07	3447492	16428	32.307103	1476239	11199	0.007586
buq	Chil2_Cb_01	1804375	5072	35.608857	455286	3485	0.007655
buq	Puc_Cb_01	2052758	10402	27.55916	934945	7188	0.007688
buq	Cb_Nel_05	3052534	15412	32.882668	1385079	10685	0.007714
buq	Chil3_Cb_12	3094624	21974	27.886986	1975456	15266	0.007728
buq	Chil4_Cb_01	4866606	22147	35.426944	1990744	15420	0.007746
buq	Cb_Nel_04	5191411	24894	31.492345	2238179	17659	0.00789
buq	Ale3_Cb_02	5821235	32182	37.187039	2894893	23371	0.008073
buq	Chil1_Cb_06	1775641	6983	30.220989	627192	5116	0.008157
buq	Chil2_Cb_02	3505730	12825	30.754958	1152122	9434	0.008188
buq	Chil3_Cb_04	2454450	9439	32.311234	848032	7015	0.008272
buq	Ale3_Cb_01	2565621	9112	33.131652	818782	7103	0.008675
buq	Cb_Chai_04	4752870	21936	29.614877	1971786	17210	0.008728
buq	Cb_Chai_03	5206681	30092	29.693999	2706194	24211	0.008947
buq	Puc_Cb_10	778231	2792	31.458816	250736	2308	0.009205
buq	Tol2_Cb_01	869618	10923	21.458487	981524	10244	0.010437
chil	TV_Cc_03	13508	26	166.942857	2329	61	0.026191
chil	Puc_Cc_01	12310	34	67.734694	3061	52	0.016988
chil	TV_Cc_01	24470	39	197.87931	3510	65	0.018519
chil	Puc_Cc_04	19863	81	64.605769	7290	99	0.01358
chil	Chg_Cc_01	263689	950	25.492623	85266	1448	0.016982
chil	Ret_Cc_05	39126	1102	29.529725	99060	105	0.00106
chil	Chil2_Cc_06	4013014	36005	69.80639	3237792	11358	0.003508

chil	Cc_Ll_01	1344269	20296	19.564907	1823728	7543	0.004136
chil	Cc_Chil2_07	562788	5872	63.439377	527072	2974	0.005642
chil	RD_Cc_01	2584910	35312	36.245597	3175836	18133	0.00571
chil	Ale4_Cc_08	2395269	28001	24.859994	2517276	15098	0.005998
chil	ST_Cc_01	3902247	38789	38.223508	3488526	21282	0.006101
chil	Cur_Cc_01	1111115	16508	21.332728	1483217	9094	0.006131
chil	Cc_LQ_02	3313338	37241	46.286184	3349326	20616	0.006155
chil	SF_Cc_01	1418286	21733	26.405595	1953089	12101	0.006196
chil	Cc_LQ_01	4177494	40250	45.609186	3619582	22638	0.006254
chil	Mal3_Cc_01	313394	6608	17.533158	593832	3812	0.006419
chil	Cur_Cc_02	954990	14195	19.739423	1275260	8193	0.006425
chil	Ale3_Cc_02	5442827	68752	38.637726	6183692	39905	0.006453
chil	VB_Cc_02	3192921	38804	33.163975	3488226	23071	0.006614
chil	Cur_Cc_03	1948034	24811	23.922289	2230116	14758	0.006618
chil	Mal4_Cc_02	1689351	25964	28.713261	2334439	15535	0.006655
chil	Nel_Cc_03	802706	10793	39.934526	970008	6485	0.006686
chil	Nel_Cc_02	409641	6120	18.62769	549932	3682	0.006695
chil	VB_Cc_01	4668239	41787	53.778617	3758223	25224	0.006712
chil	Tra_Cc_02	3931458	39977	44.271765	3595293	25163	0.006999
chil	Tra_Cc_01	4060332	40551	45.450507	3647128	25731	0.007055
chil	Chg_Cc_02	4754970	41929	56.492915	3771713	26722	0.007085
chil	Mal5_Cc_02	2427761	33399	23.162597	3002599	21414	0.007132
chil	Mal5_Cc_01	3905768	37675	38.424206	3389002	24306	0.007172
chil	Tol2_Cc_01	1897349	28826	30.888232	2591951	19430	0.007496
chil	Tol1_Cc_03	2616186	32838	38.082239	2953047	22281	0.007545
chil	Cc_Ct_01	2702743	33754	33.715671	3036233	24109	0.00794
chil	Ret_Cc_02	347639	4219	19.953753	378664	3027	0.007994
chil	Nah1_Cc_03	2526803	34499	31.866753	3102899	25498	0.008217
chil	Tol1_Cc_01	281655	3647	17.282344	327518	2729	0.008332
chil	Nah1_Cc_02	2136594	43868	21.293609	3944371	33264	0.008433
chil	Cur_Nn_04	1631410	18410	36.917513	1654352	14403	0.008706
dar	Puy_Cd_06	707146	25139	23.4394	2259977	10820	0.004788
dar	Puy_Cd_05	2349306	38505	56.23676	3463496	16587	0.004789
dar	Chil6_Cd_01	2177725	38402	52.913814	3455001	19653	0.005688
dar	Chil6_Cd_02	575024	22037	22.40087	1981148	11345	0.005726
dar	Kat_Cd_05	367585	17339	14.105454	1557993	9325	0.005985
dar	Cd_Chai_02	2027757	47428	37.430296	4266043	25910	0.006074
dar	Cd_Chai_03	2179044	38420	51.778833	3457012	21021	0.006081
dar	Chil2_Cd_06	81034	2854	12.638729	256329	1568	0.006117
dar	Chil3_Cd_01	1958690	35274	49.294034	3173641	19445	0.006127
dar	Chil3_Cd_02	2074548	37276	50.407814	3353584	20703	0.006173
dar	Kat_Cd_06	732346	25951	22.519889	2333404	14520	0.006223

dar	Chil2_Cd_07	1378769	33979	36.588538	3057030	20138	0.006587
dar	Chil1_Csp_08	2078296	37764	50.993208	3398152	22424	0.006599
dar	Chil1_Csp_09	728595	23505	26.298158	2113185	14064	0.006655
mag	Mal3_Cc_02	3059381	39486	65.113401	3552109	19552	0.005504
mag	Mal5_Cm_01	3363961	41235	71.21026	3709322	21331	0.005751
mag	Tol2_Cm_02	1041502	27338	30.151263	2458543	14247	0.005795
mag	Mal4_Cc_03	159190	5069	18.147165	455468	2664	0.005849
mag	Tol2_Cm_03	1524283	31551	42.494428	2838218	16838	0.005933
mag	Nah5_Cm_03	1226696	30261	31.113756	2721832	18355	0.006744
mag	Nah3_Cm_04	1928997	36113	41.56293	3248873	22083	0.006797
mag	Nel_Cm_01	1118306	29803	31.122102	2680915	19781	0.007378
mag	Nel_Cm_02	267462	7940	19.380785	713718	5327	0.007464
mag	Ale2_Cd_01	141719	4698	18.387538	422151	3155	0.007474
mag	Puc_Cm_03	550801	18588	21.757951	1670669	12889	0.007715
mag	Puc_Cm_04	1494049	33586	34.786787	3022331	23331	0.00772
mag	Tv_Cm_01	145279	4369	13.450813	392360	3170	0.008079
mag	Ale4_Cd_07	1126396	34673	26.929035	3117816	27493	0.008818
	Average	2059815.229	21946.938	38.43721359	38.43721	38.43721359	38.43721359

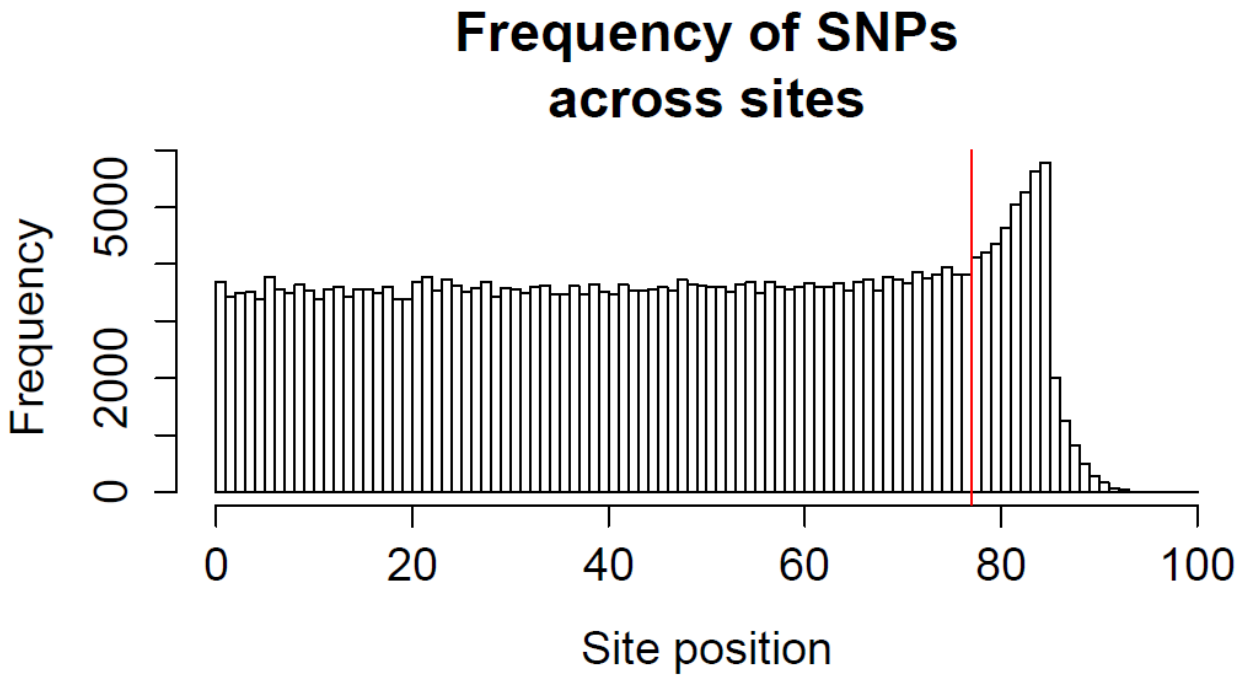

Figure S1: Frequency of SNPs across sequence sites (positions) before trimming.

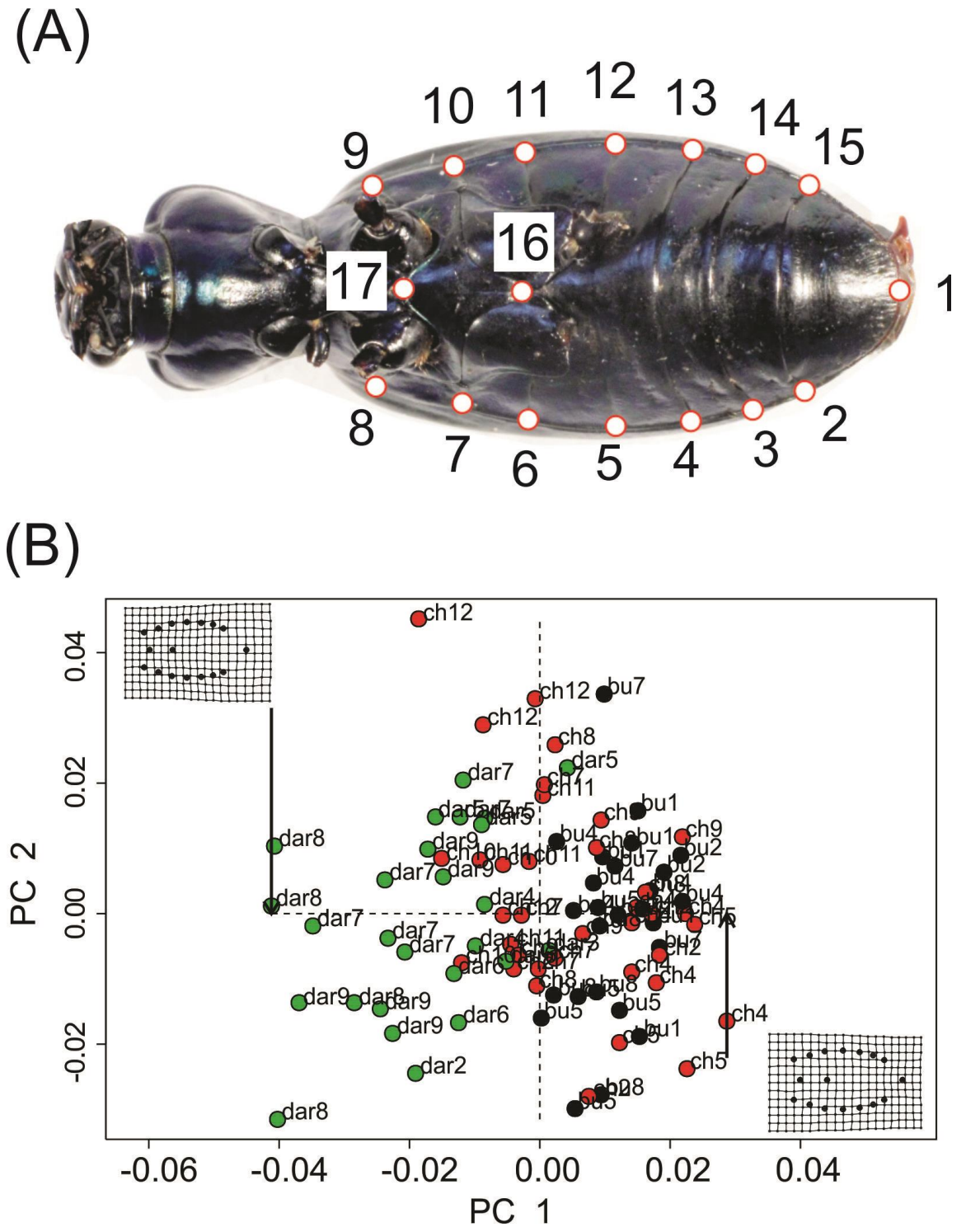

Figure S2: (A) Map of 17 landmarks used for the geometric morphometric analysis. (B) Morphological space represented by principal components 1 and 2 that resulted from the principal component analysis of the geometric morphometric data. Deformation grids are shown at the upper left and bottom right corners. Each dot represents an individual and its color the species group it belongs. Red, *Ceroglossus chilensis*, black, *C. buqueti*, and green, *C. darwini*.

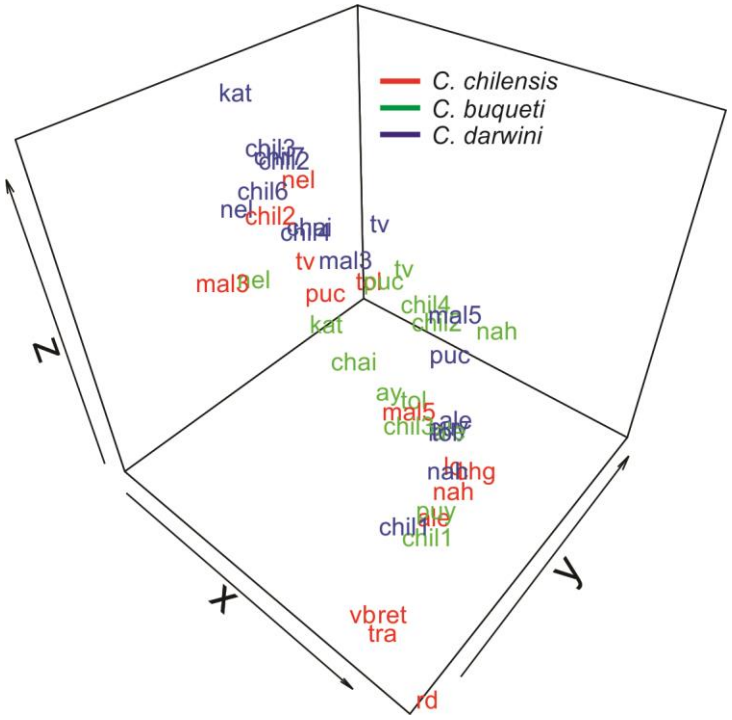

Figure S3: Tridimensional color space for *Ceroglossus* subspecies created from a tetrahedral coordinate system to calculate colour distance between color morphs. Labels match population abreviations and their colour indicates what species group they belong to. Axes correspond to x, y, and z color coordinates from the projected reflectance data (Muñoz-Ramírez et al. 2016).

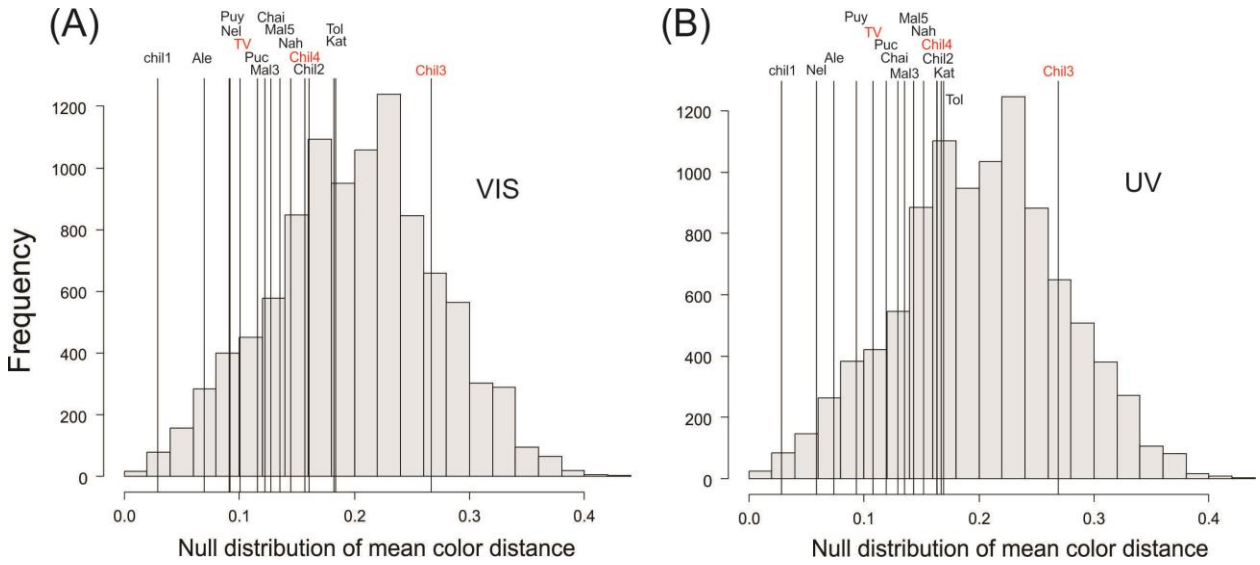

Figure S4: Degree of mimicry for all localities with 2 or 3 co-mimics species based their mean color distance. The histograms represent null distributions of distances among mimics obtained by calculating 10000 mean distances from 3 randomly selected points from a color space. (A) Color distances based on a VIS visual model color space (mean= 0.203). (B) Color distances based on a UV visual model color space (mean= 0.199). Vertical lines indicate observed values for a given site locality (site labels are as those indicated in table 3.1). Red labels show sites with samples that are not represented in the BPP analyses. For details on color data see Muñoz-Ramírez et al. (2016).

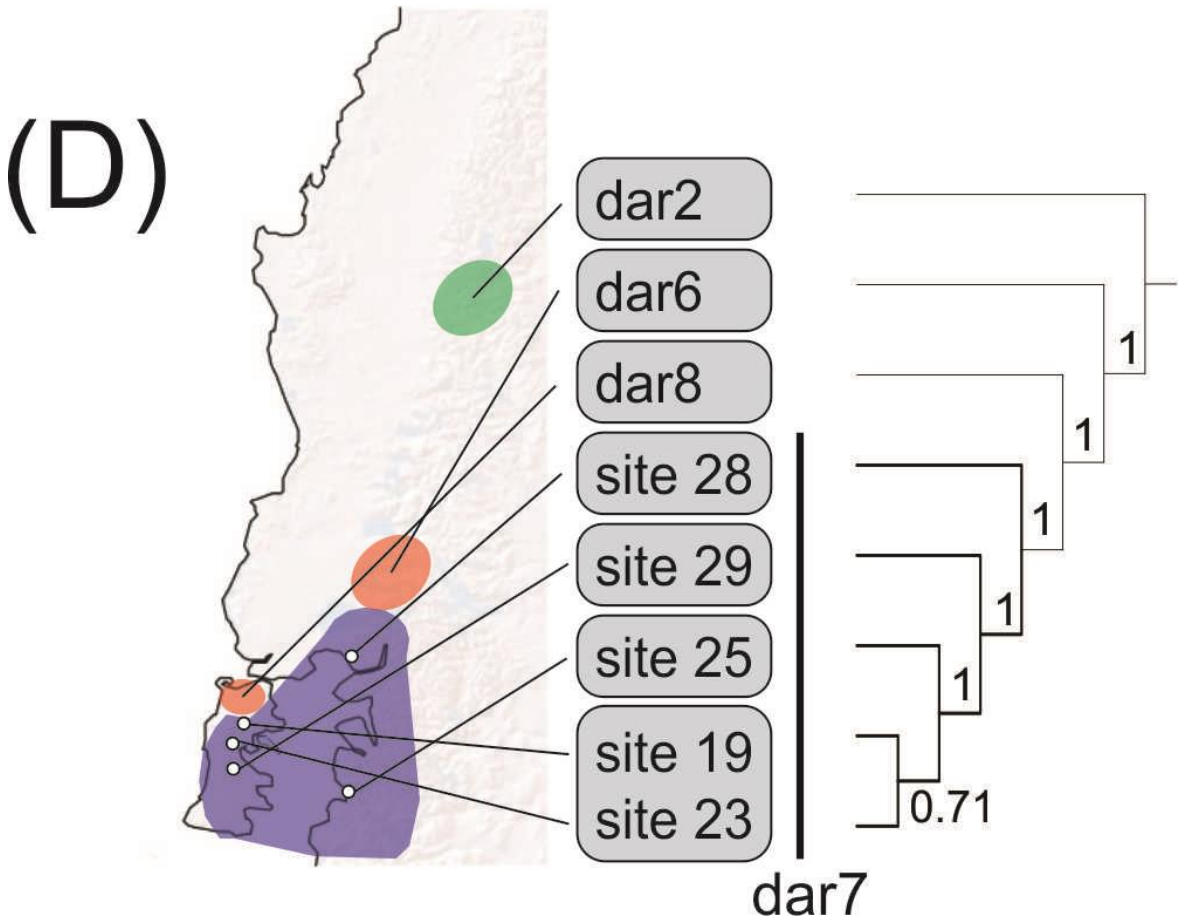

Figure S5: Distribution map species tree for *C. darwini darwini* color morph showing the five sites used for species delimitation analyses with BPP. Color areas correspond to additional morphs within the same species complex used as outgroups. Note that sites 25, 28, and 29 and sites (19 plus 23) were supported as species. Population tree was estimated with SVDQuartets implemented in PAUP (Swofford 2002).

CHAPTER 4: PHYLOGENETIC TESTS OF THE ROLE OF MIMICRY IN THE DIVERSIFICATION OF MIMETIC GROUND BEETLES

4.1 ABSTRACT

Müllerian mimicry has been suggested to provide ideal conditions for coevolution, yet the evidence supporting this idea has been controversial. Here we test this idea with the ground beetle genus *Ceroglossus*, a recently discovered Müllerian system. We used phylogenetic congruence between species as a measurement of co-divergence (which in turn suggest coevolution) and the variation in color match between species (as a measurement of the degree of mimicry) to evaluate the role of mimicry in coevolution. We found high phylogenetic congruence between species which was supported not only by topological congruence, but also temporal congruence. However, we did not find a relationship between the degree of mimicry and the magnitude of phylogenetic congruence. These results suggest that although a pattern of co-divergence was supported, the role of mimicry on the generation of this pattern was not. These findings challenge the classic idea that Müllerian mimicry should promote coevolution and raise the question whether mimicry evolves before or after phenotypic differentiation.

4.2 INTRODUCTION

Müllerian mimetic species have been studied for many decades as a textbook example of natural selection, and the high diversity of color morphs that is often present within species have stimulated the study of the mechanisms explaining and maintaining biodiversity. For example, the well-studied butterfly genus *Heliconius* not only exemplifies the role of selection on phenotypic evolution (Ruxton et al. 2004; Futuyma 2013), but also the debate about general processes explaining the extremely high biodiversity present in the Neotropical region (Knapp and Mallet 2003; Arias et al. 2014). While there is no dispute of the significant contributions studies of mimetic butterflies have made, studying disparate taxa from other regions is still fundamental to understand how general the lessons learnt from such classical systems are (Pfennig 2012).

For example, although Müllerian mimicry is a theory about convergence, mimicry systems are often very diverse, with multiple color races forming mosaics of matching phenotypes across the geographic distribution of co-mimic species (Joron and Mallet 1998; Sherratt 2006; Marek and Bond 2009; Mallet 2010; Wilson et al. 2012). It is not clear how this diversity originates in the first place (Joron and Mallet 1998; Knapp and Mallet 2003; Aubier and Sherratt 2015), but it is thought that once it arises, coevolution between the interacting species might play an important role (Thompson 1989; Cuthill and Charleston 2015). Müllerian mimicry has long been regarded as an important example of mutualism because co-mimic species share the cost of teaching predators about their unpalatability (Mallet 1999; Ruxton et al. 2004). It has been argued that, due to this mutualistic condition, Müllerian mimicry can be an important driver of coevolution (Thompson 1989; Cuthill and Charleston 2015). In *Heliconius* butterflies, for example, phylogenetic and phylogeographic data have recently supported this view as divergence between aposematic races shows strong patterns of co-divergence across co-mimic species (Cuthill and Charleston 2012, 2015). An alternative to coevolution would be the diversification of one species first, followed later by the diversification of the co-mimics to adapt to the phenotypic diversity already established. The later situation should not lead to co-divergence as the diversification of the

younger co-mimic is not constrained to follow the same branching pattern of the model. To understand to what extent any of these hypotheses apply to a mimicry system, well resolved and calibrated phylogenies are essential.

Another conundrum about diversity within Müllerian mimicry systems is that the origin of diversity is difficult to explain (Joron and Mallet 1998; Knapp and Mallet 2003; Aubier and Sherratt 2015), despite mechanisms maintaining diversity once it arises are well understood (e.g., frequency-dependenet selection; Mallet & Barton 1989; Sherratt 2006; Sherratt 2006; Chouteau & Angers 2011). Positive frequency dependent selection is expected to promote homogeneity in an aposematic signal because a common phenotype is favored due to its high abundance, whereas new (and therefore rarer) phenotypes are strongly selected against. How then high regional diversity can be originated in Müllerian mimicry in the first place? Different hypotheses, ranging from population drift to adaptation, have been proposed to initiate the within-species phenotypic diversity characterizing mimicry systems. For example, in *Heliconius* butterflies, one hypothesis centers on the initiation of phenotypic differences during glacial periods as a result of population isolation in multiple forest refugia (Sheppard et al. 1985), whereas other hypotheses invoke adaptation to local environmental conditions unrelated to mimicry (Ruxton *et al.* 2004), or a combination of relaxed natural selection (Benson 1982) and high genetic drift (Mallet 2010).

The ground beetle genus *Ceroglossus* (Coleoptera: Carabidae) provides a good opportunity to independently investigate questions about the evolution of diversity in Müllerian mimicry. The genus *Ceroglossus* contains phenotypically diverse species endemic to the temperate forest of Southern South America. These species exhibit high polymorphism in regards to body coloration and have been recently associated with Müllerian Mimicry (Jiroux 2006; Muñoz-Ramírez and Knowles 2016) due to the covariation of elytral color across co-distributed species. Additionally, species usually exhibit

conspicuous coloration (bright, metallic colors) and possess deterrent chemical defenses produced in abdominal glands (Jiroux 2006). The genus has been subdivided into four major species groups or species complexes, and like in several other Müllerian mimicry systems (e.g. Chouteau and Angers, 2011; Marek and Bond, 2009; Merrill et al., 2015), species groups have extensive overlapping distributions with multiple geographic color morphs matching their generic counterparts in several areas across their overlapping range (Okamoto et al. 2001; Muñoz-Ramírez et al. 2016). However, a unique feature of *Ceroglossus* is that the degree of mimicry varies across areas, with localities harboring species with high or low color matching (Muñoz-Ramírez *et al*. 2016). This characteristic may provide opportunities to assess whether the degree of mimicry can predict patterns of coevolution because low color matching might reflect areas with a lack of a shared evolutionary history and therefore, low phylogenetic congruence between species (Cuthill and Charleston 2015). Molecular phylogenetic analyses with mitochondrial DNA (Okamoto et al. 2001; Muñoz-Ramírez, 2015) have confirmed the monophyly of the four major species groups supporting previous morphological studies (Jirous 1996; 2006). However, internal relationships between color morphs within species groups have not been resolved because pervasive incomplete lineage sorting complicate single-locus phylogenetic reconstructions in recently diverged taxa/populations (Knowles and Carstens 2007b; Huang et al. 2010). In order to understand coevolution patterns within *Ceroglossus*, it is critical to count with resolved within-species phylogenetic trees that can depict population relationships despite the difficulties arising from incomplete lineage sorting.

The temperate areas of South America have a unique biodiversity and diversification history that distinguish them from other areas in the continent as a different biogeographic region (Morrone 2006). Pleistocene glacial cycles are among the most important factors shaping diversity patterns in southern South American forests with important glacier advances covering large areas during glacial periods (Hulton et al. 2002; Sugden et al. 2005) that have impacted the evolution of taxa (Allnutt et al. 1999;

Mathiasen and Premoli 2010; Sérsic et al. 2011). Unlike in tropical areas of South America, the direct impact of glaciers (advances and retreats) in the temperate regions could have had a more influential role in species distributions, and population isolation could have been facilitated by the more fragmented landscape. Thus, the opportunity for phenotypic differentiation between isolated populations could have been, at least in part, facilitated during glacial cycles.

In order to better understand how mimicry has evolved in C*eroglossus* ground beetles, we address the following specific questions, 1) is there evidence of coevolution between co-distributed species of Ceroglossus? and 2) Is the diversification of intraspecific color morphs consistent with an origin within the Pleistocene? Because a reliable investigation of these questions requires robust phylogenetic reconstructions, here we conduct a number of analyses combining coalescent-based phylogenetic methods and different data types. Specifically, we couple the use of thousands of RADSeq loci to estimate robust phylogenetic relationships between intraspecific lineages with a time-calibrated phylogeny from mitochondrial DNA, and spectral color data to test whether the degree of coevolution (if any) is reflective of the degree of mimicry between species.

4.3 MATERIALS AND METHODS

Sampling and DNA extraction

Samples were obtained for all four major species groups within the genus *Ceroglossus* (Jiroux 2006), and which have been widely supported by recent phylogenetics studies (Okamoto 2001; Muñoz-Ramírez 2015; Muñoz-Ramírez et al. 2016). Within each species, samples were chosen to largely represent the species distribution and subspecies diversity (Jiroux 2006). We focus our study on the three species groups or clades that have the largest geographic overlap in South-Central Chile (*C. chilensis*, *C. buqueti*, and the *C. darwini* group), so these groups were represented by a highest number

of individuals. Hereafter, we refer to these three main species complexes as species, and the phenotypic variation within these species as color morphs. The species *C. suturalis*, which geographic distribution extends further south was included only in the mitochondrial DNA (mtDNA) phylogenetic analyses to provide the overall phylogenetic context. Specimens were preserved in Ethanol 100°. All the material is stored at the Museum of Zoology, University of Michigan (UMMZ). Total DNA was extracted from legs using the DNeasy Blood & Tissue Kit (Cat. No. 69581; Qiagen Inc) following the manufacturer's protocol. The only difference with the standard protocol was that we use water, not buffer to store the DNA to improve subsequent RADSeq protocol steps and avoid excessive salt concentration in case DNA needed to be concentrated.

Genomic (RADseq) data acquisition

A total of 96 samples, representing the three main co-mimic species (*C. chilensis*, *C. buqueti* and the *C. darwini* group) were selected for collecting Next Generation Sequencing data via RADSeq (Table S1). Extracted DNA was barcoded for each individual and processed into a reduced-complexity library using a double-digestion, restriction-fragment-based procedure (for details, see Peterson et al., 2012). Briefly, DNA was doubly digested with EcoRI and MseI restriction enzymes, followed by the ligation of Illumina adaptor sequences and unique barcodes. Ligation products were pooled among samples and size-selected for two fragment size ranges: between 180 and 280 (lane 1) and between 350 and 450 (lane 2) base pairs using a Pippin Prep (Sage Science) machine. Each of these two size-selected products was separately amplified by iProofTM High-Fidelity DNA Polymerase (BIO-RAD) with 10 cycles. The products were sequenced in two separate lanes (one per each fragment size product to increase coverage) at The Centre for Applied Genomics (Hospital for Sick Children, Toronto, Canada) on the Illumina HiSeq2500 platform to generate 100-bp, single-end reads. Sequences were demultiplexed, and reads with an average Phred score of at least 20 and an unambiguous barcode and restriction cut site

were retained (raw genomic data available on Dryad: doi:xxxxxxx/dryad.xxxxxx). Sequences were demultiplexed using process_radtags.pl, which is distributed as part of the Stacks pipeline (Catchen et al. 2013). Only reads with Phred scores ≥ 32, no adaptor contamination, and unambiguous barcode and restriction cut sites were retained. Demultiplexed reads from the two lanes were then combined in a single data set and then processed via iPyRAD v.0.4.1 (Eaton 2014). Parameter settings as provided in the 'params.txt' files are available from the author upon request. A clustering similarity threshold of 0.9 and a minimum depth of cluster of 6 for base calling (i.e. clusters with lower coverage were excluded) were used. Reads with more than 4 sites with a Phred quality score lower than 20 were also excluded. We first generated a data set by setting a minimum of 20 individuals per locus (min_samples_locus = 20 in in the param file) for exploratory analyses and quality checking. A plot for the distribution of SNPs across locus positions revealed an unexpected peak approximately between positions 80 and 85 (Fig. S1, Supporting information), which most likely correspond to issues related to gap insertions during the alignment procedure (Deren Eaton pers. com.). Accordingly, we trimmed this portion from all loci in all subsequent data output generated by ipyRAD, by using the trim_overhang parameter. Final datasets consisted of loci with a minimum length of 80 bp. Of the 96 individuals included in the Illumina library, ten individuals were removed due to their low number of reads and loci (figure S2, in the Appendix). We also excluded one additional individual with no precise geographic location. After processing, data had on average 2059815 reads per individual, 21946 loci per individual, and an average depth of 38.4 reads per loci.

mtDNA data acquisition

We used published sequences of *Ceroglossus* (Muñoz-Ramírez 2016; Muñoz-Ramírez *et al*. 2016) along with newly generated ones of the mtDNA COI gene (~680 bp). The newly generated sequences were amplified for all individuals using the universal primers LCO1490 5'-

GGTCAACAAATCATAAAGATATTGG-3' and HCO2198 5'-TAAACTTCAGGGTGACCAAAAAATCA-3' (Folmer *et al*. 1994). Each PCR reaction contained 1µl of extracted DNA, 2 µl of 10x buffer, 1.5µl of MgCl2, 1µl of 10mM dNTPs, 0.4 µl of 1% BSA, 0.8µl of each primer (10µM), 0.06µl of Tag DNA polymerase (Invitrogen, USA), and ddH2O to make a total of 25µl reaction. A standard PCR profile with one-minute duration for each step, a total of 35 cycles, and a final extension of 10 minutes at 72°C was followed. The annealing temperature was 52°C. PCR products were sequenced on an ABI Model 3730 XL sequencer by the Sequencing Core, University of Michigan, USA. Chromatograms were edited in CodonCode Aligner version 3.0.3. and then imported in Bioedit 7.2.5 (Hall *et al*. 2011). Sequences were then aligned using the ClustalW algorithm implemented in Bioedit and checked via amino acid coding in MEGA 6.0 (Tamura *et al*. 2013) to test for unexpected frame shift errors or stop codons. All sequences were deposited in GenBank, with accession numbers KT997732, KT997737, KT997740, KT997744–45, KT997747, KT997750, KT997752–54, KT997760–61, KT997764–65, KT997768, and KT997771–82.

Phylogenetic analyses

Phylogenetic analyses with the RADSeq data: An estimate of the phylogeny based on RADseq loci was obtained using a coalescent-based approach and by concatenation. Specifically, a coalescent species tree method was used to estimate intraspecific relationships within species. The species tree analyses was performed in SVDQuartets (Chifman and Kubatko 2014), which is available as part of the software PAUP version 4.0 (Swofford 2002), that accounts for both mutational and coalescent stochasticity, scales well with genomic datasets, and allows for missing data (Chifman and Kubatko 2014). SVDQuartets was run using the exhaustive option (it finds all possible quartets) and using the taxon partition option with color morphs as the partitions. Tree inference was conducted with the QFM quartet assembly algorithm under the multispecies coalescent model (Chifman and Kubatko 2014), and branch support was assessed by running 200 bootstrap replicates. Three independent runs of SVDquartets were conducted

in the program PAUP* 4.0 (Swofford, 2003) to assess topological convergence, each of which included 200 bootstrap replicates and exhaustive quartet sampling.

A phylogeny was also estimated from a concatenated data set of RADseq loci. Because our test of phylogenetic concordance (see below) requires a tree with branch lengths, the tree was estimated using maximum likelihood (ML) in the program RAxML v.8.1.16 (Stamatakis, 2014) with a GTR + Γ model of nucleotide evolution. Support was assessed by 200 nonparametric bootstrap replicates, followed by a search for the best-scoring maximum likelihood tree.

mtDNA phylogenetic reconstruction and dating: Because mtDNA provides a reasonable means to date phylogenetic analyses as there are several calibrations studies available in the literature, we conduct calibrations using mtDNA data. Sequences from the COI (cox1-A) gene region, obtained by following the protocol described in Muñoz-Ramírez (2015), were used as the molecular marker to infer a calibrated phylogenetic tree using the software BEAST v2.4.4 (Bouckaert et al. 2014). Sequences were first imported into BEAUTi (included as part of the BEAST package) to set model parameters and MCMC settings and then loaded as a XML file into BEAST to conduct the Bayesian phylogenetic analysis. To calibrate our phylogeny, we used a mutation rate of 0.0113 substitutions per site per million year per lineage, following a recent calibration for the COI region in carabid beetles (Andújar et al. 2012). A HKY + G model of sequence evolution, with four gamma categories was set as the substitution model. The strict clock model was selected as the clock model and a coalescent constant population model was selected as the tree prior. MCMC chains were run for a total of 100 million generations sampling every 10 000 generations. Convergence of the MCMC chains was checked in TRACER, ensuring effective sample sizes (ESS) were above 200. After convergence was verified, the trees were summarized as the maximum clade credibility tree in TreeAnnotator v2.4.4 (part of the BEAST package), discarding the first 20% of the trees as burnin.

Test of co-divergence

To investigate whether there is evidence of coevolution between the three main *Ceroglossus* species complexes, we tested for co-divergence patterns by comparing the pattern of intraspecific patristic distances between sites/color morphs across species using the ML tree inferred from the RADSeq data set. For each species pair, we identified all the sites in which both species were present and had phylogenetic data. Then, for each species, we computed all pairwise patristic distance between sites (figure S1 in Appendix shows the tree used to calculate patristic distances). Finally, species were plotted against each other matching their patristic distances for the same pair of sites (each data point represents the patristic distance between a pair of sites shared between species 1 and species 2). To assess how likely a pattern of correlated phylogenetic distances could arise under a scenario of no co-divergence, we implemented an additional test in which we randomized the phylogenetic position of the color morphs to simulate lack of co-divergence. Within each of the three major species groups, we randomized the phylogenetic position and branch lengths of the color morphs and calculated the correlation across taxa based on these random relationships and branch lengths. We repeated this procedure 1000 times to build a null distributions of the correlation coefficient for each pair of species and calculated the probability of obtaining by chance correlation values equal or higher than the observed values. To obtain this probability we simply divided the number of simulated correlation values that were equal or higher than the observed values by the total number of simulated values (n= 1000).

Because *Ceroglossus* beetles exhibit varying degrees of mimicry across areas (i.e. areas with high and low color matching between species), we also investigated whether there is a role for the degree of mimicry on the strength of co-divergence in *Ceroglossus*. For this purpose, we assessed whether the fit of the phylogenetic congruence between species varied as a function of the degree of mimicry. For each species pair, we tested the correlation between the residuals of the linear regression between species's

patristic distances and the color similarity between species. A positive correlation between the residuals and color similarity would provide evidence that mimicry plays a positive role on the generation of phylogenetic congruence between species. Color similarity was estimated as the mean color distance between species within localities using color data published in Munoz-Ramirez et al. (2016). Patristic distances were computed using the function *fastDist* from the R-package *phytools* (Revell 2012), whereas the Pearson's correlation test, as implemented in R (R Development Core Team 2013), was used to assess the statistical significance of correlations.

4.4 RESULTS

RADSeq and species tree

The ML and SVDQuartets species tree analyses of the RADSeq dataset produced consistent results. The three species groups included in the study were recovered as reciprocally monophyletic with high bootstrap support for most internal clades (figure 4.2A and 4.2B). Each main clade representing species groups contained subclades dividing north and south populations or subspecies. Within the *C. chilensis* species group, the north subclade encompassed four subspecies *C. c. fallaciosus*, *C. c. colchahuensis*, *C. c. chilensis*, and *C. c. cyanicollis*. The south clade grouped eight subspecies, *C. c. evenoui*, *C. c. selandonicus*, *C. c. gloriossus*, *C. c. resplendens*, *C. c. kratzianus*, and *C. c. solieri*. The phylogenetic position of two other subspecies, *C. c. ficheti* and *C. c. latemarginatus*, was not consistent across the ML and the SVDQuartet species tree as they appeared more closely related to the north subclade in the ML tree, while for the SVDQuartet tree, they appeared more closely related to the south subclade . The ML reconstruction confirms the conflictive position of these subspecies as they cluster closer to the north subclade in this tree. The *C. buqueti* species group also divided into a north and a south subclade. The north subclade contained subspecies *C. b. deuvei*, *C. b. cherquencoensis*, and *C. b.*

subnitens, whereas the south subclade contained *C. b. andestus*, *C. b. buqueti*, *C. b. calvus*, *C. b. sybarita*, and *C. b. chiloensis*. The *C. darwini* species group was divided into two main subclades in general agreement with previously described species. A north subclade matched the species *C. magellanicus* and grouped the subspecies *C. m. dolhemi*, *C. m. boeufi*, *C. m. similis*, *C. m. caburgansis*, and *C. d. ugartei*, while a south clade matched the species *C. darwini* including the subspecies *C. d. reedi*, *C. d. darwini*, and the species *C. speciosus* as the sister of the other two. Similarly to the *C. chilensis* group, there was one lineage, represented by the subspecies *C. d. ugartei*, whose grouping within the north clade was not highly supported. Its inclusion within the north group (*C. magellanicus s.s.*) had only moderate bootstrap support in the SVDQuartet species tree, whereas it appeared more closely related to the south clade in the ML tree.

mtDNA tree

The calibrated Bayesian tree recovered all four species groups (*C. chilensis*, *C. buqueti*, *C. darwini*, and *C. suturalis*) as monophyletic with high Bayesian posterior probabilities. In general, all species groups except *C. suturalis*, exhibited some degree of overlap in their timing of origin. The *C. darwini* species group showed the oldest time of origin with a mean time to the MRCA of 4.13 Mya (95% HPD interval: 2.75 Mya – 5.58 Mya). The MRCA of the *C. chilensis* species group dates back to 2.64 Mya (95% HPD interval: 1.87 Mya – 3.46 Mya), while the MRCA of *C. buqueti* originated 3.1 Mya (95% HPD interval: 2.25 Mya – 4.06 Mya). The *Ceroglossus suturalis* species group was the most recently evolved lineage with an age of 2.2 My (95% HPD interval: 1.35 Mya – 2.75 Mya). The MRCA of all four species dated to 9.5 Mya (95% HPD interval: 7.1 Mya – 12.1 Mya) placing the origin of the current species in the Middle Miocene.

Results from the test of co-divergence

We found statistically significant correlations between the phylogenetic histories of all three species pairs as indicated by our co-divergence test (Table 4.2 and figure 4.3). The highest correlation was found between *C. chilensis* and *C. darwini*. Correlations between *C. chilensis* and *C. buqueti* and between *C. buqueti* and *C. darwini* were similarly high and nearly as high as that of *C. chilensis* and *C. darwini*. The results were also significant when compared to simulations under a model of no co-divergence (Figure S2). Based on this analysis, the probability that a high correlation between species can arise under a scenario of no co-divergence was p= 0.013 for the species pair of *C. chilensis* and *C. buqueti*, p= 0.004 for the species pair of *C. buqueti* and *C. darwini*, and p= 0.001 for the species pair of *C. buqueti* and *C. darwini*.

The test of the role of mimicry on co-divergence, which consisted on correlations between the residuals of the phylogenetic congruence test and the degree of mimicry (color matching) between species, yielded no-significant results for all species comparisons (see Table 4.2), suggesting species co-divergence patterns were not affected by the degree of mimicry.

4.5 DISCUSSION

Codivergence but not coevolution among mimics

Knowing whether coevolution played a role on the diversification of a Müllerian radiation is important because it shed lights on how diversity can evolve in Müllerian mimicry. The results of this study broadly agree with a history of co-divergence among species of the mimetic ground beetle genus *Ceroglossus*. First, results show high phylogenetic congruence among species and second, the time-calibrated phylogeny is consistent with temporal congruence. These results may suggest a role of mimicry on coevolution. However, our test of the role of mimicry on codivergence (i.e. correlation test between phylogenetic residuals versus degree of color matching; Table 4.2) showed that the variation in the degree of mimicry was not correlated with the degree of phylogenetic congruence suggesting that,

despite the positive evidence for co-divergence, mimicry might not be implicated in coevolution. This challenges previous suggestions that Müllerian mimicry causes coevolution, and provides room for questioning whether mimicry evolves before or after speciation/race formation.

The hypothesis of coevolution in mimicry systems has been controversial (Mallet 1999; Sherratt 2008). Although Müllerian mimicry may provide excellent conditions for coevolution (Gilbert 1983; Joron and Mallet 1998; Futuyma 2013), the evidence for this association has been elusive. For example, when analyzing the evidence from one of the most studied Müllerian systems, the *Heliconius* butterflies, is not until recently that coevolution has gained support. At first, evidence coming from the analysis of phylogenetic information and few loci did not support the idea of coevolution (e.g. Brower 1996; Mallet *et al.* 1996; Flanagan *et al.* 2004). However, the accumulation of additional data and more powerful phylogenetic analyses have provided new evidence that agrees with a history of coevolution (Hines et al. 2011; Cuthill and Charleston 2012, 2015). Under the coevolution hypothesis, diversity evolves as a direct consequence of species interactions. For example, if some mechanism facilitated the divergence of the ancestral population of a mimic species into two color morphs, the other mimic would be under a selective pressure to diversify as well in order to adapt to the newly formed morphs. This process can repeat several times with any of the two species diversifying first and triggering the differentiation of the other, producing a high diversity of intraspecific color morphs in both species matching each other and forming a mimetic mosaic. In other words, the evolution of the diversity we see today is the result of reciprocal evolutionary change and therefore, it requires close ecological interaction of species. On the other hand, under the hypothesis of no coevolution, evolution of diversity would be unrelated to reciprocal evolutionary change. This implies that the evolution of diversity in at least one of the co-mimics (the "model") might not have evolved as a response of adaptation for mimicry, suggesting that other mechanisms might be necessary to generate an initial amount of diversity to serve as a template for the co-mimic (i.e. it could evolve by habitat fragmentation with no gene flow between fragments).

Regardless of the actual mechanisms causing diversity, under this scenario localized color match between species could evolve once polymorphism is already present, perhaps, by filtering of color morphs. In other words, existing polymorphism might be sorted in such a way that interspecific morphs that match are preserved due to improved fitness for all the species involved. This is not to say that mimicry is not involved in the process, but its role would not be associated to the promotion of the polymorphism, but solely on the preservation of a pattern of color covariation among species complexes. This alternative hypothesis, therefore, emphasize Mimicry as a consequence of rather than a cause for diversity in mimetic systems.

The species analyzed here have a relatively high degree of overlap in geographic range, although one species, *C. chilensis*, extends further north into areas where other *Ceroglossus* species are rare of absent (fig. 4.1; Jiroux 2006). It is interesting to notice that in the range where *C. chilensis* is the only species found, body coloration does not vary as much as within the range where it overlaps with the other species (Figure 4.1, Chapter 2). Although we did not evaluate this aspect, this lack of color variation in allopatry may suggest that species interactions between *Ceroglossus'* species are important for color diversification. In other Müllerian systems, color pattern variation within species strongly correlates between co-mimics (Brower 1994; Marek and Bond 2009) suggesting that species interactions play a role on color variation. However, some aposematic taxa can also be phenotypically diverse even in the absence of co-mimics (Brown et al. 2010), suggesting that species interactions and mimicry might not be the only mechanisms involved in color variation. Processes like strong genetic drift and a relaxation of selective pressures, population isolation, and local adaptation not related to mimicry have been suggested as potential mechanisms to explain diversity in aposematic species (Mallet 2010).

A reasonable prediction that can be made if we assume that mimicry is an important driver of coevolution is that phylogenetic congruence should be higher when the degree of mimicry is higher. The

geographic variation in the degree of mimicry in *Ceroglossus* comes handy to test this prediction. We did not find differences in phylogenetic congruence between species in regards to the degree of mimicry. In other words, areas with lower degree of mimicry exhibited similarly high degrees of phylogenetic congruence than areas with high degree of mimicry (Table 4.2). This result may open room for other mechanisms as drivers of the phylogenetic congruence between *Ceroglossus* species. For example, general phylogeographic structure is commonly found between non-mimetic co-distributed taxa in comparative phylogeographic analysis (Avise 1992; Hickerson et al. 2010; Satler and Carstens 2016). A long history of co-distribution and exposure to common past events (e.g. barriers, glaciations) can affect the phylogeographic or phylogenetic structure of taxa similarly, especially if the taxa exhibit similarities in some biological traits like dispersal capabilities, or physiological tolerance (Papadopoulou and Knowles 2016). Therefore, our results challenge the common view that mimicry promotes diversification and suggest that other potential mechanism might explain co-divergence.

Origin of color diversity

Although the mechanisms that maintain regional color polymorphism in Müllerian mimicry systems are well understood (Sherratt 2006; Aubier and Sherratt 2015; Aubier et al. 2017b), there is still debate on what processes originate the polymorphism in the first place (Mallet et al. 1996; Mallet 2010). The hypotheses, that have been suggested motivated on studies on butterflies, are i) population isolation during glaciations (Sheppard et al. 1985), ii) local adaptation not related to mimicry (Ruxton et al. 2004), and iii) genetic drift under conditions of low predation pressures (Mallet 2010). Our data does not currently allow a formal test of these hypotheses in *Ceroglossus*, but suggest the plausibility of the Pleistocene isolation hypothesis. Our calibrated phylogeny indicates that most branching events within species groups occurred during the Pleistocene (2.6 Mya to 11 Kya). The south of Chile was heavily impacted by the glacial cycles during this period and great extensions of land were covered by ice

(Hulton et al. 2002; Sugden et al. 2005). Although several studies have shown results consistent with extensive areas of complete biotic exclusion (Victoriano et al. 2008; Nuñez et al. 2010; Muñoz-Ramírez et al. 2014), some have suggested that cryptic refugia were plausible (e.g. Xu *et al.* 2009; Vera-Escalona *et al.* 2012). In addition, evidence suggest that the temperate forest could have been highly fragmented in areas that were close to the margins of the glacial ice sheet (Victoriano et al. 2008) and even further away due to the increase in aridity during this period (Armesto et al. 1994; Villagrán and Armesto 2005). Our phylogenetic analyses show signals of glacial impact in the branching pattern of *Ceroglossus*. For instance, there is a tendency of shorter branch lengths between southern populations in all species groups, in agreement with a higher glacial impact at higher latitudes. Although these evidences do not prove that the origin of regional polymorphism in *Ceroglossus* was due to the Pleistocene isolation hypothesis, they do suggest that the conditions required under this hypothesis were all in place.

4.6 CONCLUSIONS

Mimicry systems are excellent models for the study of diversity and their drivers. In this study we have found that mimetic species of *Ceroglossus* show significant patterns of co-divergence, but we did not find evidence of a role of mimicry underlying this pattern. This finding has important implications for understanding the evolution of mimicry and its role on biodiversity. Our results are consistent with co-divergence patterns found in the classic *Heliconius* study system in that there was phylogenetic and temporal congruence between species, suggesting that patterns of co-divergence can be a more general characteristic of mimicry systems. However, the lack of correlation between phylogenetic congruence and degree of color matching (degree of mimicry) suggests that other processes, not mimicry, could be driving co-divergence patterns in *Ceroglossus*. Taken together, the implication is that Müllerian mimicry may not necessarily be a promoter, but rather a consequence of polymorphism.

4.7 TABLES

Table 4.1: Localities where molecular data were collected and its distribution across the main species groups, *Ceroglossus chilensis* (ch), *C. buqueti* (bu), *C. darwini* (da), and *C. suturalis* (su).

Site	Latitude	Longitude	RADSeq			MtDNA			
			ch	bu	da	ch	bu	da	su
Radal	-35.4459	-71.0411	x			x			
Los Queules	-35.9900	-72.7003	x			x			
Retiro	-36.0908	-71.7834	x			x			
Villa Babiera	-36.3922	-71.5429	x						
San Fabian	-36.5500	-71.4310	x			x			
Las Trancas	-36.8040	-71.6456	x			x			
Chiguayante	-36.9355	-73.0011	x			x			
San Pedro	-36.8994	-73.1245				x			
Nahuelbuta	-37.8193	-73.0283	x	x	x	x	x	x	
Contulmo	-38.0128	-73.1874	x			x		x	
Llacolen	-38.1500	-71.2997	x			x			
Tirua	-38.3783	-73.5044				x			
Tolhuaca1	-38.2220	-71.7504	x			x			
Tolhuaca2	-38.2220	-71.7504	x	x	x	x	x	x	
Malalcahuello Bajo	-38.4361	-71.5258	x		x	x			
Malalcahuello Bajo	-38.4658	-71.5193	x			x			
Manzanares	-38.4682	-71.7164	x			x			
Malalcahuello Alto	-38.4710	-71.5760	x		x	x		x	
Tunel Las Raices (North)	-38.5138	-71.5137	x			x			
Caleta Queule	-39.4653	-72.9956				x		x	
Tunel Las Raices (South)	-38.55751	-71.4971	x			x			
Caburga	-39.0589	-71.6894						x	
Pucon	-39.3508	-71.9680	x	x	x	x	x	x	
Termas Vergara	-39.5098	-71.8928	x	x	x			x	
Neltume	-39.8511	-71.9256	x	x	x	x	x	x	
Mafil	-39.7029	-72.9185							x
PN Alerce Costero	-40.1967	-73.4321	x	x	x	x	x	x	x
PN Puyehue	-40.6641	-72.1720	x	x	x		x	x	
Huerquehue	-39.1386	-71.6664					x		
Katalapi	-41.5142	-72.7554		x	x		x	x	
Chiloe 1	-41.8820	-73.8799		x	x		x	x	
Chiloe 2	-42.1195	-73.8066	x	x	x	x	x	x	
Chiloe 3	-42.3996	-73.8507		x	x		x	x	
Chiloe 4	-42.6481	-74.0653		x			x	x	x
Chiloe 5	-42.6216	-74.1077							x

Chiloe 6	-42.7792	-73.7958		x			x	
Chaiten	-42.9097	-72.7074	x	x		x	x	
Aysen (AyRM)	-45.6335	-72.9895	x			x		x
RN Coyhaique	-45.5320	-71.8400						x
Nahuelbuta	-37.8163	-73.0094						

Table 4.2: Results from the correlation test between the patristic distances of different *Ceroglossus* species. In addition to a general correlation test with all the data for each pair of species (all comparisions), the same correlation test was conducted for the 50% of the data with higher similarity (lower mean color distance between species) and 50% of the data with lower similarity (higher mean color distance between species).

		Sp1 vs Sp2		residuals(sp1~sp2) vs mimicry match		residuals(sp2~sp1) vs mimicry match	
Species 1	Species 2	R2	P-value	R2	P-value	R2	P-value
C. chilensis	C. buqueti	0.6498	0.0049	0.1954	0.2008	0.0006	0.9487
C. chilensis	C. darwini	0.7809	0.0000	0.0551	0.3059	0.0019	0.8496
C. buqueti	C. darwini	0.6436	0.0000	0.0000	0.9769	0.0001	0.9559

4.8 FIGURES

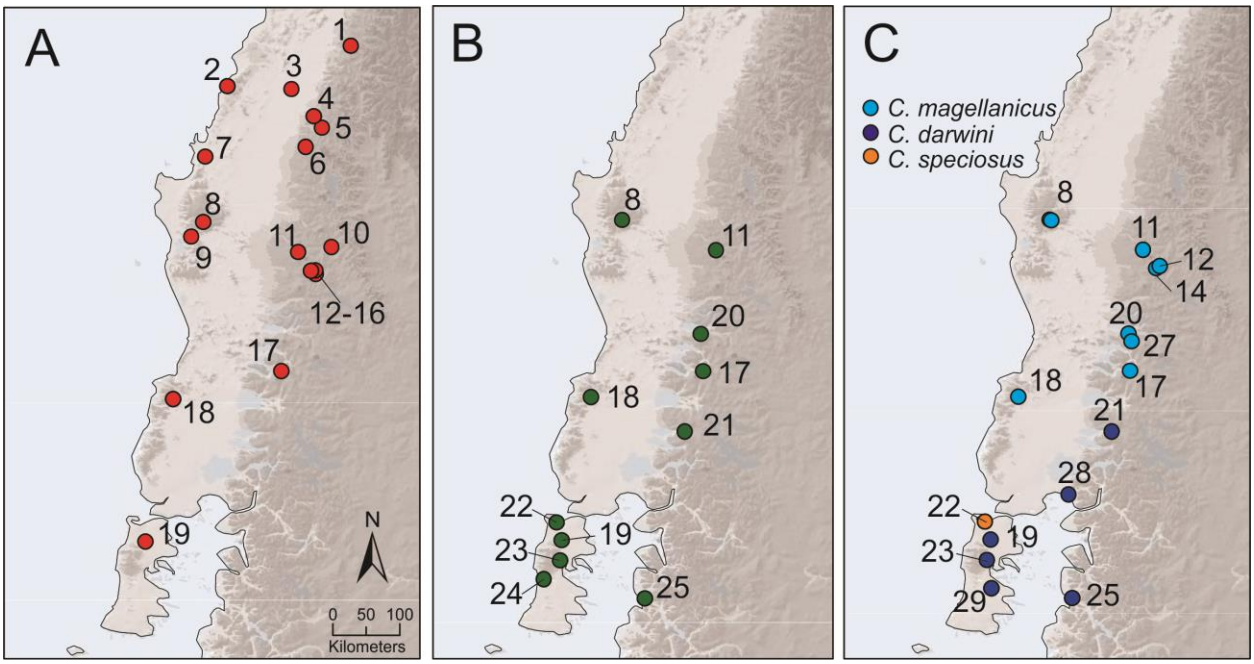

Figure 4.1: Distribution and RADSeq sampling of the three main species groups that are the focus of this study, *Ceroglossus chilensis* (A), *Ceroglossus buqueti* (B), and *Ceroglossus darwini* (C).

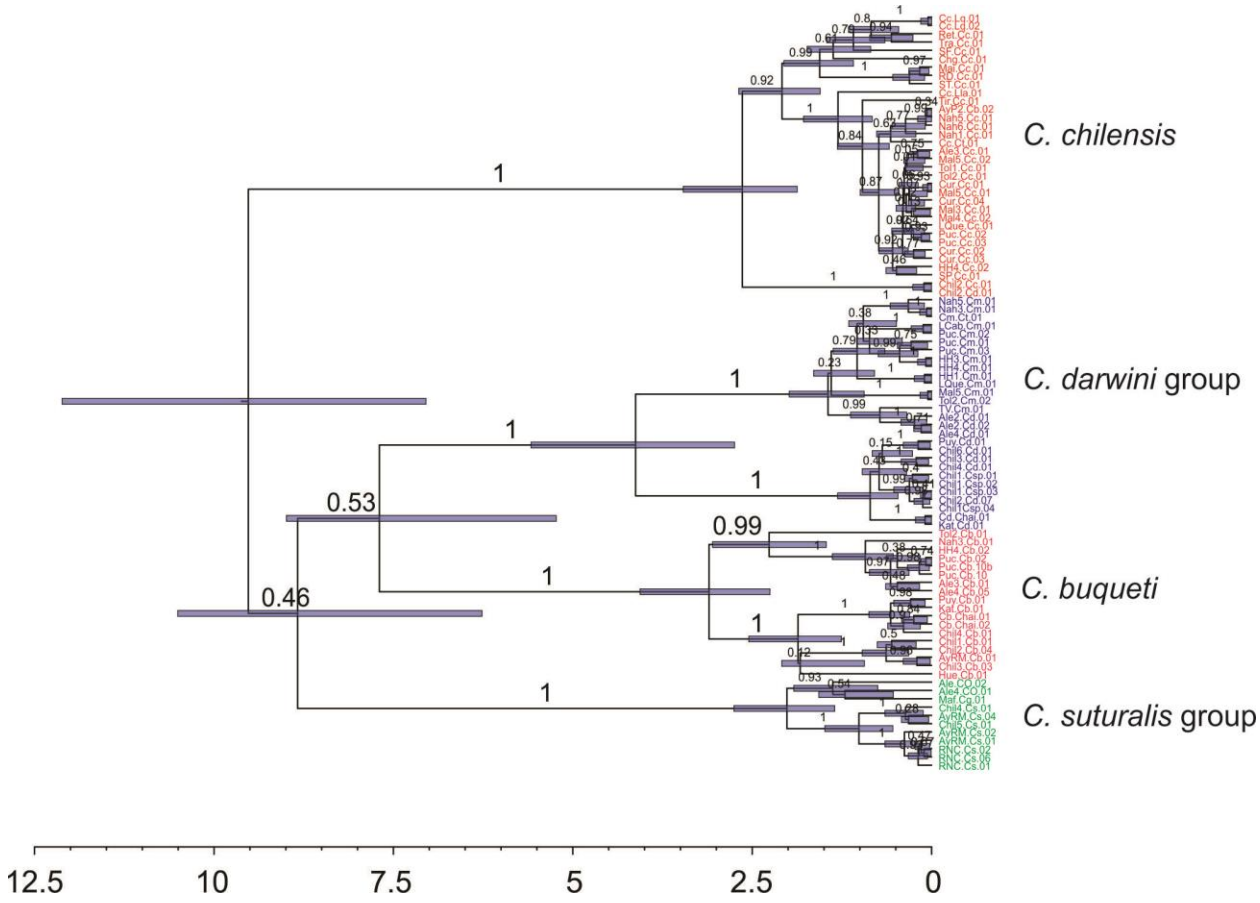

Figure 4.2: Time-calibrated phylogeny reconstructed by Bayesian inference in BEAST (Bouckaert et al. 2014) using sequences from the mtDNA COI region of 91 *Ceroglossus* individuals sampled across all four species groups.

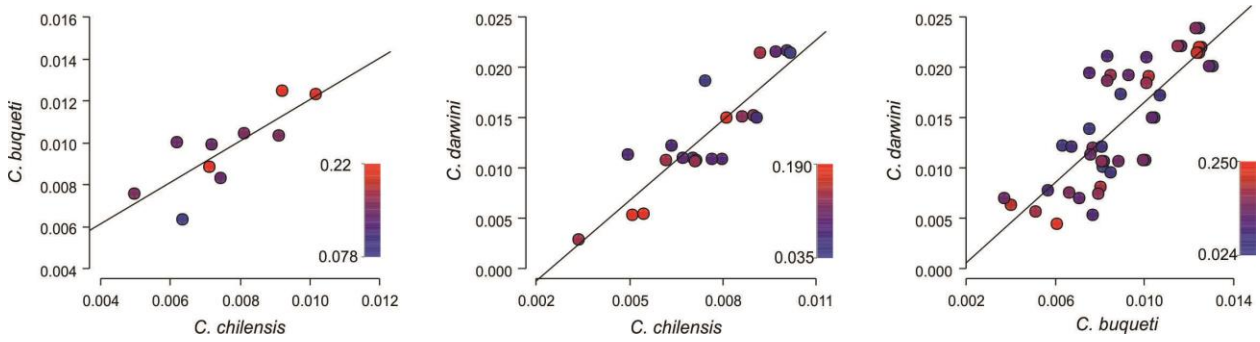

Figure 4.3: Test of co-divergence. Each graph represents the relationship between the patristic distances between two species. Each point represents the patristic distance between the color morphs of two different localities in which both species were present. Color of points indicates the average color similarity (degree of mimicry) between species, with blue indicating higher similarity (lower color distance) and red indicating lower similarity (higher color distance).

4.9 APPENDIX

Table S1: Summary of data after processing in ipyRAD. The first 10 samples (highlighted in grey) were removed for phylogenetic analyses due to their low number of reads. Averages at the bottom of the table do not include removed samples.

species	sample	reads_raw	Nloci	avg_depth_stat	nsites	nhetero	heterozygosity
buq	TV_Cb_03	71363	142	63.098765	12732	181	0.014216
buq	TV_Cb_02	577680	326	129.764069	29284	732	0.024997
buq	Kat_Cb_05	278165	357	32.423154	32040	650	0.020287
buq	Kat_Cb_04	567099	783	40.966738	70246	999	0.014221
buq	Tol2_Cb_02	2854346	23006	28.675301	2068263	10602	0.005126
buq	Nah3_Cb_03	2542010	18743	25.460221	1684195	8810	0.005231
buq	Cb_Ay_02	1580721	9962	18.829544	895026	5003	0.00559
buq	Nah3_Cb_01	699109	4984	19.459598	447677	2601	0.00581
buq	Puy_Cb_01	5194428	26536	33.039832	2385884	15187	0.006365
buq	Puy_Cb_02	9265081	36878	43.416671	3316821	21954	0.006619
buq	Chil4_Cb_05	5355180	34324	63.981347	3087604	21697	0.007027
buq	Cb_Ay_01	1177698	4213	18.525056	378213	2756	0.007287
buq	Chil3_Cb_05	1298484	6779	25.624561	609175	4582	0.007522
buq	Puc_Cb_02	638667	5012	19.24631	450409	3399	0.007546
buq	Chil1_Cb_07	3447492	16428	32.307103	1476239	11199	0.007586
buq	Chil2_Cb_01	1804375	5072	35.608857	455286	3485	0.007655
buq	Puc_Cb_01	2052758	10402	27.55916	934945	7188	0.007688
buq	Cb_Nel_05	3052534	15412	32.882668	1385079	10685	0.007714
buq	Chil3_Cb_12	3094624	21974	27.886986	1975456	15266	0.007728
buq	Chil4_Cb_01	4866606	22147	35.426944	1990744	15420	0.007746
buq	Cb_Nel_04	5191411	24894	31.492345	2238179	17659	0.00789
buq	Ale3_Cb_02	5821235	32182	37.187039	2894893	23371	0.008073
buq	Chil1_Cb_06	1775641	6983	30.220989	627192	5116	0.008157
buq	Chil2_Cb_02	3505730	12825	30.754958	1152122	9434	0.008188
buq	Chil3_Cb_04	2454450	9439	32.311234	848032	7015	0.008272
buq	Ale3_Cb_01	2565621	9112	33.131652	818782	7103	0.008675
buq	Cb_Chai_04	4752870	21936	29.614877	1971786	17210	0.008728
buq	Cb_Chai_03	5206681	30092	29.693999	2706194	24211	0.008947
buq	Puc_Cb_10	778231	2792	31.458816	250736	2308	0.009205
buq	Tol2_Cb_01	869618	10923	21.458487	981524	10244	0.010437
chil	TV_Cc_03	13508	26	166.942857	2329	61	0.026191
chil	Puc_Cc_01	12310	34	67.734694	3061	52	0.016988
chil	TV_Cc_01	24470	39	197.87931	3510	65	0.018519
chil	Puc_Cc_04	19863	81	64.605769	7290	99	0.01358
chil	Chg_Cc_01	263689	950	25.492623	85266	1448	0.016982

chil	Ret_Cc_05	39126	1102	29.529725	99060	105	0.00106
chil	Chil2_Cc_06	4013014	36005	69.80639	3237792	11358	0.003508
chil	Cc_Ll_01	1344269	20296	19.564907	1823728	7543	0.004136
chil	Cc_Chil2_07	562788	5872	63.439377	527072	2974	0.005642
chil	RD_Cc_01	2584910	35312	36.245597	3175836	18133	0.00571
chil	Ale4_Cc_08	2395269	28001	24.859994	2517276	15098	0.005998
chil	ST_Cc_01	3902247	38789	38.223508	3488526	21282	0.006101
chil	Cur_Cc_01	1111115	16508	21.332728	1483217	9094	0.006131
chil	Cc_LQ_02	3313338	37241	46.286184	3349326	20616	0.006155
chil	SF_Cc_01	1418286	21733	26.405595	1953089	12101	0.006196
chil	Cc_LQ_01	4177494	40250	45.609186	3619582	22638	0.006254
chil	Mal3_Cc_01	313394	6608	17.533158	593832	3812	0.006419
chil	Cur_Cc_02	954990	14195	19.739423	1275260	8193	0.006425
chil	Ale3_Cc_02	5442827	68752	38.637726	6183692	39905	0.006453
chil	VB_Cc_02	3192921	38804	33.163975	3488226	23071	0.006614
chil	Cur_Cc_03	1948034	24811	23.922289	2230116	14758	0.006618
chil	Mal4_Cc_02	1689351	25964	28.713261	2334439	15535	0.006655
chil	Nel_Cc_03	802706	10793	39.934526	970008	6485	0.006686
chil	Nel_Cc_02	409641	6120	18.62769	549932	3682	0.006695
chil	VB_Cc_01	4668239	41787	53.778617	3758223	25224	0.006712
chil	Tra_Cc_02	3931458	39977	44.271765	3595293	25163	0.006999
chil	Tra_Cc_01	4060332	40551	45.450507	3647128	25731	0.007055
chil	Chg_Cc_02	4754970	41929	56.492915	3771713	26722	0.007085
chil	Mal5_Cc_02	2427761	33399	23.162597	3002599	21414	0.007132
chil	Mal5_Cc_01	3905768	37675	38.424206	3389002	24306	0.007172
chil	Tol2_Cc_01	1897349	28826	30.888232	2591951	19430	0.007496
chil	Tol1_Cc_03	2616186	32838	38.082239	2953047	22281	0.007545
chil	Cc_Ct_01	2702743	33754	33.715671	3036233	24109	0.00794
chil	Ret_Cc_02	347639	4219	19.953753	378664	3027	0.007994
chil	Nah1_Cc_03	2526803	34499	31.866753	3102899	25498	0.008217
chil	Tol1_Cc_01	281655	3647	17.282344	327518	2729	0.008332
chil	Nah1_Cc_02	2136594	43868	21.293609	3944371	33264	0.008433
chil	Cur_Nn_04	1631410	18410	36.917513	1654352	14403	0.008706
dar	Puy_Cd_06	707146	25139	23.4394	2259977	10820	0.004788
dar	Puy_Cd_05	2349306	38505	56.23676	3463496	16587	0.004789
dar	Chil6_Cd_01	2177725	38402	52.913814	3455001	19653	0.005688
dar	Chil6_Cd_02	575024	22037	22.40087	1981148	11345	0.005726
dar	Kat_Cd_05	367585	17339	14.105454	1557993	9325	0.005985
dar	Cd_Chai_02	2027757	47428	37.430296	4266043	25910	0.006074
dar	Cd_Chai_03	2179044	38420	51.778833	3457012	21021	0.006081
dar	Chil2_Cd_06	81034	2854	12.638729	256329	1568	0.006117
dar	Chil3_Cd_01	1958690	35274	49.294034	3173641	19445	0.006127

dar	Chil3_Cd_02	2074548	37276	50.407814	3353584	20703	0.006173
dar	Kat_Cd_06	732346	25951	22.519889	2333404	14520	0.006223
dar	Chil2_Cd_07	1378769	33979	36.588538	3057030	20138	0.006587
dar	Chil1_Csp_08	2078296	37764	50.993208	3398152	22424	0.006599
dar	Chil1_Csp_09	728595	23505	26.298158	2113185	14064	0.006655
mag	Mal3_Cc_02	3059381	39486	65.113401	3552109	19552	0.005504
mag	Mal5_Cm_01	3363961	41235	71.21026	3709322	21331	0.005751
mag	Tol2_Cm_02	1041502	27338	30.151263	2458543	14247	0.005795
mag	Mal4_Cc_03	159190	5069	18.147165	455468	2664	0.005849
mag	Tol2_Cm_03	1524283	31551	42.494428	2838218	16838	0.005933
mag	Nah5_Cm_03	1226696	30261	31.113756	2721832	18355	0.006744
mag	Nah3_Cm_04	1928997	36113	41.56293	3248873	22083	0.006797
mag	Nel_Cm_01	1118306	29803	31.122102	2680915	19781	0.007378
mag	Nel_Cm_02	267462	7940	19.380785	713718	5327	0.007464
mag	Ale2_Cd_01	141719	4698	18.387538	422151	3155	0.007474
mag	Puc_Cm_03	550801	18588	21.757951	1670669	12889	0.007715
mag	Puc_Cm_04	1494049	33586	34.786787	3022331	23331	0.00772
mag	Tv_Cm_01	145279	4369	13.450813	392360	3170	0.008079
mag	Ale4_Cd_07	1126396	34673	26.929035	3117816	27493	0.008818
	Average	2059815.229	21946.938	38.43721359	38.43721	38.43721359	38.43721359

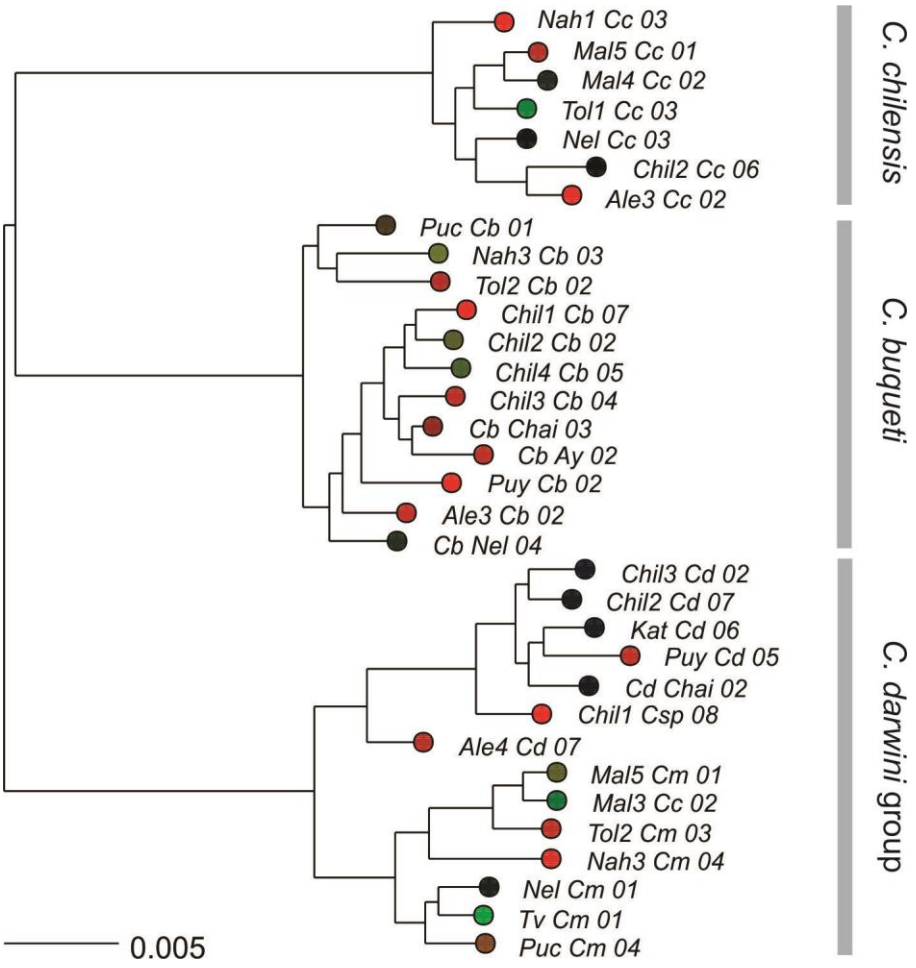

Figure S1: Maximum likelihood tree for the RADSeq data used for the species co-divergence test. The tree only contains samples from sites that are shared between at least 2 species. Color at tips represents elytral coloration of color morphs represented at those tips.

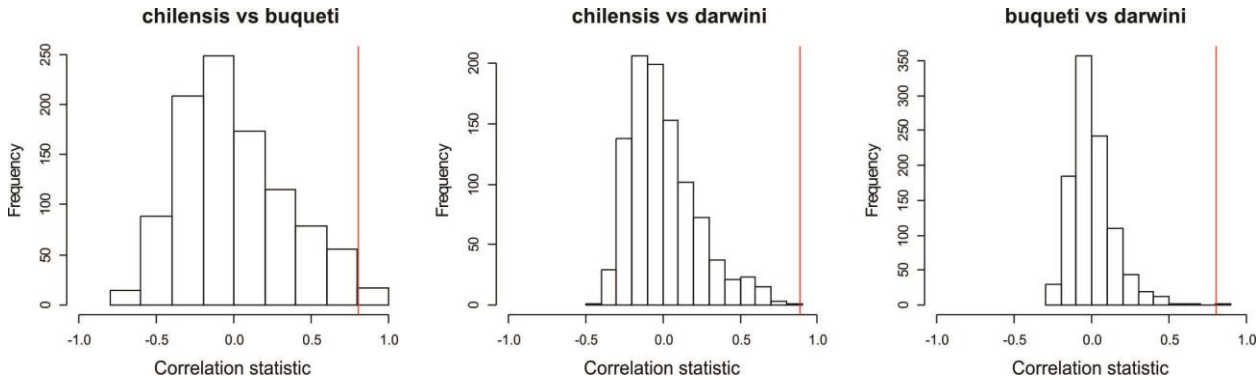

Figure S2: Results from a simulation analysis to test the significance of the co-divergence test. The test consisted on randomly reshuffling tips within species and calculating the coefficient of correlation between the species based on the new randomized relationships. The coefficients of correlation from 1000 simulations (distributions) were compared to the observed correlation (vertical red line) to provide a test of significance.

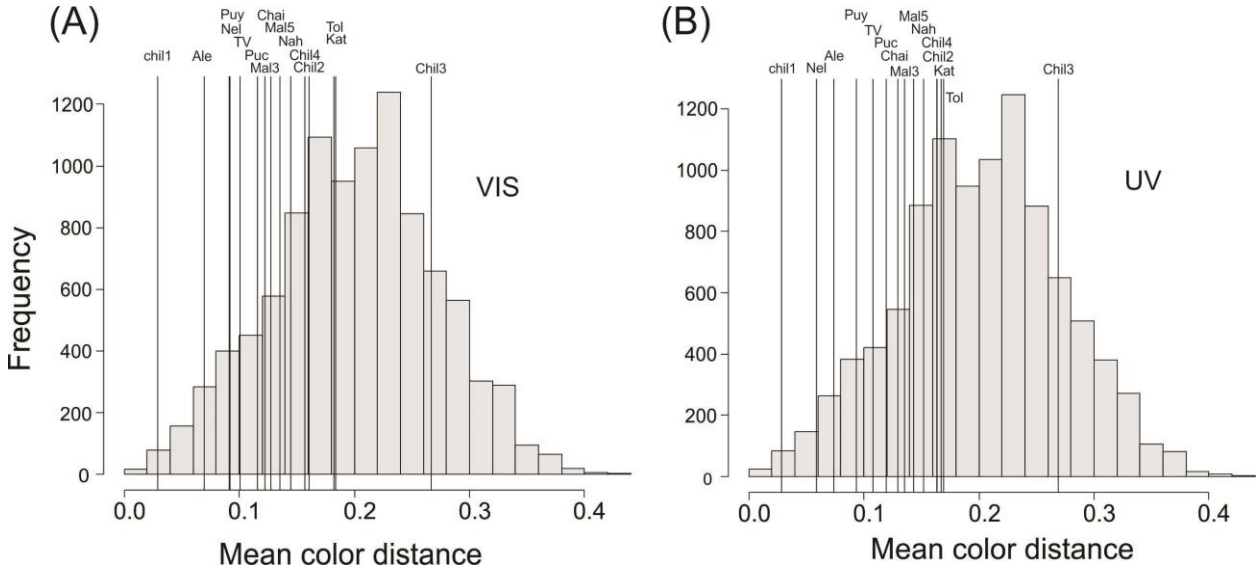

Figure S4: Degree of mimicry for all localities with 2 or 3 co-mimic species based on their mean color distance. The histograms represent null distributions of mean distances obtained randomly from points in the color space (10000 mean values, each calculated from 3 randomly selected points), were each point represents the mean color of one site of one species. (A) Color distances based on a VIS visual model color space (mean= 0.203). (B) Color distances based on a UV visual model color space (mean= 0.199). Vertical lines indicate observed color distance values between species for a given locality (site labels are as those indicated in table 4.1). Color data was taken from Muñoz-Ramírez et al. 2016.

CHAPTER 5: CONCLUSION

This dissertation uncover a fascinating new mimicry system—the ground beetle genus Ceroglossus—that exhibits striking and unique characteristics that make it specially suitable to study a range of questions in ecology and evolutionary biology. Here I used the remarkable geographic variation in the degree of phenotypic matching (color) of this system to study the role of mimicry in speciation and coevolution. The results revealed no significant effect of the degree of mimicry in either speciation or coevolution at the regional scale in this system. This is the first time that the degree of mimicry is accounted for to understand these processes at a regional scale and the results suggest that the role of mimicry on speciation and diversification is complex and requires further study. In particular, my results challenge the idea that mimicry must cause speciation due to positive frequency dependent selection and suggest that without other processes like assortative mating or some particular genetic architecture, speciation is harder to achieve. In addition, these results also suggest that mimicry may be just a consequence of speciation, not the cause as it has been argued in other mimicry systems (e.g. (Jiggins et al. 2004; Cuthill and Charleston 2012, 2015). Perhaps more importantly, this study exemplifies the need for studying other model systems because the particularities they may offer (e.g. mimicry variation, genetics of underlying traits, biogeographic context) can greatly increase our understanding of mimicry evolution and its role on diversity.

The study of the genus *Ceroglossus* warrants several future directions. For example, because the main focus of mimicry research has been on to explain the remarkable power of natural selection to produce accurate mimics, the *Ceroglossus* system, on the contrary, may encourage a shift toward

understanding the factors that prevents mimicry or maintain phenotypic mismatching. Chapter 2 highlighted several hypotheses that could explain why inaccurate mimicry is present across the distribution of the genus including variation in selective pressures for mimicry, differential levels of gene flow between areas with different color morphs, and the lack of sufficient time to complete color convergence (evolution in progress). By studying these questions we may get a deeper understanding on the tradeoffs in the evolution of mimicry and the role of historical events, aspects that would be more difficult to study in groups with lower or no variation of mimicry across space.

In speciation research, ecological speciation has gained important momentum in recent years. Mimicry has been implied as an important driver of ecological speciation because color divergence, which results from ecological divergence, has been linked with reproductive isolation in butterflies (Jiggins 2008). In these butterflies, mate preferences are linked with color patterns causing that color-differentiated populations may experience assortative mating. However, the ecological speciation literature has also suggested that the sole presence of strong natural selection (without any other additional process) can be sufficient to cause some degree of reproductive isolation (Nosil 2012) because strong selection can cause high migrant mortality and hybrid inviability. The variation in color matching in *Ceroglossus* provides an excellent opportunity to test whether color divergence can cause speciation because it not only allows testing genetic structure across color morphs, but also disentangling potentially confounding factors like assortative mating. For example, a natural experiment could evaluate genetic structure across areas with different levels of mimicry and use color matching as a proxy to predict levels of selection. Then, processes other than mimicry could be responsible for genetic structure (between color morphs of one species) if similarly high genetic structure is found between areas with high color match versus between areas with low color matching. Thus, by predicting levels of genetic structure under different levels of selection, other factors such as assortative mating or other overlooked barriers could be ruled out.

Müllerian mimicry has been a powerful model system to study ecology and evolution (Gilbert 1983; Ruxton et al. 2004; Futuyma 2013). However, there are still many questions that require further testing and consideration. By studying new mimicry systems with disparate ecologies we will be able not only to test the generality of the mimicry theory learnt from more classic systems, but also to approach several basic questions from a different perspective. *Ceroglossus* offers a great opportunity to increase our understanding on the processes involved in Müllerian mimicry and promises to be an excellent complement to other classic Müllerian systems to study drivers of biodiversity.

BIBLIOGRAPHY

Adams D.C., Otárola-Castillo E. 2013. Geomorph: An r package for the collection and analysis of geometric morphometric shape data. Methods Ecol. Evol. 4:393–399.

Agapow P.-M., Bininda-Emonds O.R., Crandall K. a, Gittleman J.L., Mace G.M., Marshall J.C., Purvis A. 2004. The impact of species concept on biodiversity studies. Q. Rev. Biol. 79:161–179.

Allnutt T.R., Newton A.C., Lara A., Premoli A.C., Armesto J.J., Vergara R., Gardner M. 1999. Genetic variation in Fitzroya cupressoides (alerce), a threatened South American conifer. Mol. Ecol. 8:975–987.

Andújar C., Serrano J., Gómez-Zurita J. 2012. Winding up the molecular clock in the genus Carabus (Coleoptera: Carabidae): assessment of methodological decisions on rate and node age estimation. BMC Evol. Biol. 12:40.

Arias C.F., Salazar C., Rosales C., Kronforst M.R., Linares M., Bermingham E., McMillan W.O. 2014. Phylogeography of Heliconius cydno and its closest relatives: Disentangling their origin and diversification. Mol. Ecol. 23:4137–4152.

Armesto J., Villagrán C., Donoso C. 1994. La historia del bosque templado chileno. Ambient. y Desarro. 66:66–72.

Aubier T.G., Elias M., Llaurens V., Chazot N. 2017a. Mutualistic mimicry enhances species diversification through spatial segregation and extension of the ecological niche space. Evolution (N. Y).:1–45.

Aubier T.G., Joron M., Sherratt T.N. 2017b. Mimicry among Unequally Defended Prey Should Be Mutualistic When Predators Sample Optimally. 189.

Aubier T.G., Sherratt T.N. 2015. Diversity in Müllerian mimicry: The optimal predator sampling strategy explains both local and regional polymorphism in prey. Evolution (N. Y). 69:2831–2845.

Avise J.C. 1992. Molecular population structure and biogeographic history of a regional fauna: a case history with lessons for conservative biology. Oikos. 63:62–76.

Benson W. 1982. Alternative models for infrageneric diversification in the humid tropics: tests with passion vine butterflies. In: Prance G., editor. Biological diversification in the tropics. New York: Columbia University Press. p. 608–640.

Bouckaert R., Heled J., Kühnert D., Vaughan T., Wu C.H., Xie D., Suchard M.A., Rambaut A., Drummond A.J. 2014. BEAST 2: A Software Platform for Bayesian Evolutionary Analysis. PLoS Comput. Biol. 10.

Brower A. V. 1994. Rapid morphological radiation and convergence among races of the butterfly Heliconius erato inferred from patterns of mitochondrial DNA evolution. Proc. Natl. Acad. Sci. U. S.

A. 91:6491–6495.

Brower A.V.Z. 1996. Parallel race formation and the evolution of mimicry in Heliconius butterflies: A phylogenetic hypothesis from mitochondrial DNA sequences. Evolution (N. Y). 50:195–221.

Brown J.L., Maan M.E., Cummings M.E., Summers K. 2010. Evidence for selection on coloration in a Panamanian poison frog: a coalescent-based approach. J. Biogeogr. 37:891–901.

Camargo A., Sites J.J. 2013. Species Delimitation : A Decade After the Renaissance. .

Catchen J., Hohenlohe P. a, Bassham S., Amores A., Cresko W. a. 2013. Stacks: an analysis tool set for population genomics. Mol. Ecol. 22:3124–40.

Chazot N., Willmott K.R., Santacruz Endara P.G., Toporov A., Hill R.I., Jiggins C.D., Elias M. 2014. Mutualistic Mimicry and Filtering by Altitude Shape the Structure of Andean Butterfly Communities. Am. Nat. 183:26–39.

Chifman J., Kubatko L. 2014. Quartet Inference from SNP Data Under the Coalescent Model. Bioinformatics.:1–8.

Chou J., Gupta A., Yaduvanshi S., Davidson R., Nute M., Mirarab S., Warnow T. 2015. A comparative study of SVDquartets and other coalescent-based species tree estimation methods. bioRxiv. 16:1–15.

Chouteau M., Angers B. 2011. The role of predators in maintaining the geographic organization of aposematic signals. Am. Nat. 178:810–7.

Chouteau M., Arias M., Joron M. 2016a. Warning signals are under positive frequency-dependent selection in nature. Proc. Natl. Acad. Sci. 113:201519216.

Chouteau M., Arias M., Joron M. 2016b. Warning signals are under positive frequency-dependent selection in nature. Proc. Natl. Acad. Sci. 113:2164–2169.

Correa A., Armesto J.J., Schlatter R.P., Rozzi R., Torres-Mura J.C. 1990. La dieta del chucao (Scelorchilus rubecola), un Passeriforme terrícola endémico del bosque templado húmedo de Sudamérica austral. Rev. Chil. Hist. Nat. 63:197–202.

Coyne J.A., Orr H.A. 2004. Speciation. .

Cuthill J.H., Charleston M. 2012. Phylogenetic codivergence supports coevolution of mimetic Heliconius butterflies. PLoS One. 7:e36464.

Cuthill J.H., Charleston M. 2015. Wing patterning genes and coevolution of Müllerian mimicry in Heliconius butterflies: support from phylogeography, co-phylogeny and divergence times. Evolution (N. Y). 69:3082–3096.

DaCosta J.M., Sorenson M.D. 2016. ddRAD-seq phylogenetics based on nucleotide, indel, and presence–absence polymorphisms: Analyses of two avian genera with contrasting histories. Mol. Phylogenet. Evol. 94:122–135.

Dalrymple R.L., Hui F.K.C., Flores-Moreno H., Kemp D.J., Moles A.T. 2015. Roses are red, violets are blue - so how much replication should you do? An assessment of variation in the colour of flowers and

birds. Biol. J. Linn. Soc. 114:69–81.

Dumbacher J.P., Fleischer R.C. 2001. Phylogenetic evidence for colour pattern convergence in toxic pitohuis: Müllerian mimicry in birds? Proc. Biol. Sci. 268:1971–6.

Dynesius M., Jansson R. 2013. Persistence of Within-Species Lineages: a Neglected Control of Speciation Rates. Evolution.:1–12.

Eaton D.A.R. 2014. PyRAD: Assembly of de novo RADseq loci for phylogenetic analyses. Bioinformatics. 30:1844–1849.

Eaton D.A.R., Spriggs E.L., Park B., Donoghue M.J. 2016. Misconceptions on Missing Data in RAD-seq Phylogenetics with a Deep-scale Example from Flowering Plants. Syst. Biol. 0:syw092.

Elias M., Gompert Z., Jiggins C., Willmott K. 2008. Mutualistic interactions drive ecological niche convergence in a diverse butterfly community. PLoS Biol. 6:2642–2649.

Endler J.A., Mielke P.W. 2005. Comparing entire colour patterns as birds see them. Biol. J. Linn. Soc. 86:405–431.

Etienne R.S., Rosindell J. 2012. Prolonging the past counteracts the pull of the present: Protracted speciation can explain observed slowdowns in diversification. Syst. Biol. 61:204–213.

Flanagan N.S., Tobler A., Davison A., Pybus O.G., Kapan D.D., Planas S., Linares M., Heckel D., McMillan W.O. 2004. Historical demography of Mullerian mimicry in the neotropical Heliconius butterflies. Proc Natl Acad Sci U S A. 101:9704–9709.

Folmer O., Black M., Hoeh W., Lutz R., Vrijenhoek R. 1994. DNA primers for amplification of mitochondrial cytochrome c oxidase subunit I from diverse metazoan invertebrates. Mol. Mar. Biol. Biotechnol. 3:294–299.

Freckleton R.P., Harvey P.H., Pagel M. 2002. Phylogenetic analysis and comparative data: a test and review of evidence. Am. Nat. 160:712–26.

Fujita M.K., Leaché A.D., Burbrink F.T., McGuire J. a, Moritz C. 2012. Coalescent-based species delimitation in an integrative taxonomy. Trends Ecol. Evol. 27:480–8.

Futuyma D. 2013. Evolution. Sinauer Associates, Inc.

Germain P. 1895. Apuntes sobre los insectos de Chile. Los carabus chilenos. An. la Univ. Chile. 90:627–683.

Gilbert L.E. 1983. Coevolution and mimicry. In: Futuyma D., Sletkin M., editors. Coevolution. p. 263–281.

Goolsby E.W., Bruggeman J., Ane C. 2016. Rphylopars: Fast Multivariate Phylogenetic Comparative Methods for Missing Data and Within-Species Variation. Methods Ecol. Evol.

Hall T., Biosciences I., Carlsbad C. 2011. BioEdit: An important software for molecular biology. GERF Bull. Biosci. 2:60–61.

Harmon L.J., Glor R.E. 2010. Poor statistical performance of the mantel test in phylogenetic comparative analyses. Evolution (N. Y). 64:2173–2178.

Harper G.R., Pfennig D.W. 2008. Selection overrides gene flow to break down maladaptive mimicry. Nature. 451:1103–6.

Hedin M., Carlson D., Coyle F. 2015. Sky island diversification meets the multispecies coalescent - Divergence in the spruce-fir moss spider (Microhexura montivaga, Araneae, Mygalomorphae) on the highest peaks of southern Appalachia. Mol. Ecol. 24:3467–3484.

Hey J., Pinho C. 2012. Population genetics and objectivity in species diagnosis. Evolution (N. Y). 66:1413–1429.

Hickerson M.J., Carstens B.C., Cavender-Bares J., Crandall K. a, Graham C.H., Johnson J.B., Rissler L., Victoriano P.F., Yoder a D. 2010. Phylogeography's past, present, and future: 10 years after Avise, 2000. Mol. Phylogenet. Evol. 54:291–301.

Hines H.M., Counterman B.A., Papa R., Albuquerque P., Moura D., Cardoso M.Z. 2011. Wing patterning gene redefines the mimetic history of Heliconius butterflies. Proc. Natl. Acad. Sci. U. S. A. 108:19666–19671.

Hotaling S., Foley M.E., Lawrence N.M., Bocanegra J., Blanco M.B., Rasoloarison R., Kappeler P.M., Barrett M.A., Yoder A.D., Weisrock D.W. 2016. Species discovery and validation in a cryptic radiation of endangered primates: coalescent-based species delimitation in Madagascar's mouse lemurs. Mol. Ecol.:2029–2045.

Huang H., He Q., Kubatko L.S., Knowles L.L. 2010. Sources of Error Inherent in Species-Tree Estimation: Impact of Mutational and Coalescent Effects on Accuracy and Implications for Choosing among Different Methods. Syst. Biol. 59:573–583.

Huang H., Lacey Knowles L. 2016. Unforeseen consequences of excluding missing data from next-generation sequences: Simulation study of rad sequences. Syst. Biol. 65:357–365.

Hulton N.R.., Purves R.., McCulloch R.., Sugden D.., Bentley M.. 2002. The Last Glacial Maximum and deglaciation in southern South America. Quat. Sci. Rev. 21:233–241.

Jiggins C.D. 2008. Ecological Speciation in Mimetic Butterflies. Bioscience. 58:541.

Jiggins C.D., Estrada C., Rodrigues a. 2004. Mimicry and the evolution of premating isolation in Heliconius melpomene Linnaeus. J. Evol. Biol. 17:680–91.

Jiggins C.D., Naisbit R.E., Coe R.L., Mallet J. 2001. Reproductive isolation caused by colour pattern mimicry. Nature. 411:302–5.

Jimenez J.E., Jaksic F.M. 1993. Variación estacional de la dieta del caburé grande (Glaucidium nanum) en Chile y su relación con la abundancia de presas. El Hornero. 13:265–271.

Jiroux E. 1996. Revision du genre Ceroglossus. Collection Systematique. .

Jiroux E. 2006. Le genre Ceroglossus, Vol. 14. .

Jiroux E. 2008. Contribution a la connaissance du genre Ceroglossus Solier, V (Coleoptera, Carabidae). Les Cah. Magellanes. 25:1–7.

Johnstone R. a. 2002. The evolution of inaccurate mimics. Nature. 418:524–6.

Joron M., Mallet J.L. 1998. Diversity in mimicry: paradox or paradigm? Trends Ecol. Evol. 13:461–6.

Kapan D.D. 2001. Three-butterfly system provides a field test of müllerian mimicry. Nature. 409:338–340.

Knapp S., Mallet J. 2003. Refuting Refugia? Science 300:71–72.

Knowles L.L., Carstens B.C. 2007a. Estimating a geographically explicit model of population divergence. Evolution. 61:477–93.

Knowles L.L., Carstens B.C. 2007b. Delimiting species without monophyletic gene trees. Syst. Biol. 56:887–95.

Maia R., Eliason C.M., Bitton P.-P., Doucet S.M., Shawkey M.D. 2013. pavo: an R package for the analysis, visualization and organization of spectral data. Methods Ecol. Evol. 4:906–913.

Mallet J. 1999. Causes and consequences of a lack of coevolution in Müllerian mimicry. Evol. Ecol. 13:777–806.

Mallet J. 2010. Shift happens! Shifting balance and the evolution of diversity in warning colour and mimicry. Ecol. Entomol. 35:90–104.

Mallet J., Barton N.H. 1989. Strong Natural Selection in a Warning-Color Hybrid Zone. Evolution (N. Y). 43:421.

Mallet J., Jiggins C.D., McMillan W.O. 1996. Evolution: Mimicry meets the mitochondrion. Curr. Biol. 6:937–940.

Mallet J., Joron M. 1999. Evolution of diversity in warning color and mimicry: polymorphisms, shifting balance, and speciation. Annu. Rev. Ecol. Syst. 30:201–233.

Marek P.E., Bond J.E. 2009. A Müllerian mimicry ring in Appalachian millipedes. Proc. Natl. Acad. Sci. U. S. A. 106:9755–60.

Mathiasen P., Premoli A.C. 2010. Out in the cold: genetic variation of Nothofagus pumilio (Nothofagaceae) provides evidence for latitudinally distinct evolutionary histories in austral South America. Mol. Ecol. 19:371–85.

Merrill R.M., Dasmahapatra K.K., Davey J.W., Dell'Aglio D.D., Hanly J.J., Huber B., Jiggins C.D., Joron M., Kozak K.M., Llaurens V., Martin S.H., Montgomery S.H., Morris J., Nadeau N.J., Pinharanda A.L., Rosser N., Thompson M.J., Vanjari S., Wallbank R.W.R., Yu Q. 2015. The diversification of Heliconius butterflies: what have we learned in 150 years? J. Evol. Biol. 28:1417–1438.

Morrone J.J. 2006. Biogeographic Areas and Transition Zones of Latin America and the Caribbean Islands Based on Panbiogeographic and Cladistic Analyses of the Entomofauna. Annu. Rev. Entomol. 51:467–494.

Müller F. 1879. Ituna and Thyridia: a remarkable case of mimicry in butterflies. Trans. Entomol. Soc. L.:xx–xxiv.

Muñoz-Ramírez C. 2015. The Phylogenetic position of Ceroglossus ochsenii GERMAIN and Ceroglossus guerini GERMAIN (Coleoptera: Carabidae), two endemic ground beetles from the Valdivian forest

of Chile. Rev. Chil. Entomol. 40:14–21.

Muñoz-Ramírez C.P., Bitton P.-P., Doucet S.M., Knowles L.L. 2016. Mimics here and there, but not everywhere: Müllerian mimicry in Ceroglossus ground beetles? Biol. Lett. 12:20160429.

Muñoz-Ramírez C.P., Unmack P.J., Habit E., Johnson J.B., Cussac V.E., Victoriano P. 2014. Phylogeography of the ancient catfish family Diplomystidae: Biogeographic, systematic, and conservation implications. Mol. Phylogenet. Evol. 73:146–160.

Noonan B.P., Comeault A.A. 2009. The role of predator selection on polymorphic aposematic poison frogs. Biol. Lett. 5:51–54.

Nosil P. 2012. Ecological speciation. Oxford University Press.

Nosil P., Crespi B.J. 2004. Does Gene Flow Constrain Adaptive Divergence or Vice Versa? a Test Using Ecomorphology and Sexual Isolation in Timema Cristinae Walking-Sticks. Evolution (N. Y). 58:102.

Nuñez J.J., Wood N.K., Rabanal F.E., Fontanella F.M., Sites W., Jack W. 2010. Amphibian phylogeography in the Antipodes : refugia and postglacial colonization b. Mol. Phylogenet. Evol.

Okamoto M., Kashiwai N., Su Z.H., Osawa S. 2001. Sympatric convergence of the color pattern in the Chilean Ceroglossus ground beetles inferred from sequence comparisons of the mitochondrial ND5 gene. J. Mol. Evol. 53:530–8.

Oksanen J., Blanchet F., Kindt R., Legendre P., O'Hara R. 2016. Vegan: community ecology package. R Packag. 2.3-3.:Available at: https://cran.r-project.org/web/packa.

Orsini L., Vanoverbeke J., Swillen I., Mergeay J., De Meester L. 2013. Drivers of population genetic differentiation in the wild: Isolation by dispersal limitation, isolation by adaptation and isolation by colonization. Mol. Ecol. 22:5983–5999.

Papadopoulou A., Knowles L.L. 2016. Toward a paradigm shift in comparative phylogeography driven by trait-based hypotheses. Proc. Natl. Acad. Sci. U. S. A. 113:8018–24.

Pena M., Rumboll M. 1998. Birds of Southern South America and Antarctica. New Jersey: Princeton.

Penney H.D., Hassall C., Skevington J.H., Abbott K.R., Sherratt T.N. 2012. A comparative analysis of the evolution of imperfect mimicry. Nature. 483:461–4.

Pfennig D. 2012. Mimicry: Ecology, evolution, and development. Curr. Zool. 58:604–607.

Pfennig D.W., Kikuchi D.W. 2012. Competition and the evolution of imperfect mimicry. Curr. Zool. 58:608–619.

Posada D. 2008. jModelTest: phylogenetic model averaging. Mol. Biol. Evol. 25:1253–1256.

De Queiroz K. 2005. Different species problems and their resolution. BioEssays. 27:1263–1269.

Rabosky A.R.D., Cox C.L., Rabosky D.L., Title P.O., Holmes I.A., Feldman A., McGuire J.A. 2016. Coral snakes predict the evolution of mimicry across New World snakes. Nat. Commun. 7:11484.

R Development Core Team. 2013. R: A language and environment for statistical computing. R

Foundation for Statistical Computing, Vienna, Austria. ISBN 3-900051-07-0, URL http://www.R-project.org/. R Found. Stat. Comput. Vienna, Austria.

Revell L.J. 2012. phytools: an R package for phylogenetic comparative biology (and other things). Methods Ecol. Evol. 3:217–223.

Rohlf F. 2013. TpsDig2, Version 2.17. .

Ronquist F., Huelsenbeck J.P. 2003. MrBayes 3: Bayesian phylogenetic inference under mixed models. Bioinformatics. 19:1572–1574.

Ruíz P. 1931. Los Ceroglossus de Chile. Rev. Chil. Hist. Nat. 40:381–425.

Runemark A., Hansson B., Pafilis P., Valakos E.D., Svensson E.I. 2010. Island biology and morphological divergence of the Skyros wall lizard Podarcis gaigeae: a combined role for local selection and genetic drift on color morph frequency divergence? BMC Evol. Biol. 10:269.

Ruxton G.D., Sherratt T.N., Speed M.P. 2004. Avoiding Attack: The Evolutionary Ecology of Crypsis, Warning Signals and Mimicry. .

Satler J.D., Carstens B.C. 2016. Phylogeographic concordance factors quantify phylogeographic congruence among co-distributed species in the Sarracenia alata pitcher plant system. Evolution (N. Y). 70:1105–1119.

Sérsic A.N., Cosacov A., Cocucci A. a., Johnson L. a., Pozner R., Avila L.J., SITES Jr. J.W., Morando M. 2011. Emerging phylogeographical patterns of plants and terrestrial vertebrates from Patagonia. Biol. J. Linn. Soc. 103:475–494.

Sheppard P.M., Turner J.R.G., Brown K.S., Benson W.W., Singer M.C. 1985. Genetics and the Evolution of Muellerian Mimicry in Heliconius Butterflies. Philos. Trans. R. Soc. B Biol. Sci. 308:433–610.

Sherratt T.N. 2002. The evolution of imperfect mimicry. Behav. Ecol. 13:821–826.

Sherratt T.N. 2006. Spatial mosaic formation through frequency-dependent selection in Mullerian mimicry complexes. J. Theor. Biol. 240:165–174.

Sherratt T.N. 2008. The evolution of Müllerian mimicry. Naturwissenschaften. 95:681–695.

Smith K.E., Halpin C.G., Rowe C. 2016. The benefits of being toxic to deter predators depends on prey body size. Behav. Ecol. 0:arw086.

Solis-Lemus C., Knowles L.L., Ane C. 2014. Bayesian species delimitation combining multiple genes and traits in a unified framework. Evolution (N. Y). 69:492–507.

Sota T., Konuma J., Fujiwara M., Shoguchi E. 2013. Genome sizes of three species in the subtribe Carabina (Coleoptera: Carabidae). Entomol. Sci. 16:122–124.

Stoddard M.C. 2012. Mimicry and masquerade from the avian visual perspective. Curr. Zool. 58:630–648.

Stoddard M.C., Prum R.O. 2008. Evolution of avian plumage color in a tetrahedral color space: a phylogenetic analysis of new world buntings. Am. Nat. 171:755–776.

Sugden D.E., Bentley M.J., Fogwill C.J., Hulton N.R.J., McCulloch R.D., Purves R.S. 2005. Late-Glacial Glacier Events in Southernmost South America: a Blend of “Northern” and “Southern” Hemispheric Climatic Signals? Geogr. Ann. Ser. A Phys. Geogr. 87:273–288.

Sukumaran J., Knowles L.L. 2017. Multispecies coalescent delimits structure, not species. Proc. Natl. Acad. Sci. 2016:201607921.

Swofford D.L. 2002. PAUP* phylogenetic analysis using parsimony (*and other methods). Version 4.0b10. Sinauer Assoc.

Tamura K., Stecher G., Peterson D., Filipski A., Kumar S. 2013. MEGA6: Molecular evolutionary genetics analysis version 6.0. Mol. Biol. Evol. 30:2725–2729.

Thompson J.N. 1989. Concepts of coevolution. Trends Ecol. Evol. 4:179–183.

Twomey E., Vestergaard J.S., Summers K. 2014. Reproductive isolation related to mimetic divergence in the poison frog Ranitomeya imitator. Nat. Commun. 5:4749.

Vera-Escalona I., D’Elía G., Gouin N., Fontanella F.M., Muñoz-Mendoza C., Sites J.W., Victoriano P.F. 2012. Lizards on ice: evidence for multiple refugia in Liolaemus pictus (Liolaemidae) during the last glacial maximum in the Southern Andean beech forests. PLoS One. 7:e48358.

Victoriano P.F., Ortiz J.C., Benavides E., Adams B.J., Sites J.W. 2008. Comparative phylogeography of codistributed species of Chilean Liolaemus (Squamata: Tropiduridae) from the central-southern Andean range. Mol. Ecol. 17:2397–416.

Villagrán C., Armesto J. 2005. Fitogeografía histórica de la Cordillera de la Costa de Chile. Historia, biodiversidad y ecología de los bosques costeros de Chile. p. 105–123.

Wang I.J., Shaffer H.B. 2008. Rapid color evolution in an aposematic species: a phylogenetic analysis of color variation in the strikingly polymorphic strawberry poison-dart frog. Evolution. 62:2742–59.

Wilson J.S., Williams K. a, Forister M.L., von Dohlen C.D., Pitts J.P. 2012. Repeated evolution in overlapping mimicry rings among North American velvet ants. Nat. Commun. 3:1272.

Wright S. 1931. Evolution in Mendelian populations. Genetics. 16:97–159.

Wright S. 1943. Isolation by Distance. Genetics. 28:114–138.

Xu J., Pérez-Losada M., Jara C.G., Crandall K. a. 2009. Pleistocene glaciation leaves deep signature on the freshwater crab Aegla alacalufi in Chilean Patagonia. Mol. Ecol. 18:904–18.

Yang Z., Rannala B. 2010. Bayesian species delimitation using multilocus sequence data. Proc. Natl. Acad. Sci. U. S. A. 107:9264–9.

Yeager J., Brown J.L., Morales V., Cummings M., Summers K. 2012. Testing for selection on color and pattern in a mimetic radiation. Curr. Zool. 58:668–676.

Zhang C., Rannala B., Yang Z. 2014. Bayesian Species Delimitation Can Be Robust to Guide-Tree Inference Errors. Syst. Biol. 63:993–1004.

Zhang C., Zhang D.-X., Zhu T., Yang Z. 2011. Evaluation of a bayesian coalescent method of species

delimitation. Syst. Biol. 60:747–61.